Identification, Molecular cloning and Functional Characterization of Novel Bioactive Peptides from Amphibian Skin Secretion

Yanjing Dong

School of Pharmacy

Faculty of Medicine, Health and Life Science

Queens University Belfast

A thesis submitted to Queen's University, Belfast, for the degree of Doctor of Philosophy

2018

Contents

Acknowledgements I

Declaration II

Abstract III

Chapter 1 General Introduction 1

1.1 Biological evolution leads to amphibian host defence 2

1.1.1 Evolutionary adaptions for changes of habitats 2

1.1.2 Increasingly endangered amphibians 3

1.2 Amphibian skin secretions & their collection 5

1.2.1 Amphibians skin secretions 5

1.2.2 Collection of frog skin secretions 6

1.3 The functional mechanisms and structures of AMPs 7

1.3.1 Membrane active modes 7

1.3.2 Targeting of key cellular processes 12

1.3.3 Immune-related activity 14

1.4 Physiochemical properties of AMPs 15

1.4.1 Length 15

1.4.2 Net charge 16

1.4.3 Amphipathicity 18

1.4.4 Hydrophobicity 18

1.4.5 Helicity 19

1.5 Anticancer peptides 19

1.5.1 Current situation of cancer therapy 20

1.5.2 Various anticancer peptides (ACPs) 21

1.5.3 Membrane-active mechanism....22
1.5.4 Non-membrane-lytic modes....24
1.6 Protease inhibitors....25
1.6.1 Protease and protease inhibitors....25
1.6.2 Amphibian skin-derived trypsin inhibitors....26
1.6.3 Kunitz-inhibitors....28
1.7 Aims and objectives of this thesis....29
Chapter 2 General Methods....31
2.1 Molecular cloning....32
2.1.1 Specimen biodata and secretion harvesting....32
2.1.2 mRNA Isolation....32
2.1.3 cDNA Library Construction....34
2.1.4 3´- RACE PCR....37
2.1.5 Gel Analysis....39
2.1.6 PCR Products Purification....40
2.1.7 Cloning....41
2.1.8 Gel Analysis....45
2.1.9 Selected PCR Products Purification....46
2.1.10 Sequencing Reaction....47
2.1.11 Extension Products Purification....48
2.1.12 Sequencing....48
2.2 Peptide Identification and Structural Analysis....49
2.2.1 RP-HPLC analysis....49
2.2.2 Fraction analysis by MALDI-TOF mass spectrometry....49
2.2.3 Sequencing of peptides by LCQ ESI quadrupole ion-trap mass spectrometry....50
2.2.4 Bioinformatic analysis of isolated peptides....50

2.3 Solid-Phase Peptide Synthesis 51

2.3.1 Preparation and synthesis 51

2.3.2 Peptide cleavage 53

2.3.3 Washing and lyophilisation 54

2.4 Synthetic Peptide Purification and Identification 54

2.5 Secondary structure analysis 55

2.6 Antimicrobial Assays 56

2.6.1 Preparation 56

2.6.2 Inoculation 56

2.6.3 MIC assay & viable cell counts 56

2.7 Bacterial Cell Membrane Permeability Assay 59

2.8 Haemolysis Assay 60

2.8.1 Preparation 60

2.8.2 Erythrocyte washing 60

2.8.3 Peptide loading 61

2.8.4 Detection 61

2.9 Anti-cancer assay 61

2.9.1 Resuscitation of frozen cell lines 62

2.9.2 Cell culture 62

2.9.3 Cell subculture (passage) 63

2.9.4 MTT assay 63

2.10 Trypsin Inhibition Assay 65

2.11 Chymotrypsin inhibition assay 66

2.12 Trypsin cleavage 66

CHAPTER 3 A Combined Molecular Cloning and Mass Spectrometric Method to Identify a Novel Peptide from the

Skin Secretion of *Odorrana hejiangensis* : Characterisation and Design of Analogues 68

3.1 Introduction 69

3.2 Methods 70

3.2.1 Specimen Biodata and Secretion Acquisition 70

3.2.2 Molecular Cloning of QUB-1568 Precursor-Encoding cDNA 71

3.2.3 Identification and Structural Analysis of Peptides in Skin Secretion 71

3.2.4 Solid-Phase Peptide Synthesis 72

3.2.5 Circular Dichroism (CD) Analysis 72

3.2.6 Minimal Inhibitory Concentration Assays 72

3.2.7 Membrane permeability assay 72

3.2.8 Haemolysis Assay 73

3.2.9 Anti-cancer assay 73

3.3 Results 74

3.3.1 Molecular cloning and sequencing analysis 74

3.3.2 Identification and structural characterisation of peptide QUB 1568 76

3.3.3 Peptide synthesis 78

3.3.4 Secondary structure analysis of peptide 79

3.3.5 Antimicrobial activity of QUB-1568 and two designed analogues 81

3.3.6 *S.aureus* membrane permeabilisation test 82

3.3.7 Haemolytic activity assay 84

3.3.8 Cell culture 85

3.4 Discussion 86

CHAPTER 4 Identification, Characterisation and modification of the Antimicrobial Peptide, QUB-3025, from the Skin Secretion of *Phyllomedusa coelestis* 91

4.1 Introduction 92

4.2 Methods 93

4.2.1 Specimen Biodata and Secretion Acquisition 93

4.2.2 Molecular Cloning of QUB-3025 Precursor-Encoding cDNA 94

4.2.3 Identification and Structural Analysis of Peptides in Skin Secretion 94

4.2.4 Solid-Phase Peptide Synthesis 95

4.2.5 Circular Dichroism (CD) Analysis 95

4.2.6 Minimal Inhibitory Concentration Assays 95

4.2.7 Membrane permeability assay 96

4.2.8 Haemolysis Assay 96

4.2.9 Anti-cancer assay 96

4.3 Results 97

4.3.1 Molecular cloning and sequencing analysis 97

4.3.2 Identification and structural characterisation of peptides 99

4.3.3 Peptide synthesis 101

4.3.4 Secondary structure analysis 102

4.3.5 Antimicrobial assays 105

4.3.6 *E.coli* membrane permeability assay 105

4.3.7 Haemolysis assay 107

4.3.8 Anti-cancer assay 107

4.4 Discussion 108

CHAPTER 5 A novel Kunitz-like trypsin inhibitor isolated from the defensive skin secretion of the Odorous frog: *Odorrana versabilis*. 114

5.1 Introduction 115

5.2 Methods 116

5.2.1 Specimen Biodata and Secretion Acquisition 116

5.2.2 Molecular Cloning of Kunitzin-OV Precursor-Encoding cDNA from a Skin Secretion-Derived cDNA Library of *O. versabilis* 117

5.2.3 Identification and Structural Analysis of Peptides in Skin Secretion..... 117

5.2.4 Solid-Phase Peptide Synthesis..... 118

5.2.5 Minimal Inhibitory Concentration Assays 119

5.2.6 Haemolysis Assay 119

5.2.7 Trypsin inhibition assay 119

5.2.8 Chymotrypsin inhibition assay 120

5.2.9 Trypsin cleavage of inhibitor peptides 120

5.3 Results 120

5.3.1 Molecular cloning and sequencing analysis of Kunitzin-OV..... 120

5.3.2 Identification and structural characterisation of peptides..... 122

5.3.3 Peptide synthesis 124

5.3.4 Antimicrobial/ Haemolysis assays 124

5.3.5 Trypsin inhibition and peptide cleavage..... 126

5.4 Discussion 127

Chapter 6 General Discussion 133

6.1 Structure/Activity relationships of AMPs..... 134

6.2 Bacterial resistance against AMPs 136

6.2.1 Biofilm..... 136

6.2.2 Proteolysis 137

6.2.3 Membrane modification 138

6.3 Combination use of AMPs and antibiotics 139

6.4 Development of therapeutic AMPs..... 139

6.5 Conclusions and prospects..... 141

References 143

Acknowledgements

First and foremost, I would like to show my most profound gratitude to Prof. Chris Shaw, Dr Tianbao Chen, Dr Mei Zhou, Dr Lei Wang and Dr Chengbang Ma, for providing me with the opportunity to study in their research group and their valuable advice in my work.

I also sincerely thank my supervisor, Dr Xinping Xi, who provided me with valuable guidance in my experiments and at every stage of the writing of this thesis. Without his patience and help, I could not have completed my thesis.

My appreciation must go to my research colleagues in the Natural Drug Discovery Group as my entire period of studying was full of happiness and joy with their help and company. Extended thanks go to Yipeng Yuan, Xiaolin Chen and Luyao Zhang, as I benefited a lot from them both in my academic and daily life.

Last but not least, I'd like to thank all my friends, especially my two lovely roommates, Zichen Shang, Jia Liu and Yujie Fu, for their encouragement and support.

Declaration

I declare that the research reported in this thesis is my work except where acknowledgement has been made. All of the work was carried out in the Natural Drug Discovery Group, School of Pharmacy, Faculty of Medicine, Life and Health Sciences, Queen's University Belfast.

I declare that for two years following the date on which the thesis is deposited in the Library of Queen's University Belfast, the thesis shall remain confidential with access or copying prohibited. Following the expiry of this period, I permit the librarian of the University to allow the nine-month report to be copied in whole or part without reference to me on the understanding that such authority applies to the provision of single copies made for study purposes or inclusion within the stock of another library. This restriction does not apply to the British Library Thesis Service. IT IS A CONDITION OF USE OF THIS THESIS THAT ANYONE WHO CONSULTS IT MUST RECOGNISE THAT THE COPYRIGHT RESTS WITH THE AUTHOR AND THAT NO QUOTATION FROM THE THESIS AND NO INFORMATION DERIVED FROM IT MAY BE PUBLISHED UNLESS THE SOURCE IS PROPERLY ACKNOWLEDGED.

Abstract

Amphibian skin is a rich source of bioactive peptides in its abundant secretions. Here in this thesis, three novel peptides were identified from three different frogs: *Odorrana hejiangensis*, *Phyllomedusa coelestis* and *Odorrana versabilis*, respectively, and then these were synthesized and subjected to a series of functional assays together with their designed analogues.

Chapter 3 describes the identification of QUB-1568 (SLILKGLASLAQKIL-NH2), a novel bioactive peptide with excellent antimicrobial activity but no anti-cancer activity. In order to attempt to improve the stability and anti-cancer activity of this peptide, the analogues, QUB-1774 (CSLILKGLASLAQKILC) and QUB-2889 (RKKRRQRRRSLILKGLASLAQKIL-NH_2), were designed and synthesised. According to the results obtained, both QUB-1774 and -2889 had antimicrobial activity against Gram positive bacteria and yeast but a higher cytotoxicity than QUB-1568. While QUB-1774 had no anti-cancer activity, QUB-2889 was found to have activity against all tested cancer cells. The addition of a cationic Tat sequence (RKKRRQRRR) to the core natural peptide sequence, successfully increased the peptide bioactivity and achieved the goal, while the results of cyclization using a disulphide bond to increase peptide stability needs further investigation.

In Chapter 4, a cDNA encoding the biosynthetic precursor of a putative novel dermaseptin peptide named QUB-3025 (ALWKDILKNVGKAAGKAVLNKVTDMVNQ-NH_2), was cloned from the skin-derived cDNA library of *Phyllomedusa coelestis*. QUB-3025 and its shorter analogue, QUB-1994 (ALWKDILKNVGKAAGKAVL-NH_2,) were synthesised by solid phase peptide synthesis. Following functional assays, the two peptides were found to possess a

similarly broad-spectrum antimicrobial activity against not only Gram-positive and Gram-negative bacteria but also against a potentially pathogenic yeast. Besides, both peptides showed weak haemolytic activity against horse erythrocytes at their effective antimicrobial concentrations. However, no significant anti-cancer activity was observed. It may suggest that the C-terminal sequence of dermaseptins makes little difference to their antimicrobial activity.

In Chapter 5, a novel peptide with trypsin inhibitory activity, was found in the skin secretion of the Chinese Bamboo Leaf Odorous frog, *Odorrana versabilis*. Based on the comparison of structures, the six-residue C-terminal disulphide bond of the novel peptide (ALKYPFRCKAAFC) was identical to the C-terminal loop of the previously reported short peptide Kunitz-type inhibitors, the kunitzins. Thus, this novel peptide was named kunitzin-OV. A synthetic replicate of kunitzin-OV was subjected to a series of functional assays, and it exhibited no significant antimicrobial activity against Gram positive and negative bacteria (*Staphylococcus aureus* and *Escherichia coli*) or yeast (*Candida albicans*). Also, little haemolytic activity was observed for this novel peptide at concentrations up to 512 μM. In the trypsin inhibitor assay, kunitzin-OV displayed a trypsin inhibitory activity with a Ki value of 3.042 μM, whereas, when Lys-9 at P1 position was substituted by Phe (F), trypsin inhibitory activity totally disappeared and a chymotrypsin optimized inhibitory activity was produced with a Ki value of 2.874 μM.

Amphibian skin secretions have again been proven to be a unique resource for an abundance of bioactive peptides and these naturally-occurring peptides are capable of targeting pathogenic cells, intracellular processes, proteins, etc., which gives them great potential to be developed as novel drugs.

Chapter 1

General Introduction

1.1 Biological evolution leads to amphibian host defence

1.1.1 Evolutionary adaptions for changes of habitats

Amphibians were the first creatures to grow lungs, and they are the transitional type from aquatic to terrestrial. In a broad sense, the Class Amphibia was divided into three subclasses: Temnospondyli, Lepospondyli and Lissamphibia (Baird 1965), with the extinction of the former two subclasses, the Lissamphibia represents all modern amphibians including frogs & toads (Anura), salamanders & newts (Caudata) and caecilians (Gymnophiona). Currently, over 7000 amphibian species are known to exist, of which almost 90% are anurans. The electronic database is accessible at http://research.amnh.org/vz/herpetology/amphibia/index.html (Frost 2015).

The dramatic changes of the living environment from aquatic to terrestrial brought about many changes such as the distinct respiratory condition, more undulating temperature, water deficiency, etc. and thus brought about significant challenges especially in physiology (Ubhi, Matthews 2018). Consequently, amphibians have developed a series of typical evolutionary adaptations in their physiological and morphological features, among which the skins adaptive traits play vital roles in conquering difficulties of survival (König et al. 2015).

The skin is an extraordinary organ and acts as a protector to keep external damaging factors away from the animal due to its direct contact with the outside environment (D'Orazio et al. 2013). Generally, the extraordinary cutaneous exocrine apparatus with abundant granular and mucous glands is the chief peculiarity of amphibian skin (Wells, Schwartz 2007). These glands connect with the outer epidermis directly through a secretory canal and are widely distributed on the dorsal surface of amphibians (Wells 1977). The granular glands can release toxic secretions under various stimulations like

predatory attack, while the discrete amounts of mucopolysaccharides secreted by mucous glands are used for keeping the skin moist (Duellman, Trueb 1994). Moreover, macro glands, which are the gathering of granular glands with the toxins in high concentration in the uncovered parts of the body, are the reflection of an enhanced defensive mechanism (König et al. 2015).

1.1.2 Increasingly endangered amphibians

The Red List Index (RLI), expounded the evaluation of biodiversity variation according to the data about all nature conservation categories of the non-governmental organization, International Union for Conservation of Nature and Natural Resources (IUCN) Red List of Endangered Species, was applied in the analysis of endangered species. This index is a significant quantitative measure for risk assessment and determination of conservation status (Butchart et al. 2007). Notably, the RLI values for amphibians changed by 3.4% from 1980 to 2004 which made them more endangered than mammals and birds, in addition, during the investigation period, the Red List categories of extinction have changed due to the worsening of the amphibians population status (662 amphibian species have been observed) (Hoffmann et al. 2010). Besides, the IUCN categories declined by three or more units for nearly 40 amphibian species, in the two decades after 1980, no less than nine amphibian species, including two unique species of the Australian genus *Rheobatrachus* and the golden toad *Incilius periglenes* from Costa Rica, disappeared (Hoffmann et al. 2010). Moreover, 95 species (with 18 species belonging to the Neotropical genus *Atelopus*) are supposed to die out with a substantial probability (Anan'eva et al. 2015).

Anurans are widespread species that are distributed extensively across all continents excluding Antarctica (Miller, Fowler 2014). Besides, frogs and toads show excellent adaptability with numerous habitats ranging from parched deserts to Arctic tundra as well

as altitudes ranging from sea level to heights of 5000m (Duellman, Trueb 1994). With environmental issues caused by human beings becoming more and more severe all over the world, the damage to habitats such as the air and water contamination, deforestation and overgrazing, turn out to be the main threats for amphibians. Besides, climate change is also a contributing factor that considerably influences environmental niches and brings new survival challenges for amphibians (Gascon 2007). Apart from this, over-collecting causes population losses of frogs and these are dramatic as well. For example, the Odorous frog, *Odorrana grahami,* was once familiar in China, but it is now uncommon mainly because of excess use as food for local consumption (Vié et al. 2009).

Furthermore, *Batrachochytrium dendrobatidis* (Bd), a recently studied severe amphibian infectious disease (caused by chytridiomycosis which is a common fungal pathogen) is another major contributor to declines and extinctions of amphibians (Berger et al. 1998). The infections, extinctions or die-offs of more than 200 amphibian species is attributed to Bd, and this fungus exists on every continent but Antarctica (Seimon et al. 2015). After infection of amphibians, Bd was found in the epidermal cells and led to pathological abnormalities include a thickening of the outer layer of skin (Berger et al. 1998). The unique physiological activities of amphibian skin which are associated with strict regulation for the exchange of respiratory gases, water, and electrolytes makes amphibians extremely vulnerable to cutaneous fungal infections (Ohmer 2016). The hypothesis about the pathogenesis of Bd, is that this fungus disrupts the standard regulatory functions of frog skin. Also, studies indicate that severe chytridiomycosis in amphibians brings about electrolyte depletion and osmotic imbalances that are sufficient to result in death (Voyles et al. 2007).

1.2 Amphibian skin secretions & their collection

1.2.1 Amphibians skin secretions

While amphibians have long been recognized for their value in traditional medicines, they are also being gradually accepted as a significant potential source of chemical substances for modern medical applications like antimicrobial peptides (AMPs) (Hocking, Babbitt 2014). In many regions of the world, amphibians are still collected by residents to meet primary health needs (Alves et al. 2013, Mohneke et al. 2011). Aside from this, there are some areas, particularly East Asia, where commercial markets exist for the use of amphibians in traditional medicinal practices, over 30 of amphibian species have been presented in Traditional Chinese Medicine alone (Ye et al. 1993).

As the regulator as well as protector of amphibians, the amphibian skin is capable of releasing secretions via the glands to maintain not only physiological homeostasis but also against potential predators (Duellman, Trueb 1994). Anurans are the principal study object of research on the biologically active components in amphibian skin secretions, and as early as in the fifties of the 20th century, it had been first proven that the biogenic amine serotonin exists in the amphibian skin secretion (Erspamer and Vialli, 1951). Over the next couple of decades, many new amphibians were used for studies of the natural products in their skin secretions and it is mainly the bioactive peptides which have been most intensely studied (Simmaco et al. 1998). These different functional peptides (like protease inhibitors, neural stimulators, immunomodulators and antimicrobials) are stored in granular skin glands and can be discharged in high concentrations under stressful or embattled situations (König et al. 2015).

Skin secretions from anurans are an abundant source of biologically active peptides and these peptides are expected to have a significant potential medicinal value with analgesic,

antiviral, antibiotic, antidiabetic and wound-healing properties as well as the potential of curing cancer, HIV and drug resistance, which are main challenges facing the 21st century medical community (Ladram, Nicolas 2016). In fact, exudates of frogs and toads skin have been used for the treatment of disease for centuries, for instance, Chansu, a rare traditional Chinese medicine made from toad venom, has an excellent effect on detoxification, detumescence and acesodyne (Hong et al. 1992). Furthermore, modern medical science has already proven the therapeutic role of Chansu in several types of cancers (Ko et al. 2005, C. Li et al. 2013, Qin et al. 2008).

1.2.2 Collection of frog skin secretions

With the growing number of studies on anuran dermal secretions, the methods of collecting such also vary. In earlier research, using either methanol or acetone to extract frog skin peptides was popular among most researchers, however, it is also an inhuman method due to the experimental procedures being somewhat rough and demanded hundreds of skins from frogs (De Caro et al. 1968). With the decreasing number of amphibians, more friendly collection methods have been applied. Intradermal injection of glucocorticoids or norepinephrine are well tolerated by the animals without symptoms of soreness and casualties are rare (Nutkins and Williams 1989). Nevertheless, when it comes to vulnerable or threatened species, to obtain permission to perform an invasive operation is almost impossible. In this case, Conlon and Leprince adopted an alternative method involved immersing frogs in a norepinephrine solution, which is a less effective stimulation but is non-invasive, hence may be more applicable for rare and endangered species (Conlon, Leprince 2010).

Apart from chemical means, electrical stimulation is an available and effective method of catalysing secretion of skin peptides without any invasion, which induces the adrenergic myocytes surrounding the granular glands to contract and subsequently leads

to the full release of the components via a holocrine mechanism. During this process, both peptides and mRNA can be obtained from the skin secretions, and the mRNA can be preserved in fresh samples by freeze-drying instantly that allows their storage life to stretch up to several years (Chen et al. 2003). Generally, the treatment is entirely animal-friendly and also presents a number of advantages: firstly, no specimen will be sacrificed during the experiments; secondly, collecting the secretions from the same individuals regularly (longitudinal sampling) ensures high accuracy and repeatability; thirdly, samples obtained in this way are free of contamination of blood, blood proteins/peptides from dissected integument; lastly, cDNA libraries can be established through the isolation of endogenous mRNA (Chen et al. 2006).

1.3 The functional mechanisms and structures of AMPs

Antimicrobial peptides have developed a wide diversity of means to achieve their activities as well as various structural properties with thousands of years of evolution, and there is an interaction effect between the function and structure of AMPs. That is, the function can influence the structure of these peptides and *vice versa* (Nguyen et al. 2011).

1.3.1 Membrane active modes

One of the critical mechanism of AMPs to achieve their activities is to interfere with the stability of bacterial bilayers. In general, a cationic charge and a prominent proportion of hydrophobic residues are two common characteristics of AMPs (Bahar, Ren 2013). The cationicity provides AMPs with a high selectivity for microbial cytoplasmic membranes which have a negative charge and enhances the interactions between AMPs and other negatively-charged moieties like nucleic acids, outer membrane lipids and

phosphorylated proteins; on the other hand, the second feature promotes the interactions with the fatty acyl chains (Kumar et al. 2018, Lohner 2001).

No matter how different the formation, length and amino acid composition are, all peptides can form an amphipathic conformation in the presence of membrane (Bahar, Ren 2013). Initially, peptides will adsorb to the membrane and in the classic modes which include toroidal pores, carpet mode and barrel stave mode (Figure 1.1), the peptides insert themselves across the membrane to constitute different pore formations in a threshold concentration (Nguyen et al. 2011).

1.3.1.1 Carpet model

In a carpet-like manner, peptide molecules lie on the membrane first and then aggregate on a small area of the bilayer to a certain amount which is enough for penetrating the bilayer and the result is destruction of the micellar structure of membranes (Bahar, Ren 2013). Cecropins are a family of antimicrobial peptides that were first isolated from insects. Gazit E et al. (Gazit et al. 1995) investigated the antimicrobial mechanism of cecropin via binding experiments and resonance energy transfer (RET) measurements to test the effectiveness of the target peptides on the bacterial membrane. The results revealed that the insect cecropins attach to the bilayer in a simple, non-cooperative way, and they do not aggregate on the cell membrane. This action mode is proposed as the carpet model.

1.3.1.2 Barrel-stave model

To achieve a barrel-stave formation, peptide molecules are first adsorbed to the cell membrane, then as the peptides perpendicularly insert into the core of the bilayer, a peptide-linked barrel-stave pore is formed (Bahar, Ren 2013). The most mentioned example of a barrel-stave structure is with alamethicin (from the fungus *Trichoderma*

viride). This linear peptide antibiotic can adapt an α-helical structure on the cell membrane, and with the aggregation of 4 to 6 molecules, alamethicin can form multi-conductance channels by the barrel-stave formation model in the membrane (Laver 1994).

1.3.1.3 Toroidal pore model

In toroidal pore formation, amphipathic peptides first lie parallel to the cell membrane, and then, with the hydrophobic side inserted into the bilayer, peptides become perpendicular to the membrane plane, and transmembrane pores are formed of alternating arranged peptides and lipids (Nguyen et al. 2011). One of the most well-known amphibian antimicrobial peptides, magainin, which is found in the skin of *Xenopus laevis*, uses toroidal pore formation during its interactions with bacteria cell membranes. According to the data obtained from oriented circular dichroism analysis and neutron in-plane scattering analyses of magainin 2, when peptides aggregate to a high local concentration, they orientate perpendicular to the lipid bilayer plane and form transmembrane pores with lipids incurved like the inner part of a torus (Ludtke et al. 1996).

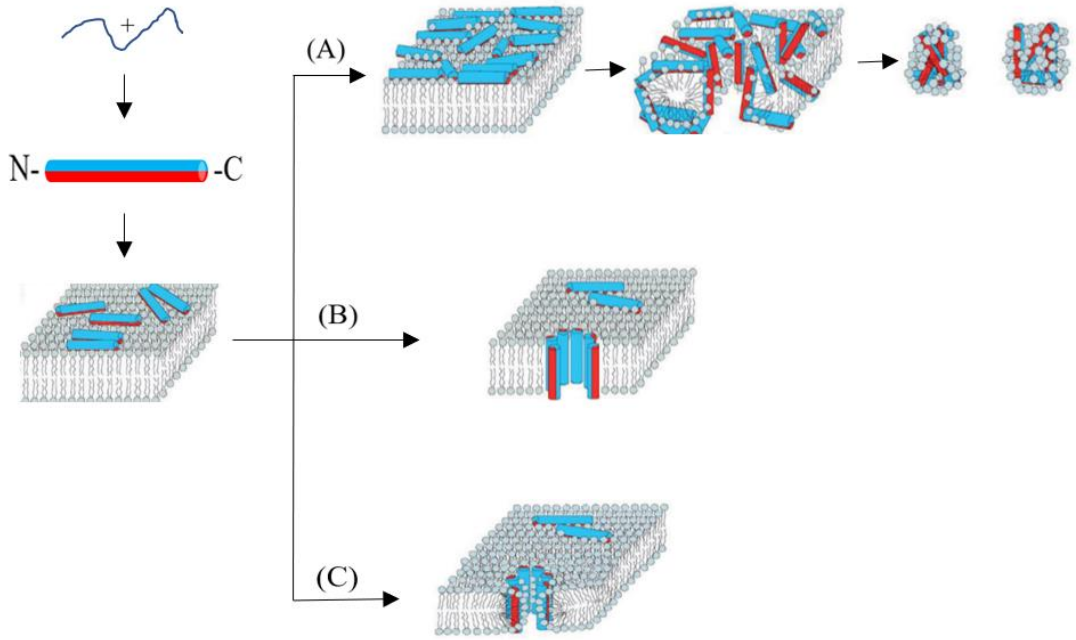

Figure 1.1 The three standard membrane-related mechanisms of AMP actions (Giuliani et al. 2008). The cationic peptides adopt an amphipathic conformation in the membranous environment, and the red part indicates the hydrophobic side and the blue part represents the hydrophilic (positively charged) side. At the initial stage, the positively charged side of peptide binds to the anionic cell membrane surface via electrostatic attractions, and the hydrophobic side is inserted into the lipid bilayer. Along with the aggregation of peptides, a threshold is reached, and membrane disruption appears in (A) carpet model: membrane is solubilized by micellization; (B) barrel-stave model: with the hydrophilic sides of peptides facing each other, peptide-linked transmembrane pores are formed; (C) toroidal pore model: transmembrane pores are formed of alternating arranged peptides and lipids, before the membrane lysis, these pores can let small molecules enter the cells.

1.3.1.4 Disordered toroidal pore formation

Besides the classical membrane disrupting modes, many other membrane-active modes also have been reported. With the application of dynamic simulations, mechanisms of AMP action can be effectively detected, and in this way, the interaction between

magainin MG-H2 and a model lipid bilayer, was described as through a disordered toroidal pore (Leontiadou et al. 2006). After peptide binding and gathering on the cellular membrane to a specific high concentration, a toroidal pore structure was formed. However, differing from the previous maintained classic toroidal pore conformation with several peptide molecules involved, in the centre of this disordered toroidal pore formation, only one peptide was present, while other peptides were located close by and lied parallel to the membrane.

1.3.1.5 Other membrane-related actions

Bacterial membranes are enriched with differently charged lipids (anionic, zwitterionic and neutral), and when cationic peptides adsorb to the cellular membrane, there is an excellent chance that individually charged lipids will be separated to form different domains (Epand, Epand 2011). This kind of segregation brings about membrane depolarization, the leakage of intercellular contents and can finally result in cell growth arrest and cell death.

Notably, a membrane-associated way for AMPs to facilitate their activity is to target oxidised lipids (Mattila et al. 2008). It is supposed that lipid oxidation could increase bacterial membrane sensitivity to AMPs with the reactive oxygen species released during phagocytosis. The α-helical AMPs, temporin B and L, have more efficient interactions with membranes containing an oxidised phosphatidylcholine lipid, the Schiff base formation between the lipid aldehyde groups and peptide amino groups plays a vital role during this process (Brogden 2005).

In more specific situations, peptides can combine with small anions across the membrane, bringing about their outflow, non-bilayer intermediates in the membrane can be induced, and the membrane potential may be dissipated without other apparent damage

(Ulmschneider 2017); or in contrast, in the molecular electroporation model, the membrane potential increases above a threshold because of the accumulation of peptides on the outer leaflet which makes the membrane instantly permeable to peptides and many other molecules (Takahashi et al. 2010).

1.3.1.6 Membrane disruption of a-helical peptides

The α-helical conformation commonly exists among AMPs and also is the most studied secondary structure of AMPs (Dennison et al. 2005). Generally, most α-helical AMPs achieve their activity by membrane disruption: the axis of the α-helix usually segregates amphipathicity of the peptides so that the peptide can lie parallel to the bilayer plane during the initial lipid interactions, with the hydrophobic side inserting into the acyl tail core and the charged side facing outside towards the phospholipid head groups (Nguyen et al. 2011). Although the formation of the α-helix may provide a more continuous hydrophobic and larger surface, it can also become a contributing factor to cytotoxicity (Takahashi et al. 2010). Peptides require a membranous environment to adopt a proper amphipathic helix and may have a proline-induced hinge or glycine-induced kink in the middle of the α-helix thus retaining antimicrobial activity but with low cytotoxicity (Lee et al. 2013). The presence of the hinge or kink partially unfolds the α-helix and separates the various functions into different regions of peptides. For example, the glycine residue in the lactoferrampin peptides separates the amphipathic helix region from the cationic region which is responsible for interacting with the membrane and attraction to the negatively-charged membrane, respectively (Haney et al. 2009).

1.3.2 Targeting of key cellular processes

Various non-lytic mechanisms can also be used by AMPs. These peptides target critical cellular process such as enzymatic activity, DNA & protein synthesis, protein folding,

outer membrane synthesis etc. to achieve their antimicrobial activity (Jenssen et al. 2006).

Many β-sheet AMPs interfere with bacterial membranes via toroidal pore formation (Tang, Hong 2009) while there are also specific β-sheet peptides with non-membrane active modes. Although tachyplesin, a β-sheet peptide from horseshoe crabs, is commonly regarded as a membrane-active peptide, it is also able to bind to the minor groove of DNA, which will influence DNA–protein interactions (Brogden 2005). The β-hairpin peptide, bovine lactoferricin, can inhibit DNA, RNA and protein synthesis after translocation to the cytoplasm. A series of protegrin I peptidomimetic analogues featuring stabilised β-hairpins, introduced a new bactericidal mechanism affecting outer membrane biosynthesis by targeting a specific protein (Srinivas et al. 2010). Furthermore, some of the human defensins are also capable of inhibiting cell wall biosynthesis enzymes in staphylococci by binding to the peptidoglycan precursor lipid II (Sass et al. 2010).

In addition, numerous extended peptides are not membrane active. The Pro-rich insect-derived pyrrhocoricin, drosocin and apidaecin peptides, interact with intracellular proteins like the heat-shock proteins DnaK and GroEL, to inhibit the DnaK ATPase activity and chaperone-assisted protein folding, respectively, to perform their antimicrobial activities (Brogden 2005). Peptides of less than 15 residues, with a significant proportion of Tryptophan and Arginine residues, can adopt defined amphipathic structures in a membranous environment; however, they are not membrane-active and, instead, they accumulate in the cytoplasm (Chan et al. 2006). The antimicrobial mechanism of these short peptides is to trap the replication fork then prevent recombination and DNA repair. For example, the first defined DNA-repair

inhibitor hexapeptide, WRWYCR, was subsequently shown to have broad bactericidal activity (Su et al. 2010).

1.3.3 Immune-related activity

Virtually all cationic peptides have direct antimicrobial activity *in vitro* especially when the peptides are tested at very high concentrations or in a dilute medium (Yeung et al. 2011). Nevertheless, *in vivo*, the modest concentrations of peptides present and/or physiological concentrations of monovalent and divalent cations, serum, and anionic macromolecules such as glycosaminoglycans, often inhibit the direct antimicrobial activities of many cationic AMPs (Bowdish et al. 2005). Hence, the primary mechanisms of some cationic peptides in host defence are probably not direct microbicidal action. For example, the human cathelicidin LL-37 can protect against Gram-positive bacterial infections when given exogenously to mice but cannot inhibit the bacterial load in tissue culture medium that contains physiologically relevant salt concentrations even at very high concentrations (100 μg/ml) (Bowdish et al. 2005). By comparison, cationic AMPs such as LL-37 show a variety of biological functions that selectively enhance and/or modulate host defence mechanisms to combat microbial infections but do not target the pathogen directly at physiological concentrations of peptides, salt and serum (Yeung, Gellatly et al. 2011).

The diverse immunomodulatory activities of AMPs include adjusting dendritic cell activation and differentiation as well as cellular differentiation pathways, boosting angiogenesis and wound healing, restraining bacterial-induced pro-inflammatory cytokine production, regulating neutrophil and epithelial cell apoptosis, motivating chemotaxis directly and/or through chemokine production (Sørensen et al. 2008).

Several frog peptides have been described to possess cytokine-mediated immunomodulatory properties and effects upon production of both pro- and anti-inflammatory cytokines base on their bacteriostatic abilities (Popovic et al. 2012). For instance, the frenatins in *Sphaenorhynchus lacteus* skin, can permeate the bacterial cell membrane to kill invading microorganisms directly and may also act to stimulate the system of adaptive immunity by motivating host macrophages to produce primarily proinflammatory cytokines (Conlon et al. 2014).

Currently, a few defensins are known to possess chemotactic activity (Soehnlein 2009). A large continuous cationic surface is a unified and common feature of the antimicrobial chemokines. Under physiological conditions, some chemokines tend to dimerise to extend the cationic surface (Chan et al. 2008). As an example, the reason why HBD-3 has high salt-insensitive activity compared to other β-defensins is that HBD-3 has a stronger tendency to dimerise (Schibli et al. 2001).

1.4 Physiochemical properties of AMPs

Due to their broad-spectrum effects and low induction of drug resistance, naturally-occurring antimicrobial peptides are regarded as potential alternatives to conventional antibiotics (Jenssen et al. 2006). However, in the case of AMPs, the potent antimicrobial activity usually comes with high cytotoxicity and to improve the situation, rational peptide design is required. The activities of AMPs are closely related to their physiochemical properties including length, net charge, amphipathicity, hydrophobicity and helicity (Alessandro et al. 2000). Rational adjustment of these characteristics can optimise their activities.

1.4.1 Length

The size of different AMPs varies, generally, they are made up of 12-50 amino acids (Papagianni 2003). Since AMPs need a certain number of amino acids (at lowest 7-8 residues) to adapt amphipathic formation in the period of interacting with the bacterial cell membrane, the chain length acts as an essential affecting element (Bahar, Ren 2013). Moreover, the molecular size of antibacterial peptides can directly influence their activities. In 2005, Takuro Niidome and his fellows (Niidome et al. 2005) investigated the relationships between chain length and antimicrobial activity of several cationic peptides H-$(LARL)_3$-$(LRAL)_n$-NH_2 (n equals 0-3), and the conclusion is antimicrobial activity decreased with the increase of peptide length, while, for haemolytic activity, the opposite happened. The truth was the long sequence tended to interact with the neutral membrane of a blood cell, thus it had difficulty in entering the bacterial inner membrane. Accordingly, the chain length should be considered as a crucial factor during the design of antimicrobial peptides.

1.4.2 Net charge

The cationicity provides AMPs with a high selectivity for microbial cytoplasmic membranes which have a negative charge and enhances the interactions between AMPs and other negatively charged moieties like nucleic acids, outer membrane lipids and phosphorylated proteins (Lohner, 2001).

Most of the AMPs are positively-charged peptides (usually +2 to +9), as the first stage of the bacterial cell membrane disruption process is the electrostatic attraction between cationic AMP and anionic membrane (Porto et al. 2012). Therefore, the net charge is crucial for the binding process, and the higher positive charge usually brings more potent antibacterial activity; however, there is a threshold, as too much positive charge also

result in greater toxic effects. For instance, L-V13K is a cationic antimicrobial peptide (with net charge +7), and a series of V13K analogues with different net charges, was designed to investigate the correlation between net charge and biological activities of AMPs (Jiang et al. 2008). The results indicated that a low level of net charge (<+4) entirely removed the bioactivities of those designed peptides, and on the contrary, a high level of net charge (+9 and +10) enhanced their antimicrobial activity but also led to a significant increase in cytotoxicity towards human erythrocytes (Jiang et al. 2008). Nevertheless, when the net charge of V13K analogues was increased progressively from +4 to +8, their effect against *Pseudomonas aeruginosa* strains was gradually promoted and haemolytic activity maintained at a relatively low level (Jiang et al. 2008).

AMPs exhibit effects of different intensities against Gram-negative bacteria, Gram-positive bacteria and eukaryotic cells (Bechinger, Gorr 2017). Bacterial membranes contain negatively charged lipids, which make them sensitive to cationic peptides. To be specific, Gram-negative bacteria have anionic lipopolysaccharide (LPS) embedded outer membrane and fewer peptidoglycan layers than Gram-positive bacteria, this can explain why some cationic AMPs have better inhibition against Gram-negative bacteria (Malanovic, Lohner 2016a). AMPs can replace the calcium and magnesium ions to bind to the anionic LPS competitively, this may promote the uptake of AMPs (Anunthawan et al. 2015). When it comes to the interaction between bacterial cell walls and AMPs, anionic cell wall components such as teichoic acid and lipoteichoic acid play vital roles (Bechinger, Gorr 2017).

Besides, eukaryotic cells like mammalian cells and fungal cells have different cell wall/membrane components. Usually, their membranes are neutral in potential and have the more stable structure (Malanovic, Lohner 2016b). For instance, polybia-CP (K. Wang et al. 2016) is an antimicrobial and also antifungal peptide isolated from the venom of

Polybia paulista – a wasp, and a series of experiments revealed that polybia-CP could interact with the polysaccharide fungal cell components, and this may be the first step of its membrane-active mode. Besides, it could also significantly stimulate the production of cellular reactive oxygen species (ROS), which can finally result in cell death.

1.4.3 Amphipathicity

The amphipathic structure is also one of the primary features of AMPs and it is essential for their bioactive activities, for example, in the amphipathic alpha-helical formation, peptides, residues are divided into the hydrophobic side and polar side (S. Zhang et al. 2016). Following the initial electrostatic attraction between the cationic peptide and microbial membrane, the hydrophobic side will insert into the bilayer and interact with the hydrophobic acyl tails, to permeate and disrupt the integrity of cell membrane (Nguyen et al. 2011). However, it is not the stronger, the better, as researchers have proven that the increase of amphipathicity comes along with higher cytotoxicity and antimicrobial activity (Wieprecht et al. 1997), and sometimes even lowers the activity against bacteria (Kondejewski et al. 1999). Additionally, the hydrophobic moment is a measure of the amphipathicity of α-helical peptides (Eisenberg et al. 1982).

1.4.4 Hydrophobicity

Besides amphipathicity, hydrophobicity is also one of the critical and commonly discussed features that is closely linked to AMP bioactivity (Yin et al. 2012). It is known that AMPs disturb the cell membrane by binding to the negatively charged lipid heads of the bilayer with their positively charged faces and inserting their hydrophobic faces into the hydrophobic tails of the bilayer. By replacing the residues on the nonpolar face of the α-helical AMP V13K_L, Chen et al. changed the peptide hydrophobicity to look into its impact on peptide activities (Chen et al. 2007). They found that along with the increase

of peptide hydrophobicity both antimicrobial and haemolytic activity strengthened, whereas, there was a boundary value for antimicrobial activity, the inhibitory activity against bacteria weakened once the hydrophobicity crossed the line (Chen et al. 2007). Hence, the enhancement of hydrophobicity made it easier for the α-helical peptide to interact with membrane hydrophobic cores of both zwitterionic phospholipids and erythrocytes. Furthermore, the action mode was changed when hydrophobicity enormously increased (Tachi et al. 2002).

1.4.5 Helicity

The correlation between AMP helicity and cytotoxicity on erythrocytes has been discussed a lot. As early as 1996, Margitta Dathe et al. (Dathe et al. 1996) discovered the correlation between peptide helicity and its bioactivity. In their study, KLAL peptide together with its D-amino acid substituted analogue were subjected to different charged membranes to detect their binding affinity. The results showed peptides with higher helicity possessed better interaction with the low charged membrane surface. Hence, the helicity of the peptide is related to their haemolysis activity since most of the eukaryotic cell membranes are electroneutral. Besides, each amino acid residue has different α-helix propensity, which is also a contributing factor to peptide α-helix formation. Among the twenty necessary amino acids, alanine has the highest tendency to form an α-helix, proline and glycine have low helix propensity, as for the remaining amino acids, their helix propensities are related to the side chain hydrophobic surface (Blaber et al. 1993).

1.5 Anticancer peptides

Although AMPs have been discussed with respect to their antibacterial activity, they have also been found to possess activity on fungi, cancer cells and viruses. The reason for this spectrum of activity of AMPs, is their diversified functional mechanisms, as despite the

membrane-action mode, AMPs can also target critical cellular processes or induce immune-related activity (Nguyen et al. 2011). Cancer is a severe threat to human life and according to the World Health Organization, it killed 8.8 million people in 2015, and globally, almost one in six people die of cancer. Cancer cells are different from healthy cells; they can ignore the body signals to die and can continue to grow and divide. Furthermore, tumour cells can detach and not stick in the right place as healthy cells do, so they are able to spread to other parts of the body (Ford, Pardee 1999).

1.5.1 Current situation of cancer therapy

Over the past decades, many therapeutic methods for different types of cancer have been developed. For instance, one of the most common treatments, chemotherapy, is curative for some cancers like some leukemias (Nastoupil et al. 2012); another common treatment, radiation, is usually applied for radiosensitive cancers and at the early stage of cancers; and in the case of localized cancers, surgery is a practical option, a whole tumour will be removed. However, limitations exist, most cancers are disseminated and cannot be completely cured, and the side effects of these therapies are also noteworthy. For instance, one or more anti-tumour drugs that are used for chemotherapy can kill rapidly dividing cells, which means except for cancer cells, other normal cells with this feature, like blood cells, and cells in the bone marrow, digestive tract and hair follicles, can also be affected (Airley 2009). Therefore, hair loss, myelosuppression and mucositis have commonly occurred during chemotherapy (Airley 2009). Besides, many anti-cancer drugs are delivered through the vascular system, while the blood vessels in neoplasms are abnormal, they cannot carry sufficient blood to the tumors, which causes drug efficacy reductions (Minchinton, Tannock 2006). In the treatment of brain tumours, chemotherapy has questionable effectiveness since most drugs cannot pass through the blood-brain barrier (Deeken, Löscher 2007).

1.5.2 Various anticancer peptides (ACPs)

Under the situation of high morbidity and relatively low cure rates, scientists have been exploring new therapeutic strategies. The anticancer peptides (ACPs) are small molecules that can permeate through tissue and get into neoplastic cells, thus they are considered to have great potential to become anticancer drugs and it is expected that synergies occur between ACPs and previously used drugs to improve the selectivity and lower the side effects (Gaspar et al. 2013). According to the figures from the CancerPPD database (http://crdd.osdd.net/raghava/cancerppd/index.php), thousands of ACPs have been found, in which amphibian species are a significant resource of most naturally-occurring ACPs with antimicrobial activity, several examples are listed in Table 1.1. It is believed that those AMPs may kill the cancer cells with an antimicrobial-like membrane-action mode, due to the negatively charged membrane of malignant cells.

Table 1.1 Examples of ten naturally-occurring amphibian ACPs, most of which are also antimicrobial peptides.

Name	Sequence	Resource	Cell line	Activity	Reference
maximin1	GIGTKILGGVKTALKGALKELA STYAN-NH_2	Chinese red belly toad *Bombina maxima*	C8166 (T cell leukaemia lymphoma)	IC50=5.72 μM	(Lai et al. 2002)
Magainin A	AIGKFLHSAKKFGKAFVGEIMN S-NH_2	African clawed frog *Xenopus laevis skin*	NCI-H182 (Small cell lung carcinoma)	IC50=7.28 μM	(Ohsaki et al. 1992)
Temporin-1CEa	FVDLKKIANIINSIF-NH_2	Chinese Brown Frog, *Rana chensinensis*	MCF-7	IC50 =12 μM	(Shang et al. 2009)

			(human breast tumour)		
GA-W4	FLWWLFKWAWK-NH_2	Brevinin-1EMa analogues	PC-3 (human prostate cancer)	IC50= 24.32 μM	(Kang et al. 2012)
citropin 1.1	GLFDVIKKVASVIGGL-NH_2	Australian green tree frog, *Litoria splendida*	Melanoma	IC50= 50 μM	(Doyle et al. 2003)
Gaegurin-6	FLPLLAGLAANFLPTIICKISYK C	Japanese wrinkled frog,*Rugosa rugosa*			(Kim et al. 2003)
Dermaseptin B2	GLWSKIKEVGKEAAKAAAKAA GKAALGAVSEAV-NH_2	Amazonian tree frog, *Phyllomedusa bicolor*	MDA-MB231 (breast carcinoma)	IC50= 8 μM	(van Zoggel et al. 2012)
Ascaphin-8	GFKDLLKGAAKALVKTVLF-NH2	North American tailed frog, *Ascaphus truei*	Hep G2 (human liver cancer)	IC50= 20 μM	(Michael Conlon et al. 2008)
palustrin-Ca	GFLDIIKDTGKEFAVKILNNLKC KLAGGCPP	American bullfrog, *Lithobates catesbeianus*	SGC-7901 (human gastric cancer)	IC50= 0.29μM	(ZHAO et al. 2011)
Dermaseptin-L1	GLWSKIKEAAKAAGKAALNAV TGLVNQGDQPS	lemur leaf frog, *Hylomantis lemur*	Hep G2 human liver cancer	IC50= 45 μM	(Conlon et al. 2007)

1.5.3 Membrane-active mechanism

As is well known, mammalian cell membranes are electroneutral due to the existence of zwitterionic lipids (e.g. phosphatidylethanolamine, phosphatidylcholine, and

sphingomyelin) (Bechinger, Gorr 2017). While the situation is the other way around for bacteria, their membranes contain an abundant amount of negatively charged phospholipids (e.g. phosphatidylglycerol, cardiolipin, and phosphatidylserine), which makes the bacterial membrane anionic and sensitive to cationic antimicrobial peptides (Malanovic, Lohner 2016a). In particular, the anionic lipopolysaccharides that embed in the outer membrane of Gram-negative bacteria also contribute to the negative potential of the bacterial membrane (Hoskin, Ramamoorthy 2008). Moreover, compared to cholesterol, the mammalian cell membrane component, peptidoglycan layers (the main component of bacterial cell wall) are highly porous and have a relatively large pore size, which makes it easier for AMPs to selectively disrupt the bacterial cell membrane (Malanovic, Lohner 2016b). The cell membrane is a crucial element for cell integrity and functions, and it protects the inner components, controls the cell selectivity and participates in a series of cellular processes. When a cell become cancerous, its cell membrane properties also change (Escribáet al. 2008).

Differing from electrically neutral normal cell membranes, neoplastic cells have electronegative membranes due to the presence of negatively charged phosphatidylserine, sialic acid residues and proteoglycans (Riedl et al. 2011), which may explain why those cationic ACPs can selectively kill the cancers by various membrane-active modes. At the very beginning, cationic peptides bind to the anionic cancer cell membranes via electrostatic attraction. Along with peptide concentration increases, the membrane becomes unstable because of the distortion and the change in osmotic pressure, furthermore, disrupting pore formations appear when peptides adapt to a long enough α-helical or β-sheet secondary structure at the membranous environment (Oelkrug et al. 2015). The anticancer peptide, d-peptide B, showed a highly selective membrane disruptive activity against mouse myeloma cells, and research revealed the

peptide efficacy was related to membrane phosphatidylserine content, which means it can selectively target this kind of anionic lipid (Iwasaki et al. 2009). Dermaseptin B2 is an ACP derived from the skin secretion of the Amazonian tree frog, *Phyllomedusa bicolor*, its antitumor mechanism against human prostate cancer cell line, PC-3, was suggested to be necrosis. At first, it proved dermaseptin B2 was not acting through apoptosis since it has no effect on PS exposure, the mitochondrial transmembrane potential nor caspase-3 activation. Then, confocal microscopy revealed that dermaseptin B2 can gather on the cancer cell membrane, and permeate into the tumour cells, which is possibly a necrotic-like pathway (van Zoggel et al. 2012).

1.5.4 Non-membrane-lytic modes

In addition, ACPs have also been reported to act in non-membrane-lytic modes. LfcinB (bovine lactoferricin) is a cationic anticancer peptide that can selectively induce the mitochondrial apoptosis pathway to kill malignant cells such as THP-1 human monocytic leukaemia cells and MDA-MB-435 breast carcinoma cells. In more detail, the LfcinB anticancer action mode involves the activation of caspases-2, -3, and -9, generation of reactive oxygen species (ROS), leading to mitochondrial membrane integrity loss, potential dissipation and cytochrome c release (Mader et al. 2005). Apart from the induction of apoptosis, other mechanisms occur such as angiogenesis inhibition, immune response meditation and DNA-related inhibition. For example, by detecting the microvessel density of the neoplastic cells *in vivo*, HNP1 (human α-defensin-1) was found to inhibit cancer cell angiogenesis, and also has the ability to mediate tumour immunity (Xu et al. 2008). The myristoylated-peptide exhibited a broad-spectrum of growth inhibition activity against eight major cancer groups at 10μM, and its action mechanism was reported as DNA synthesis inhibition (Ourth 2011). The action modes of anticancer peptides are briefly summarised in Figure1.2 below.

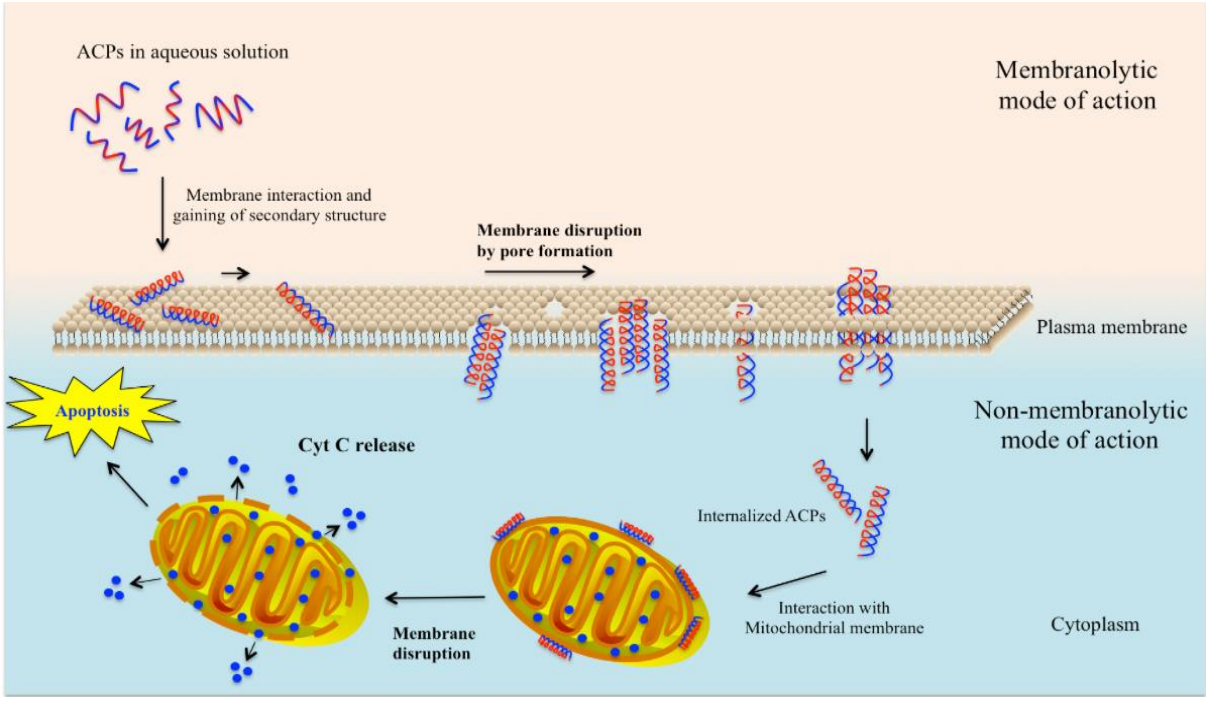

Figure 1.2 Different anticancer mechanisms of ACPs. http://crdd.osdd.net/raghava/cancerppd/index.php

In general, those small cationic peptides have a great potential to become clinical dugs since they have potent activity and high selectivity, besides, their non-receptor action modes are not easy to invoke resistance. However, there are also disadvantages as, just like AMPs, most anticancer peptides are sensitive to proteolytic cleavage, and their production is not cost-effective. Accordingly, combination of ACPs and present anticancer agents and therapies should go a considerable way to improve the cure rate of cancers.

1.6 Protease inhibitors

1.6.1 Protease and protease inhibitors

Proteases are essential enzymes involved in many physiological reactions (e.g. food protein digestion, the complement system and apoptosis pathways) and they can be found in animals, plants, bacteria and even viruses (López-Otín, Bond 2008). These enzymes

function in catalysing proteolysis, which is necessary for protein production, degradation and many cellular processes. Inside organisms, endogenous inhibitors interact with proteases to keep a dynamic balance of protease enzymatic function, and in this way, the regulation of proteolysis is achieved. Once abnormal proteolytic activity occurs, it can result in digestive system disorders, infectious disease, inflammatory disease and many other health issues (Drag, Salvesen 2010). Accordingly, regulation of abnormal proteolysis represents a potential target of therapeutic interventions, and the practical way is to replace endogenous inhibitors or dose overproducing proteases with specific inhibitors (Nixon, Wood 2006).

Protease inhibitors (PIs) are pervasive molecules in organisms, and they are commonly involved in potential drug design for the treatment of cancer, hypertension, inflammation, diabetes and protozoan infections (McKerrow et al. 2008). In 2004, based on similarities detectable at the level of amino acid sequence, Neil D. Rawlings and his colleagues (Rawlings et al. 2004) identified 48 protease inhibitor families, and according to the MEROPS database, there are now 99 families of inhibitors (https://www.ebi.ac.uk/merops/cgi-bin/family_index?type=I). While in many studies, researchers like to classify protease inhibitors through their catalytic types, thus, inhibitors can be classified as serine-, cysteine-, aspartic and metallopeptidase inhibitors (Krowarsch et al. 2003).

1.6.2 Amphibian skin-derived trypsin inhibitors

Skin secretions from amphibians are an abundant source of multi-functional bioactive peptides, and these peptides are expected to possess great pharmaceutical potential like protease inhibitors, neural stimulation, immunomodulatory, antimicrobial, anticancer, etc. (Bahar, Ren 2013). By their different structure domains, protease inhibitors from amphibian secretions can be identified as Kazal-, Bowman-Birk and Kunitz-type

(Proaño-Bolaños, Li et al.2017). Kazal-type inhibitors have been isolated from phyllomedusine frogs (Li, Wang et al.2012), the Splendid leaf frog (Proaño-Bolaños, Li et al.2017), Bowman-Birk inhibitors from *Odorrana* frogs (M. Wang, L. Wang et al.2012), and Kunitz-type inhibitors from the in Tomato frog (Conlon, Kim. 2000.) and ranid frogs (Chen, Wang et al. 2016). A simple comparison of these three protease inhibitors is shown in Table 1.2.

Table 1.2 Comparison of family, structure and inhibition of peptidase of Kunitz-, Kazal- and Bowman-birk inhibitors.

Protease inhibitors	***MEROPS inhibitor family***	***Structure***	***Inhibition of peptidase family***	***Examples***
Kazal	I1, clan IA	a large quantity of extended chain, two short alpha-helices and a 3-stranded anti-parallel beta sheet, contain 1-7 Kazal repeats	serine peptidases of the S1 family	thrombin inhibitor from *Rhodnius prolixus (Friedrich et al. 1993)*
Kunitz	I2, clan IB	A disulfide rich α+β fold, about 50 to 60 AAs, α/β proteins with few secondary structures, the fold is	serine peptidases of the S1 family,	aprotinin (bovine pancreatic trypsin inhibitor, BPTI)

		constrained by three disulphide bonds		(Kunitz, Northrop 1936)
Bowman-Birk	I12, clan IF	A duplicated structure and generally possess two distinct inhibitory sites	serine peptidases of the S1 family, but also inhibit S3 peptidases	trypsin inhibitor from *Hordeum vulgare (Odani et al. 1983)*

1.6.3 Kunitz-inhibitors

Serine proteases and their cognate inhibitors play fundamental roles in cellular biology, and inhibitors of serine proteases are the most studied and are classified into several families based on sequence homology, the location of the reactive site, structural characteristics and mechanism of action (L. Yang et al. 2017). Kunitz-type inhibitors are constituted by 50 to 60 amino acid residues and stabilized by a disulphide bond rich structure. Bovine pancreatic trypsin inhibitor (BPTI) is the classic member of this family of proteins and was the first Kunitz-type protease inhibitor described, it has relatively broad specificity inhibiting trypsin as well as chymotrypsin and elastase-like serine (pro) enzymes (Smith et al. 2016). Kunitz inhibitors are thus known as BPTI-like proteins and belong to the I2 family of peptidase inhibitors (Ranasinghe, McManus 2013).

Kunitz-inhibitors inhibit peptidases through non-covalent interactions like the enzyme–substrate Michaelis complex (Smith et al. 2016). Without any changes of confirmation, the inhibitors block the active site of the serine protease, and an antiparallel β-sheet is formed between the enzyme and its inhibitor. The so-called protease-binding loop refers to an extended, solvent-exposed and convex fragment that is in charge of protease

inhibitory activity, and the location of the reactive site (P1-P'1 peptide bond) is in the most exposed part of this loop. Crossing from the P3 to P'3 position, the protease-binding loop is highly complementary to the concave enzyme active site. The P1 position is the primary decisive factor of the inhibition selectivity, for examples, lysine and arginine always occupy the P1 of trypsin inhibitors. Apart from the P1 position, the P'1 position also plays a vital role in protease inhibitory activities. Take BPTI-like inhibitors as an example, their P'1 site is mostly occupied by alanine and rarely by glycine, and this alanine/glycine has been reported to be the indispensable factor of protease inhibition (Ranasinghe, McManus 2013).

Kunitz domains are stable as stand-alone peptides, able to recognise specific protein structures and work as competitive protease inhibitors, and these properties have led to attempts at developing biopharmaceutical drugs from Kunitz domains (Ladner, Ley 2006). The mechanisms for these beneficial effects include inhibition of kallikrein, preservation of platelet (PLT) membranes, inhibition of neutrophil activation, and a reduction in fibrinolysis (Smith et al. 2016). Several randomised controlled trials have shown that aprotinin decreases perioperative bleeding and the need for allogeneic blood transfusions (Chivasso et al. 2018). Another example is ecallantide (trade name Kalbitor), an inhibitor of the protein kallikrein and a 60-amino acid polypeptide which was developed from a Kunitz domain through phage display to mimic antibodies inhibiting kallikrein. It is a drug used for the treatment of hereditary angioedema (HAE) and in the prevention of blood loss in cardiothoracic surgery (Lehmann 2008).

1.7 Aims and objectives of this thesis

1. Bioactive peptides in frog skin secretions

To identify novel bioactive peptides from the skin secretions of three different frogs: *Odorrana hejiangensis*, *Phyllomedusa coelestis* and *Odorrana versabilis*. Numbers of multifunctional peptides were also isolated from both *Odorrana* and *Phyllomedusa* frog species (Bian et al. 2018, Mechlia et al. 2018, J. Liu et al. 2012).

2. Identification and characterisation of isolated peptides

Molecular cloning will be applied to obtain the cDNA encoding the biosynthetic precursor of putative novel peptides from skin secretion, with the combination of high-performance liquid chromatography analysis and tandem mass spectrometry technology the peptide sequences can be confirmed.

3. Peptide synthesis

To obtain the synthetic replicates of the naturally-occurring peptides, solid phase peptide synthesis will be employed and by using reverse-phase high-performance liquid chromatography, synthetic peptides can be purified.

4. Functional assays

To confirm the bioactivities of obtained peptides, the synthetic replicates will be subjected to a series of functional assays, such as antimicrobial assays, haemolytic assays, anti-cancer assays, membrane permeability assays and also trypsin inhibitory assays.

Chapter 2

General Methods

2.1 Molecular cloning

2.1.1 Specimen biodata and secretion harvesting

Based on the principle of animal conservation, we collected the frog skin secretion from the dorsal skin by mild transdermal electrical stimulation, which is an available and effective method of catalysing excretion of skin peptides without any invasion and sacrifice. The skins were used only in the situation of ageing or unnatural death.

Adult specimens of *Odorrana hejiangensis*, *Phyllomedusa coelestis* and *Odorrana versabilis* were captured and maintained in a purpose-designed amphibian facility at 20-25℃ under a 12h-light/12h-dark cycle and were fed multivitamin-loaded crickets three times per week for at least four weeks before secretion harvesting.

The dorsal skin surface was stimulated by gentle transdermal electrical stimulation (6V DC;4ms pulse-width; 50 Hz) through platinum electrodes for two periods of 20s. The resultant viscous white secretion was washed from the skin with deionised water, snap-frozen in liquid nitrogen finally lyophilised and stored a -20 ℃ before analysis. All procedures were subjected to ethical approval and carried out under appropriate UK animal research personal and project licenses.

2.1.2 mRNA Isolation

The Dynabeads® mRNA DIRECT™ Kit (Invitrogen, Lithuania) was used to isolate pure mRNA directly from crude samples. Dynabeads mRNA DIRECT™ Kit includes Dynabeads Oligo $(dT)_{25}$ and lysis/binding, washing, elution, regeneration and storage buffers. The outline for isolating mRNA using Dynabeads Oligo $(dT)_{25}$ is shown in **Figure 2.1**.

Five mg of skin secretion was weighed into a tube and centrifuged briefly by an Eppendorf Centrifuge 5424 (Eppendorf, Germany). One millilitre of lysis/binding buffer was added and the powder was dissolved by vortexing for 3 minutes then the tube was kept on ice for 1 minute. This procedure was repeated 5 times. After entirely dissolving, the sample solution was centrifuged at 18,000 × g for 5 ~10 minutes. Two hundred and fifty microliters of beads were transferred into a tube, and these beads were shaking uniformly prior to transfer. The tube was put in the magnetic rack, and then the supernatant was removed. Two hundred and fifty microliter of lysis/binding buffer was added to wash the beads, and the supernatant was abandoned after washing.

In the mixing step, the sample supernatant was removed into the beads directly, and the mixture was shaken gently for 3 minutes then the tube was kept on ice for 2 minutes. This procedure was repeated four times. After 20 minutes, the supernatant was discarded, and the beads were remained. Five hundred microliter of washing buffer A was added to wash the beads/mRNA complex three times. After that, 500 microliter of washing buffer B was added to wash the beads/mRNA complex 2 times. Followed washing was the elution step. Eighteen microliters of Tris-HCl was added into the complex tube then the tube was put in a heating block (80℃) for 2 minutes. At the last stage of isolation, the tube was put into the magnetic rack and the supernatant was removed and placed on ice immediately.

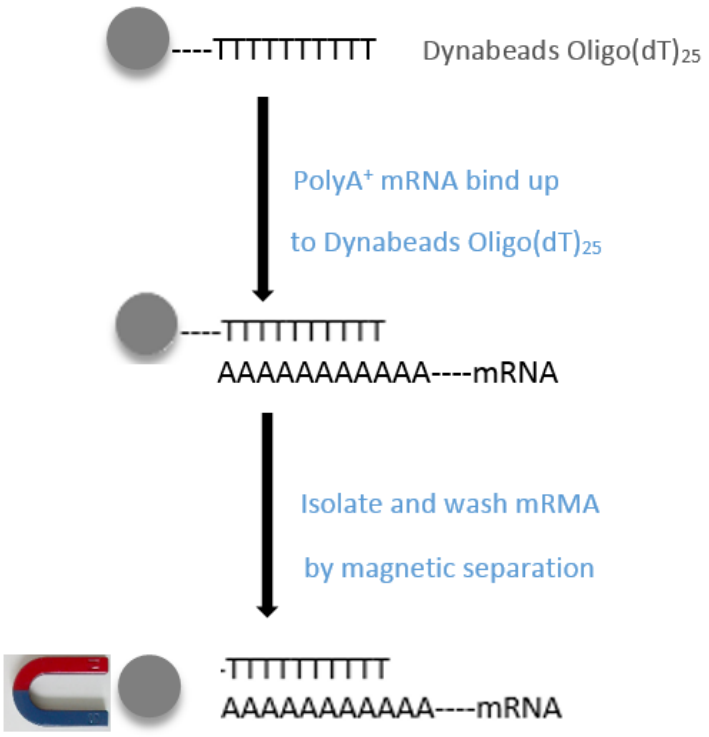

Figure 2.1 Outline for isolating poly-A mRNA using Dynabeads Oligo $(dT)_{25}$.

2.1.3 cDNA Library Construction

Preparation of sample: The BD SMART RACE Kit (BD Bioscience Clontech, UK) was used here for the construction of two separate cDNA libraries: 5'-RACE-Ready cDNA library and 3'-RACE-Ready cDNA library. The cDNA for 5'-RACE was synthesised using the 5'-RACE CDS Primer (5'-CDS) and the BD SMART II A oligo as described in Table 2.1. 5'-CDS has two degenerate nucleotide positions at the 3' end, which can position the primer at the start of the poly A^+ tail. The 3'-RACE cDNA was synthesised using a traditional reverse transcription procedure, but with a special oligo(dT) primer. This 3'-RACE CDS Primer A (3'-CDS) primer includes the lock-docking nucleotide positions as in the 5'-CDS primer and also has a portion of the BD SMART sequence at its 5' end.

5 ´- tubes and 3 ´- tubes were prepared as in Table 2.1 below, and all the tubes were incubated in the heating block at 70℃ for 2 minutes then put on ice for 2 minutes.

Table 2.1 Components of 5 ´- tubes and 3 ´- tubes.

*BD SMART II™ A Oligonucleotide:

5'-AAGCAGTGGTATCAACGCAGAGTACGCGGG-3'

3'-RACE CDS Primer A (3'-CDS):

5'-AAGCAGTGGTATCAACGCAGAGTAC $(T)_{30}$VN-3'

(N = A, C, G, or T; V = A, G, or C)

5'-RACE CDS Primer (5'-CDS):5'–$(T)_{25}$VN–3' (N = A, C, G, or T; V = A, G, or C)

5 ´- tubes	3 ´- tubes
3μL sample	4μL sample
1μL 5´- CDS primer (10 μM)	1μL 3´- CDS primer (10 μM)
1μL BD SMART Oligo (10 μM)	

Preparation of master mix: The master mix was prepared with 2μL first-strand buffer, 1μL DTT (20 mM) and 1μL dNTP (10 nM), and then the mixture was centrifuged briefly. 4μL master mix was added to each 5 ´- and 3 ´- tube (9μL in total each tube), and reagents were mixed by pipetting. After that, 1μL reverse transcriptase (100 Uint/ μl) was added to each tube (10μL in total), then the tubes were centrifuged briefly (Table 2.2).

Table 2.2 The components of cDNA library master mix.

Reagent	**volume**

5×First-Strand Buffer	2 µl
DTT (20 mM)	1 µl
dNTP Mix (10 nM)	1 µl
BD RTase (100 Uint/ µl)	1 µl

Extension: sample tubes were put into the Labnet Thermocycler, with the temperature set to 42℃, for 1.5 hours. After that, the tubes were centrifuged briefly and then 50µL PCR water was added into each tube. All the tubes were centrifuged briefly to mix the mixture and remove bubbles, then tubes were then put into Labnet Thermocycler, at 72℃ for 7 minutes. After extension, the products were stored at -20℃. Figure 2.2 and Figure 2.3 show the mechanism of 5'- and 3'-cDNA library construction respectively.

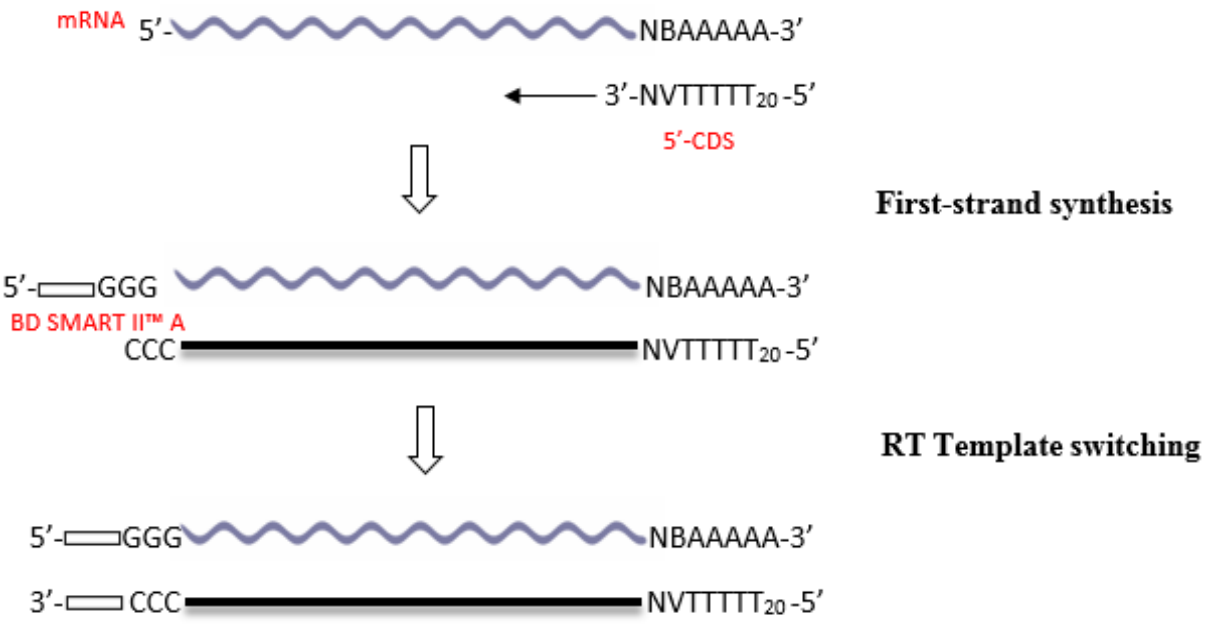

Figure 2.2 Mechanism of 5'-cDNA library construction. First-strand synthesis is primed by 5'-RACE CDS Primer. After reverse transcriptase reaches the end of the mRNA template and adds several dC residues. The BD SMART II A Oligo-nucleotide anneals to the tail of the cDNA and serves as an extended template.

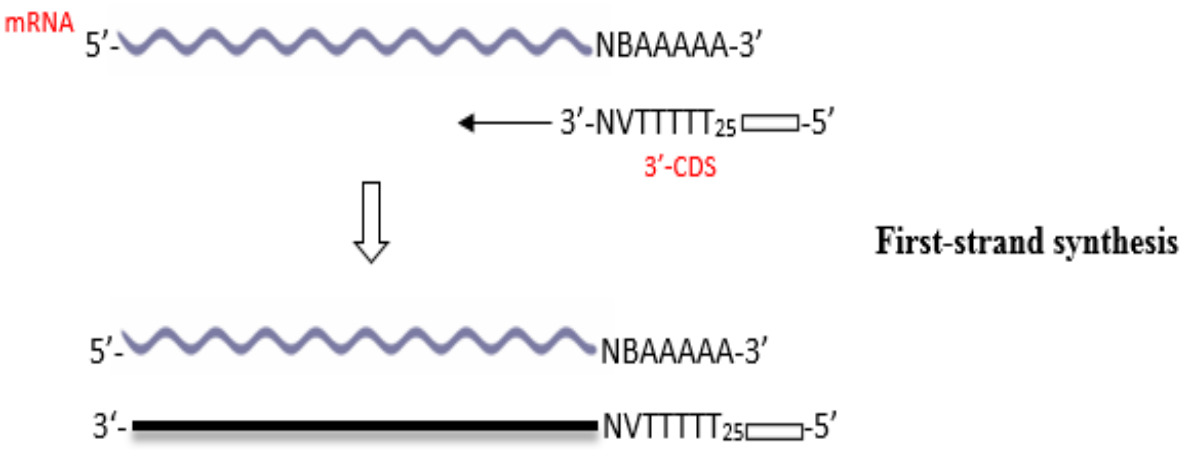

Figure 2.3 Mechanism of 3'-cDNA library construction. (block = BD SMART II A sequence)

2.1.4. 3 ´- RACE PCR

The BD SMART™ RACE cDNA Amplification Kit (BD Bioscience Clontech, UK) was used for performing both 5'- and 3'-rapid amplification of cDNA ends (RACE). By incorporating the BD SMART sequence into both the 3'-RACE-Ready cDNA libraries, 3'-RACE PCR reactions can be primed using the Nested Universal Primer A (NUP), which recognises the BD SMART sequence, in conjunction with distinct gene-specific primers.

The master mix was prepared as in Table 2.3 below. Zero point five microliter of degenerate sense primer, which was designed to a highly conserved domain of the 5'-untranslated region of previously characterised antimicrobial peptide cDNAs from *Rana* species, was added to the master mix tube and centrifuged briefly. Then, the complex was divided equally into two tubes, then the same amount of 3 ´- cDNA library and PCR water (control) were separately added into different tubes. The complex of each tube was divided equally into another two tubes, then PCR was run with different annealing temperatures. The PCR cycling procedure was as follows. Initial denaturation step: 60

seconds at 94 ℃; 35cycles: denaturation 30 seconds at 94 ℃, primer annealing for 30 seconds at 53 ℃; extension for 180 seconds at 72 ℃. Mechanism of the 3'-RACE reactions was showed in Figure 2.4.

Table 2.3 Master Mix for 3'-RACE PCR.

*Nested Universal Primer A (NUP):5'–AAGCAGTGGTATCAACGCAGAGT–3'

PCR H_2O	2.1μL
10×Advantage Buffer	1μL
NUP*(20 μM)	1μL
dNTP (10 mM)	0.2μL
50× Advantage 2 Polymerase Mix	0.2μL
Master Mix	4.5μL (each tube)

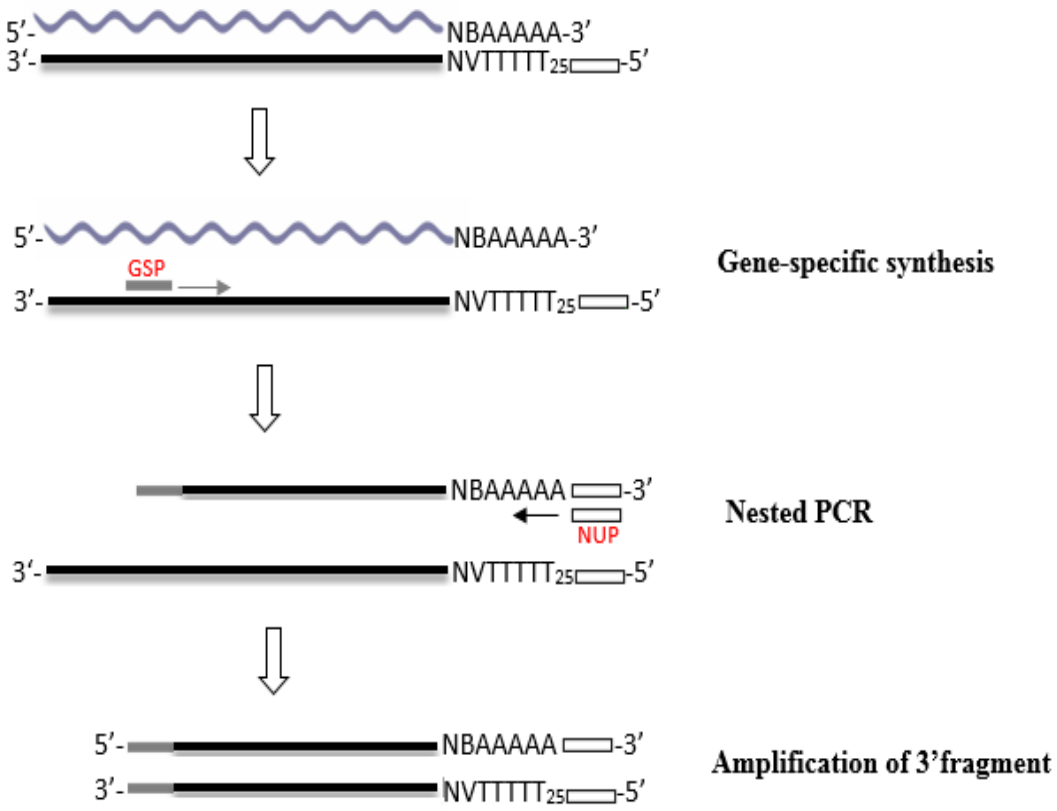

Figure 2.4 Mechanism of the 3'-RACE reactions. (block means BD SMART II A sequence)

2.1.5 Gel Analysis

To analyse RACE PCR products, 0.45g of Agarose (Invitrogen, UK) was weighed into a flask, then 35mL fresh prepared 1 × Tris/Borate/EDTA (TBE) buffer (Invitrogen, UK) was added into the flask. The mixture was heated in a microwave to dissolve the agarose and cooled down to room temperature, then 2.5μL of 10 mg/ml Ethidium Bromide (EB) (Sigma-Aldrich, USA) was added, and the mixture was gently shaken to mix thoroughly. After that, the mixture was poured into the gel-electrophoresis tank. It took around 45 minutes for the gel to mould, then both gel-forming gate and 8-well comb were taken away, and sufficient running buffer (1 × TBE Buffer) was filled to submerge the solid gel.

Before running gel analysis, 0.5μL loading dye (Promega, USA) and 1.5μL PCR sample were mixed and added into each well of the gel, 2.0μL of 100bp DNA ladder (BioLabs, UK) was added into the first well to serve as a marker for PCR products size measurement. After that, the gel electrophoresis was run with electrodes charged at 90v, for 30 minutes, followed by band detection and photographic image recording under the UV trans-illuminator BioDoc-It® Imaging System (NVP, Cambridge, UK).

2.1.6 PCR Products Purification

An E.Z.N.A.® Cycle Prue Kit (Omega Bio-Tek, USA) was employed to purify PCR product, in which DNA was bound to silica-based filter membraned during washing steps and eluted for collection.

One hundred microliter of CP Buffer was added into the PCR products tube, and the compounds were mixed thoroughly by pipetting. The mixture was transferred into the HiBind® DNA mini column and was centrifuged at 13000 ×g in an Eppendorf Centrifuge 5424 (Eppendorf, Germany) for 1 minute, and then the flow-through was discarded.

To wash the products through the cartridge, 700μL of DNA Washing Buffer was added into the column, and the column was centrifuged at 13000 ×g for 1minute to discard the flow-through. After that, 500μL of DNA Washing Buffer was added into the column, and then the centrifugation step was repeated. Followed the washing steps, the column was again centrifuged at 16000 ×g for 2 minutes.

For DNA elution, the cartridge of the HiBind® DNA mini column was placed in a 1.5mL tube, 30μL PCR water was directly added to the centre of the cartridge, and then the tube was incubated at room temperature for 2 minutes. After this, the column was centrifuged at 16000 ×g for 2 minutes to collect the elution, then the cartridge was discarded. In the

end, the sample concentrated for 1.5 hours in a concentrator (Eppendorf, UK) and the sample tube was sealed with parafilm and stored at -20℃.

2.1.7 Cloning

The pGEM ® -T Easy Vector System (Promege, USA) is used for the cloning of PCR products. The DNA products with adenine (A) at both ends of the strand could bind to and insert into the site of the pGEM®-T Easy Vector with thymine (T) via A-T base pairing. The system contains pGEM ® -T Easy Vector which contains multiple restriction sites within the multiple cloning regions., a 2X Rapid Ligation Buffer for ligation of PCR products and T4 DNA Ligase promoters flanking a multiple cloning regions.

2.1.7.1 Ligation:

Five microliter of PCR water were added into the tube to resuspend purified products, and the mixture was mixed thoroughly using a vortex for 30 seconds. The resuspended sample, pGEM ® -T Easy Vector and T4 DNA Ligase were briefly centrifuged before use, and the 2X Rapid Ligation Buffer was mixed vigorously by vortexing before each use. Ligation reactions were set up as described in Table 2.4 below. The reactions were mixed by pipetting and incubated for 1 hour at room temperature. Then the reactions were incubated overnight at 4℃.

Table 2.4 Master mix for ligation.

Reagents	Volume
2X Rapid Ligation Buffer	2.5µL
pGEM ® -T Easy Vector (50ng/ µl)	0.5µL
Sample	1.5µL

T4 DNA Ligase (3 Unit/ µl)	0.5µL
Final Volume	5µL

2.1.7.2 Transformation

For the preparation of LB Agar, 3.2g LB Agar was dissolved in 100mL double deionised water, the solution was then autoclaved. After that, 275µL ampicillin was added, and the solution was mixed thoroughly by shaking. Twelve millilitres of the mixed solution were pipetted into each Petri dish and spread uniformly. These plates were placed upside down and stored at 4℃ overnight.

To prepare the sample, 50µL of -80℃ stored JM109 High Efficiency Competent *E. coli* cells (>108 CFU/µg) (Promega, USA) were placed on ice and added in one tube together with 2.5µL ligation products, and the mixture tube was then kept on ice for 20 minutes. The reactions were incubated at 42℃ for 47 seconds, then immediately cooled on ice for 2 minutes. This was a crucial step for DNA recombination. After cooling down, 950µL of S.O.C medium (Invitrogen, USA) were added into the reaction tube and then the reactions were incubated in the shaking incubator at 37℃ for 2.5 hours.

During the incubation period, the plates for transformation were prepared. One hundred microliter of isopropyl β-D-1-thiogalactopyranoside (IPTG) (0.1 M) (Promega, USA) was placed on each previously prepared plate, and 20µL 5-bromo-4-chloro-3-indolyl-β-D-galactopyranoside (X-Gal) (50mg/ml) (Promega, USA) was then spread on the plates. These plates were placed upside down and incubated at 37℃ for 20~30 minutes. Followed that was the transformation step: 110µL of the transformed ready sample was spread evenly in each plate, then those plates were placed upside down in the incubator at 37℃ for 14~15 hours.

2.1.7.3 White and Blue Colony Screening

Plates for white and blue colony screening were prepared as the transformation step: one hundred microliter of isopropyl β-D-1-thiogalactopyranoside (IPTG) (0.1 M) (Promega, USA) was spread on each previously prepared LB plate, and 20μL 5-bromo-4-chloro-3-indolyl-β-D-galactopyranoside (X-Gal) (50mg/ml) (Promega, USA) was then spread on the plates. These plates were placed upside down and incubated at 37℃ for 20~30 minutes.

The back side of each newly prepared Petri dish was divided into 18 areas by drawing grids (Figure 2.5), and each area was numbered. The rounded white colonies that contained recombinant plasmid DNA were circled on the back side of each Petri dish from the transformation step. An inoculation loop was employed to remove circled colonies by drawing the continuous line resembling 'Z' as showed in Figure 2.5, in which every colony corresponded to one area of the newly prepared plate, and the loop was sterilised by a Bunsen burner each time after removing one colony. After screening had finished, these plates were placed upside down in the incubator at 37℃ for 14~15 hours for further selection.

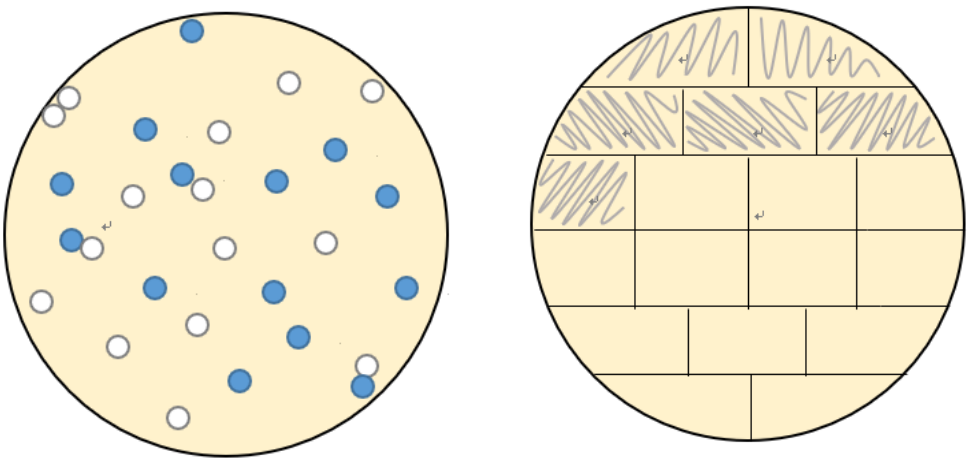

Figure 2.5 Examples of white and blue ready plate and the selected colonies plate.

2.1.7.4 Isolation of Recombinant Plasmid DNA

After incubation, twenty microliter of PCR water were added into each PCR tube, and the desired pure white colonies were removed from the plates into PCR tubes, a vortex was used to suspend the recombinant DNA for 10~15 seconds. After the suspension, these tubes were incubated in a heating block at 100℃ for 5 minutes and then immediately transformed on ice for 5 minutes. To the end, the mixture was mixed by vortexing for 20~30 seconds and then centrifuged at 16873×g for 5 minutes, and the supernatant was retained and stored at -20℃.

2.1.7.5 Cloning PCR

The master mix for cloning PCR was prepared as in Table 2.5 below. The master mix was mixed by vortexing, and 2.5μL of the DNA supernatant was added. The reactions were mixed by pipetting, and reaction tubes were briefly centrifuged to eliminate bubbles, in the end, PCR reactions were carried out as shown in Table 2.6.

Table 2.5 The components of master mix for cloning PCR.

Reagents	**Volume**
PCR H_2O	31.25μL
5xCloning Buffer	10μL
dNTP (10 mM)	1μL
M13 Forward Primer (20 μM)	2.5μL
M13 Reverse Primer (20 μM)	2.5μL
go/my Taq Polymerase (5 Unit/μl)	0.25μL
Final volume	47.5μL

Table 2.6 The cycles of Cloning PCR

Number of cycles	Procedure	Temperature	Time
1 cycle	Initial denaturation	94 ℃	1 min
31 cycles	Denaturation	94 ℃	30 s
	Annealing	55 ℃	30 s
	Extension	72 ℃	3 min
1 cycle	Final extension	72 ℃	3 min
1 cycle	Preservation	4 ℃	7 min

2.1.8 Gel Analysis

The gel analysis was performed in the same way as in section 2.1.5. However, in this analysis loading dye was no longer required: To analyse RACE PCR products, 0.45g of Agarose (Invitrogen, UK) was weighed in a flask, then 35mL fresh prepared 1× Tris/Borate/EDTA (TBE) buffer (Invitrogen, UK) was added into the flask. The mixture was heated in a microwave to dissolve the agarose and cooled down to room temperature, then 2.5μL of 10 mg/ml Ethidium Bromide (EB) (Sigma-Aldrich, USA) was added, and the mixture was gently shaken to mix thoroughly. After that, the mixture was poured into the gel-electrophoresis tank. It took around 45 minutes for the gel to be moulded, then both gel-forming gate and 8-well comb were taken away, and sufficient running buffer (1×TBE Buffer) was filled to submerge the solid gel.

Before running gel analysis, 1.5μL PCR sample was added into each well of the gel, 2.0μL of 100bp DNA ladder (BioLabs, UK) was added into the first well to serve as a marker for PCR products size measurement. After that, the gel electrophoresis was run

with electrodes charged at 90v for 30 minutes, followed by band detection and photographic image recording under the UV trans-illuminator BioDoc-It® Imaging System (NVP, Cambridge, UK).

2.1.9 Selected PCR Products Purification

An E.Z.N.A.® Cycle Prue Kit (Omega Bio-Tek, USA) was employed to purify PCR products, in which DNA was bound to a silica-based filter membrane during washing steps and eluted for collection.

One hundred microliter of CP Buffer was added into the PCR products tube, and the compounds were mixed thoroughly by pipetting. The mixture was transferred into the HiBind® DNA mini column and was centrifuged at 13000 ×g in an Eppendorf Centrifuge 5424 (Eppendorf, Germany) for 1 minute, and then the flow-through was discarded.

To wash the products through the cartridge, 700μL of DNA Washing Buffer was added into the column, and the column was centrifuged at 13000 ×g for 1minute to discard the flow-through. After that, 500μL of DNA Washing Buffer was added into the column, and then the centrifugation step was repeated. Followed the washing steps, the column was again centrifuged at 16000 ×g for 2 minutes.

For DNA elution, the cartridge of the HiBind® DNA mini column was placed in a 1.5mL tube, 30μL PCR water was directly added to the centre of the cartridge, and then the tube was incubated at room temperature for 2 minutes. After this, the column was centrifuged at 16000 ×g for 2 minutes to collect the elution, then the cartridge was discarded. In the end, the sample concentrated for 1.5 hours in a concentrator (Eppendorf, UK) and the sample tube was sealed with parafilm and stored at -20℃.

2.1.10 Sequencing Reaction

A BigDye® Terminator v3.1 Cycle Sequencing Kit (Applied Biosystems, USA) was applied in this step, in which the sequence was detected by fluorescence during DNA extension and termination processes.

The master mix for the sequencing reaction was prepared as in Table 2.7 below. Sequencing Reaction: 18.4μL master mix and 1.85μL purification products were added into a PCR tube and the reactions were mixed by pipetting. The reaction tube was briefly centrifuged to eliminate bubbles, then the PCR cycles (Table 2.8) were employed via the Labnet Thermocycler.

Table 2.7 The components of master Mix for the sequencing reaction.

Reagents	Volume
PCR H2O	12.4μL
5xSequencing Reaction Buffer	3.5μL
2.5× Ready Mix	2.8μL
M13F	1.2μL
Final volume	19.9μL

Table 2.8 The cycles of Sequencing PCR

Number of cycles	Procedure	Temperature	Time
1 cycle	Initial denaturation	96 ℃	1 min
	Denaturation	96 ℃	20 s
30 cycles	Annealing	55 ℃	10 s
	Extension	60 ℃	4 min

1 cycle	Preservation	4 ℃	7 min

2.1.11 Extension Products Purification

At first, 72μL 95% ethanol (Sigma-Aldrich, USA) was added to each tube of the extension products, and sample solution was mixed by pipetting. Ten microliter of deionised water were added in a 1.5mL tube, and the mixed sample was transferred into the tube, the reactions were mixed by vortexing for 10~20 seconds. After that, the reactions were incubated at room temperature for 20 minutes, then centrifuged at 16873×g for 20 minutes in an Eppendorf Centrifuge 5424 (Eppendorf, Germany). The supernatant was discarded carefully and immediately. In a similar operation, 260μL of 70% ethanol was added into the tube, and the reactions were mixed by vortexing for 20~30 seconds. After centrifugation for 10 min, the supernatant was discarded.

To volatilise the ethanol, tubes were uncapped and heated at 95℃ for 1 minute and then incubated at room temperature for 1 minute. A further step involved the use of the concentrator (Eppendorf, UK), in which samples were vacuum-dried for 1 hour. Finally, all tubes were sealed with parafilm and stored at room temperature.

2.1.12 Sequencing

Before sequencing, the tubes containing purified products were uncapped and heated at 95℃ for 1 minute and then incubated at room temperature for another 1 minute. After 10μL of highly-deionised formamide (HiDi) was added into the tube, the reactions were vortexed for 37 seconds and then briefly centrifuged. In the next step, these products were subsequently heated at 95℃ for 4.5 minutes and then kept on ice for 3.5 minutes. Finally, 10μL of each product were added into one corresponding well of a 96-well Thermal Cycler (ThermoFisher Scientific, USA) without any air bubbles, and the sample plate was sequenced by an ABI 3730 automated sequencer (Applied Biosystems, USA).

2.2 Peptide Identification and Structural Analysis

2.2.1 RP-HPLC analysis

The skin secretion of the frog was extracted with a mixture of ethanol (Sigma-Aldrich, USA) and 0.7 M hydrogen chloride (HCl) (Sigma-Aldrich, USA) in a ratio of 3:1. Then the extract was air-dried and dissolved in 0.3 ml of 0.05/99.5 (v/v) trifluoroacetic acid (TFA) (Sigma-Aldrich, USA) /water. After this, the sample solution was centrifuged to clarify of micro-particulates, and the supernatant was injected and pumped directly onto an HPLC column (Jupiter C-5, 5 μm particle, 300 Å pore, 250 mm × 10 mm, Phenomenex, UK) for fractionation. A reverse phase HPLC system (Amersham Biosciences) was applied with the gradient formed from 0.05/99.5 (v/v) TFA/water as buffer A to 0.05/29.95/70.0 (v/v/v) TFA/water/acetonitrile as buffer B in 240 minutes for peptides elution, and fractions were collected automatically at 1 minute intervals. The effluent was constantly monitored by a UV detector set at 214 nm (λ).

2.2.2 Fraction analysis by MALDI-TOF mass spectrometry

In this study, CHCA was used as the matrix for MALDI-TOF MS (Matrix-assisted Laser Desorption Ionization time-of-flight mass spectrometry) experiments. There were two ways of preparation of matrix-solution, one was 500 μL ACN in 500 μL water then 0.5 μL TFA was added (50%ACN in 0.05%TFA solution), and another was 700 μL ACN in 300 μL water then 0.2 μL TFA was added. For sample loading, 2 μL of the sample (peptide solution or reverse HPLC fraction) was loaded and dried on the 96-well-plate, 1 μL CHCA solution was then dropped to cover the sample spot. After the mixture dried, the plate was subjected to Voyager DE Biospectrometry (Voyager DE, PerSeptive Biosystems, Framingham, MA, USA) for monitoring the mass and purity of peptides.

2.2.3 Sequencing of peptides by LCQ ESI quadrupole ion-trap mass spectrometry

The skin secretion was stored in solution form and desalted. In the beginning, the liquid sample was introduced from the HPLC system. Then it entered the ESI needle, and 4.50kV spray voltage was applied (with the flow rate of sheath gas and aux gas was 20arb and 5arb respectively). The sample was ionised and sprayed into very fine droplets. After this, the ion beam was focused and transferred from the high-pressure ion source to the mass analyser (a quadrupole ion trap which could store fragment and other selected ions) by ion guides (usually contained a mixture of square quadrupoles and round octupoles depending on the version of the instrument). During this process, the kinetic energy of transmitted ions was reduced, and interfering ions were excluded. Finally, ions passed through the detector for further analysis. The data for MS/MS fragmentation of peptides were obtained and then subjected to a molecular cloning peptide database for confirmation of its identification and structural characterisation.

2.2.4 Bioinformatic analysis of isolated peptides

The physicochemical properties of the peptides, such as the number of amino acids, molecular weight, theoretical pI, net charge and grand average of hydropathicity, were computed by an online peptide analysis programme, ExPASy-ProtParam tool https://web.expasy.org/protparam/. Primary sequence similarities comparison were carried out by the online protein comparison software, Basic Local Alignment Search Tool (BLAST)-NCBI-NIH https://blast.ncbi.nlm.nih.gov/Blast.cgi. While the helical wheel projections of peptides were obtained theough the online tool, Helical Wheel Projections - RZ Lab

http://rzlab.ucr.edu/scripts/wheel/wheel.cgi?sequence=ABCDEFGHIJLKMNOP&submit=Submit.

2.3 Solid-Phase Peptide Synthesis

Solid-phase peptide synthesis (SPPS), which is the standard method for synthesizing peptides and proteins in the lab, serves for the synthesis of natural peptides that are difficult to express in bacteria, peptide/protein backbone modification, the integration of unnatural amino acids, as well as the synthesis of D-proteins which consist of D-amino acids.

In this study, all the peptides were synthesised automatically via the solid phase peptide synthesis, and a standard 9-fluorenylmethoxycarbonyl (Fmoc) chemistry on an automated solid phase 2-Channel peptide synthesiser (TRIBUTE®, Gyros Protein Technologies).

2.3.1 Preparation and synthesis

The dry amino acids mixed with2-(1H-benzotriazol-1-yl)-1,1,3,3-tetramethyluronium hexafluorophosphate (HBTU) (379.3 g/mol, 455.16g/1.2mol, Novabiochem®) were weighed and transferred into the acetone-cleaned amino acid vials, then the vials were sealed with caps and stepas (4 times each amino acid should be weight to synthesize 0.3 mmol peptide, thus 1.2 mmol amino acid in the sequence). After that, 0.3mmol resin (*) was weighed and added to the reaction vessel. Two kinds of resins were utilized in this section, Rink Amide MBHA resin (0.65mmol/g, Novabiochem®) for peptides ended with C-terminal amidation, while Wang resin (Sigma-Aldrich) for normal peptides with a carboxyl group at C-terminus.

*resin (g) = (peptide 0.3mmol)/ (loading Substitution mmol/g)

The peptide was synthesised by use of a Tribute Peptide Synthesizer using Fmoc SPPS from C-terminal to N-terminal. First and foremost, the inline solvent filters and the source of Nitrogen were checked, the reagent bottles were vented, then enough reagents were added for synthesis. After the reagent bottles were pressurised and primed, the reaction vessels with resin were loaded and the program was edited. Followed was the washing operations for the solvent bottles and reaction vessels. The next was peptide sequence loading step, selected a reaction vessel, start and stop position on the carousel and the coupling program for each amino acid. Finally, the Run button was pressed to start the synthesis.

Generally, the principle (Table 2.9) of solid phase peptide synthesis involved repeat cycles of deblocking, washing, coupling, washing, in addition to a final deblock step. In detail, at the beginning of the cycle, the amino acids with N-terminus protected by Fmoc were dissolved in N, N-Dimethylformamide (DMF, ⩾99%, SIGMA, D158550-2.5L), and the Fmoc groups were removed from the N-terminal amine group by 20% piperidine (99%, SIGMA,104094-1L) in DMF (v/v). After that, deprotection reagents were washed away by DMF to provide a clean environment for coupling. Then, a new protected amino acid, which was dissolved in DMF and with its carboxyl group combined with activating reagent 11% 4-Methylmorpholine (NMM, 99%, SIGMA, M56557-500ML) in 89% DMF (v/v), was then coupled with the first amino acid via a peptide bond that catalyzed by HBTU. Following was another washing step in which coupling reagents were washed away to provide a clean environment for deprotection which the start of the next cycle. This process was continued until all the amino acids were coupled on the peptide chain. At last, there was a final deprotection reaction for the N-terminal protecting group of the last amino acid, and the solvent DMF was finally washed away by Dichloromethane

(DCM, SIGMA, 32222). The synthetic peptide was then dried in a vacuum desiccator overnight.

Table 2.9 The main principle of solid phase peptide synthesis: repeat cycles of deblocking, washing, coupling, washing.

Action	Reagent
Washing	DMF
N-terminal deblocking	Piperidine/DMF(1:4)
Washing	DMF
C-terminal activation	NMM/DMF(11:89)

2.3.2 Peptide cleavage

The synthetic peptide was subjected to a cleavage reaction to remove the side chain protecting groups and the solid support. For cleavage, the washed and dried resin was weighed and placed in a 50ml round-bottomed flask. Then, the cleavage cocktail* (25ml/g) was added into the flask, and the cleavage reaction was performed with stirring at room temperature for around 4 hours. After the cleavage step, the Buchner funnel was used to filter the cleavage mixture into a 50ml round-bottomed flask, and the filtrate was concentrated by a rotary evaporator to near dryness or 3-4ml (the water bath should be kept at less than 30℃). Finally, diethyl-ether (Et2O) was added into the concentrated solution for peptide precipitation in a 50ml universal tube overnight at -20 ℃.

*cleavage cocktail: 94% Trifluoroacetic acid, 2% Thioanisole, 2% 1,2-Ethanedithiol, 2% deionized water

2.3.3 Washing and lyophilisation

Followed peptide precipitation, the tube of synthetic peptide was centrifuged at 2,500 × g for 5 min and the supernatant was discarded carefully, then, about 45mL Et2O was added into the tube. The tube was subsequently centrifuged, and the supernatant was removed. This process was repeated three times. After washing finished, Et2O was volatilized at room temperature overnight. The peptide powder was dissolved with HPLC solution A/B* and the peptide solution was then lyophilised with -55℃ Liquid Nitrogen for 65 hours.

*Solution A: 99.95% H_2O and 0.05% TFA

Solution B: 80% acetonitrile, ACN, 19.95% H_2O and 0.05% TFA

For peptide containing a cysteine residue, oxidation was required before lyophilization, and in this step, hydrogen peroxide, which was added to 2% of total volume, was added into the peptide solution.

2.4 Synthetic Peptide Purification and Identification

Peptide preparation: one milligram of lyophilised peptide powder was dissolved in 1mL of HPLC solution with the ratio of solution A and solution B as 1:1 (v/v). To make a sufficient dissolution of peptide, the solution was vortexed for about 5 mins. After that, the clear supernatant, which was also the sample, was obtained by a 5-min centrifugation at 18,000 × g for 5 min in an Eppendorf Centrifuge 5424 (Eppendorf, Germany).

Before sample injection, an HPLC column (Jupiter C18, 5μm particle, 300A pore, 250mm×10mm, Phenomenex, UK) attached to the Cecil Adept CE4200 HPLC system (Amersham Biosciences) was equilibrated in Buffer A for at least 30 min. Then the column was eluted with a linear gradient from 100% A: 0% B to 0% A: 100% B in 80

min at a flow rate of 1 ml/min with a simultaneous 214nm wavelength detection. The fractions at each peak were collected separately in tubes and utilised for identification. Finally, solution B was pumped to wash the column for 30 min.

The Voyager Biospectromery MALDI-TOF mass spectrometer (Voyager, USA) was applied to not only detect whether the target peptide was successfully synthesized by SPPS, but also confirm the purity of the peptide. Two microliter of each collected HPLC fraction were loaded and spotted separately onto the MALDI ground-steel target plate and air-dried. After that, one μl of CHCA matrix solution* (10mg/ml) was loaded onto each sample and then air dried. Followed the MALDI-TOF mass analysis of the dried complex, by comparing the mass-to-charge ratios (m/z) with the calculated molecular mass of peptide, the elution site of the pure peptide in the HPLC was confirmed.

* CHCA matrix solution: α -cyano-4-hydroxycinnamic acid (CHCA) in 20% ACN/0.1% TFA water solution (v/v)

2.5 Secondary structure analysis

A JASCO J-815 CD spectrometer (Jasco, Essex, UK) was employed to perform the analysis of peptide secondary structures. Each peptide was dissolved in 10 mM ammonium acetate and ten mM ammonium acetate with 50% TFE, respectively, to reach a concentration of 100 μM, in a 1 mm high precision quartz cell (Hellma Analytics, Essex, UK). All CD spectra were obtained at 20℃ from 250 nm to 190 nm at a scanning speed of 100 nm/min. The bandwidth was 1 nm, and the data pitch was 0.5 nm.

2.6 Antimicrobial Assays

2.6.1 Preparation

Preparation of Phosphate buffered saline (PBS): one tablet was added into 200ml ddH2O and shaken until dissolved. The solution was then autoclaved.

Peptide stock solution (concentration: 512 $\times 10^2$μM): 10mg peptide was dissolved in PBS, alternatively, for peptides that could not be dissolved in PBS, dimethylsulphoxide (DMSO) was applied.

Müller-Hinton agar (MHA) plate: 2 tubes of 10 mL MHA were dissolved for each plate at 100℃ in water bath and then cooled to 55℃. After 5min, MHA was decanted into the plastic Petri dish, distributed uniformly and dried.

2.6.2 Inoculation

Six kinds of microorganism were used: *Staphylococcus aureus (S.aureus), Escherichia coli* (*E.coli*), *Candida albicans* (*C.albicans*), *Methicillin-resistant Staphylococcus aureus (MRSA), Pseudomonas aeruginosa (P.aeruginosa) and Enterococcus faecalis (E.faecalis),* all of which had been stored in the -20℃ freezer. One bead of bacterial culture was transferred from the frozen stock into a flask of 100mL Muellar Hinton Broth (MHB) using an inoculation loop, and the flask was then placed in a shaking incubator at 37℃ overnight (16~20 hours).

2.6.3 MIC assay & viable cell counts

2.6.3.1 Subculture

Five hundred microliter of the overnight growth was transferred into the bottle of pre-warmed 20mL Muellar Hinton Broth (MHB), then the bottle was put in the shaking incubator, continuing growth until Log phase. The optical density (OD) could reflect the

metabolic activity and cell cycle phase of the bacterium, and the OD of the bacterial culture was measured by a UV spectrophotometer at λ=550nm. The OD and corresponding concentration of each organism are shown in Table 2.10.

Table 2.10 OD values and corresponding concentration of tested microorganisms.

*cfu indicates colony form unit.

Organism	OD	Concentration(cfu*/ml)
Gram+	0.23	1×10^8
Gram-	0.4	1×10^8
C.albicans	0.15	1×10^6

When the OD met the required conditions, a dilution step was implemented. 0.1mL subculture bacterial solution of both Gram-positive bacteria and Gram-negative bacteria were diluted by 19.9ml fresh MHB, while 2mL subculture solution of *C.albicans* was diluted by 18mL fresh MHB.

2.6.3.2 Minimal inhibitory concentration (MIC) assay

The peptide stock solution was double-diluted to obtain a range of concentrations of peptide (512, 256, 128, 64, 32, 16, 8, 4, 2, 1 $\times 10^2$μM), and antimicrobial assay was carried out to detect the minimum inhibitory concentration of each peptide solution on *Staphylococcus aureus (S.aureus), Escherichia coli* (*E.coli*), *Candida albicans* (*C.albicans*), *Methicillin-resistant Staphylococcus aureus (MRSA), Pseudomonas aeruginosa (P.aeruginosa) and Enterococcus faecalis (E.faecalis).* Subsequently, sample and controls were loaded into 96-well-plates as Figure 2.6 shows. After sample loading, the plate was placed on the shaker for 5~10 minutes for mixing and then incubated overnight at 37℃. The MIC detection used a Synergy HT plate reader (BioTek,

USA) at the absorbance of 550nm for each well. The bacteria cell % viability was calculated according to the formula below:

$$\text{Cell viability\%} = (OD_{Sample} - OD_{MHB}) / (OD_{Growth/DMSO} - OD_{MHB}) \times 100\%.$$

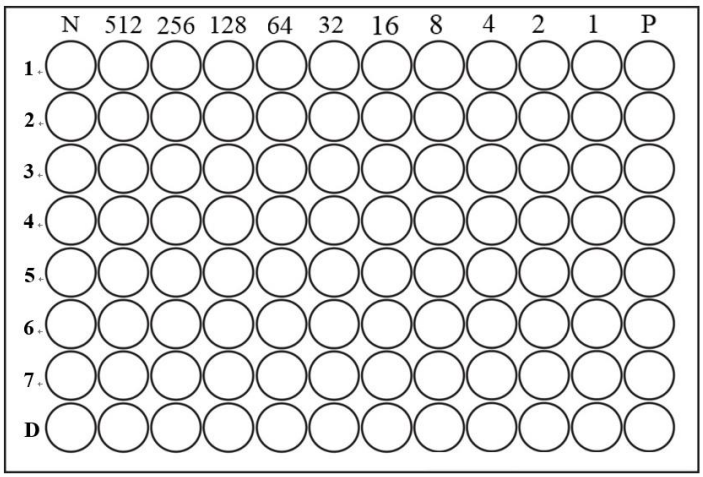

Figure 2.6 Diagram of MIC 96-well-plate for sample loading. All the samples and controls were arranged on the 96-well plate with seven replications.

Negative control (N):100 μL sterile MHB

Positive control (P):100 μL diluted bacterial subculture

Sample: 1 μL peptide solution + 99 μL diluted bacterial subculture

DMSO control (D):1 μL DMSO + 99 μL diluted bacterial subculture

Viable cell counts

Six microtubes were needed for each organism, and 900 μL PBS were added to each tube previously. One hundred microliter diluted subculture were transferred into the first tube and then ten-fold dilutions were applied to achieve a series of diluted solutions (10^1 to 10^6 times dilution). Twenty microliter of subculture from each tube were dropped onto the MHA plate, and three replications were made for each concentration. Followed air-drying, the MHA plate was incubated at 37℃ overnight. When the viable count of cells

was assessed, colony quantity in each drop was counted in a countable grid, then the original concentration* was calculated in the subculture. The calculated result was expected to at least meet the concentration of 5×10^5 cfu/ml.

* original concentration = counted number/$3\times10^n\times50$ (n=diluted times)

2.7 Bacterial Cell Membrane Permeability Assay

The membrane permeability assay was carried out using SYTOX Green Nucleic Acid Stain (Life technologies, Carlsbad, CA, USA). Bacteria were incubated in Tryptic Soy Broth (TSB) (Sigma–Aldrich, St. Louis, MO, USA) at 37 ℃ overnight, after which 200 µL of bacterial culture was inoculated into 25 mL TSB and incubated at 37 ◦C for three h to achieve the logarithmic growth phase. Then, bacterial cells were harvested by centrifugation at 1000 × g for 10 min at 4 ◦C, followed by two cell washing processes with 5% TSB in 0.85% NaCl solution.

The washed bacterial cells were suspended in 5%TSB to achieve 1×10^8 CFU/mL which was detectable at OD 590 nm = 0.7. Each well of the sample groups in a black 96 well plate (Fisher Scientific, Leicestershire, UK) contained a volume of 50 µL of bacterial suspension and 50 µL of peptide solution. Each well of the negative control group was constituted by a volume of 50 µL of bacterial suspension and 40 µL of 5% TSB. The positive control group was established by using 70% isopropanol-permeabilised bacterial cells and was made by a volume of 50 µL of permeabilised bacterial cell suspension and 40 µL of 5% TSB. Ten µL of SYTOX green nucleic acid stain was added to each well to a final concentration of 5 µM. Meanwhile, the background fluorescence was measured using a volume of 90 µL 5% TSB and ten µL SYTOX green nucleic acid stain at the same concentration. The black plate was incubated for two h at 37 ◦C in the dark.

The fluorescent intensity of each well was recorded using an ELISA plate reader (Biolise BioTek EL808, Winooski, VT, USA) with excitation at 485 nm and emission at 528nm.

2.8 Haemolysis Assay

2.8.1 Preparation

Preparation of phosphate-buffered saline (PBS): two tablets were added into 400ml double deionized and shaken until dissolved. The solution was then autoclaved.

Peptide stock solution (concentration: 1024 μM): the synthetic peptide was dissolved in PBS. 1%v of dimethylsulphoxide (DMSO) was applied if the peptide could not be dissolved in PBS.

Triton-100 stock: 20% Triton-100 solution was prepared.

2.8.2 Erythrocyte washing

Two millilitres of fresh defibrinated horse blood (TCS Bioscience Ltd, UK) was transferred into a 50mL tube, and the tube was centrifuged at 930 ×g for 5 minutes, after that, the supernatant was discarded (to remove the serum and keep the erythrocytes at the bottom of the tube) and 30mL prepared PBS solution was added to wash the erythrocytes (by gentle orbital shaking) and to remove the broken blood cells. The tube was centrifuged at 930 ×g for 5 minutes, and then the supernatant was discarded. This step was repeated until the supernatant was clear. Then, to obtain an even 4% (v/v) erythrocyte suspension, the universal tube was refilled with autoclaved PBS solution to reach the final volume of 50mL and gently shaken on an orbital shaker.

2.8.3 Peptide loading

The peptide stock solution was double-diluted to obtain a range of concentrations of peptide (1024, 512, 256, 128, 64, 32, 16, 8, 4, 2 μM), 20% Triton-100 stock solution was

10-fold diluted as positive control*, besides, PBS solution served as the negative control*. Two hundred microliter of each concentration of peptide solution was added into a 1.5mL tube, and 5 duplications were applied, then the same volume of 4% erythrocyte suspension was slowly added into each tube. Finally, erythrocyte suspension was half diluted to 2% (v/v) in each tube, and final peptide concentrations ranged from 512 to 1 μM. The tubes were then put in an incubator (Genlab Limited, UK) at 37℃ for 2 hours.

* Positive control: 200μL 2% Triton X-100 + 200μL 4% erythrocyte suspension

* Negative control: 200μL PBS + 200μL 4% erythrocyte suspension

2.8.4 Detection

After incubation had finished, all of the tubes were centrifuged at 930×g for 5 minutes, and 100μL supernatant of each tube was added into a 96-well plate. Then haemolysis detection was conducted by using a Synergy HT plate reader (BioTek, USA) at the absorbance of 570 nm wavelength for each well, and the haemolysis % was calculated via the following formula:

$$\text{Haemolysis\%} = (OD_{Sample} - OD_{Negative}) / (OD_{Positive} - OD_{Negative}) \times 100\%.$$

2.9 Anti-cancer assay

Five human cancer cell lines: MDA-MB-435S (ATCC-HTB-129), PC-3 (ATCC-CRL-1435), H157 (ATCC-CRL-5802), U251MG (ECACC-09063001) and MCF-7 (ATCC-HTB-22) were used in the anti-cancer assay. All cell lines were cultured in the complete medium supplemented with 10% (v/v) fetal bovine serum (FBS) (Sigma-Aldrich, St. Louis, MO, USA) and 1% (v/v) penicillin-streptomycin (Invitrogen, Paisley, UK).

Table 2.11 Five cell lines and their corresponding culture media.

Cell line	Tumour type	Basic Medium
PC-3	Human prostate cancer	RPMI-1640 (Invitrogen, Paisley, UK)
NCI-H157	Non-small cell lung cancer	RPMI-1640
U251MG	Human neuronal glioblastoma	DMEM (Invitrogen, Paisley, UK)
MDA-MB-435S	melanocyte, Melanoma	DMEM
MCF-7	breast cancer cell	DMEM

2.9.1 Resuscitation of frozen cell lines

All the five cell lines were frozen at -80℃ and they were thawed in a 37℃ water bath (Grant JB Aqua 12, UK) by gently shaking before use. Two millilitres of cell stock suspension was slowly added dropwise into a 75cm^2 flask which contained 15mL of the pre-warmed medium, which could dilute the DMSO concentration in the stock solution. The cell morphology was observed under a microscope and the flask was then placed in the incubator (37℃, 5%CO2) overnight.

2.9 2 Cell culture

This step was aimed at removing the DMSO, avoiding cancer cell adhesion and also supplying sufficient nutrients for cell growth. All the old medium was pipetted out and discarded, and 10mL pre-warmed PBS solution was transferred into the flask to wash out the adherent cells. Then the PBS solution was discarded and 15mL of fresh medium was

pipetted into the flask. Prior to overnight incubation (37℃, 5% CO_2), the cell morphology was observed by a microscope.

2.9.3 Cell subculture (passage)

When the confluence of cells was over 80%, it was necessary to separate cells into a new environment for better growth. In detail, the old medium was discarded, and the flask was washed with 10mL of pre-warmed PBS. After the washing procedure, 1000 μL trypsin was added to digest and detach the monolayer cells from the flask. Following around 5 minutes of incubation, 10mL of fresh medium was required to terminate the digestion and adherent cells were dispersed by gently pipetting. All the cell suspension was subsequently transferred to a 15mL centrifuge tube and centrifuged at 380 ×g for 5 minutes. After centrifugation, the supernatant was discarded, and cells were re-suspended with a 5mL fresh medium. In the end, a proper volume of cell suspension was transferred into the flask and cultured for further experiments.

2.9.4 MTT assay

The MTT assay is one of the most versatile and popular tests for determination of cell growth rates which is widely used in the testing of drug action, cytotoxic agents and screening other biologically active compounds. This assay involves the conversion of the water-soluble MTT (3-(4,5-dimethylthiazol-2-yl)-2,5-diphenyltetrazolium bromide) to an insoluble formazan, which has a purple colour. The formazan is then solubilized, and the concentration determined by optical density at 570 nm. The MTT cell viability assay can be performed when the secondary passaged cells covered 90% of the culture flask.

Cell quantification: 50 μL of the cell suspension (obtained in the subculture step) was mixed with 0.4% (w/v) trypan blue/PBS solution (which is a vital stain used to colour dead tissues or cells blue selectively) at the ratio of 1:1. An AS1000 Improved Neubauer

haemocytometer (Hawksley, UK) was required for cell quantification, both sides of the chamber (eight squares) were filled with the dyed cell suspension. Subsequently, the haemocytometer was observed, and the viable cells were counted by use of a microscope. The cell concentration was calculated by the formula below:

$$\text{Cell concentration (cells/mL)} = N_{mean} \times D \times 10^4$$

In which N_{mean} represented the mean number of viable cells among the counted squares, D indicated the dilution factor (D=2, Trypan Blue: cells=1:1, v/v).

Plate seeding: a 96-well plate was needed for seeding cells, and the desired cell concentration of each well was 5×10^3 cells per 100 μL (5×10^4 cells/ml). The required volume of medium and cell suspension (obtained in the subculture step) were calculated and mixed in one tube, and the diluted cell suspension was then transferred into a reservoir. Subsequently, 100μL of the diluted cell suspension was added in each well of 96-well plate. The plate was then incubated 37℃, 5% CO_2 overnight.

Starvation: after 24 hours of incubation, a starvation procedure was required. The old medium in the 96-well plate was removed and discarded, PBS solution was applied to clean the plate. Then, fresh medium (without FBS) was added, and the plate was placed into the incubator for 6hr. The peptide stoke was dissolved in DMSO (the concentration was 10^{-2}mol/L), and it was diluted to working concentrations ranging from 10^{-4} mol/L to 10^{-9} mol/L before use. Followed the starvation step, the old medium was discarded and then the peptide solution and 10^3 times diluted DMSO (vehicle control) were loaded with five replicates into the 96-well plate. The plate was incubated at 37℃, 5% CO_2 overnight.

MTT loading and detection: 10μL MTT was added into each well of the plate, and then the plate was subsequently incubated for 4~6hr. All the liquid in the 96-well plate was removed and abandoned, and 100 μL DMSO was added into each well. For the sake of

complete reaction, the plate was placed in a shaking incubator for 10 minutes to mix uniformly. After that, the cell viability detection was conducted by Synergy HT plate reader (BioTek, USA) at the absorbance of 570nm for each well.

2.10 Trypsin Inhibition Assay

Peptides were dissolved in PBS solution (pH 7.4), and the ten-fold dilution was performed to obtain a series of working solutions with four different concentrations: 10^{-3}, 10^{-4}, 10^{-5} and 10^{-6}M. Meanwhile, the trypsin was dissolved in 1 mM HCl to achieve 1 μg/ml working solution, and the substrate stock solution (10mM in DMF) was diluted with an appropriate volume of PBS solution (pH 7.4) to achieve 50 μM working solution. The sequence of the substrate was Z-Gly-Gly-Arg-AMC (616.67 g/mol), and Km was 73.6 μM based on the previous data.

After the preparation of the above reagents, three groups: blank groups*, positive control* groups and sample groups, were utilised in this assay. The sample groups were characterised by sixteen different concentrations of the peptide each with two replicates. In detail, each peptide working solution was subdivided into another gradient with four concentrations: 20 μl, 15 μl, 10 μl and 5 μl of particular peptide solution was mixed respectively with corresponding volumes of PBS to obtain a total volume of 20 μl, together with 180 μl substrate working solution and 10 μl trypsin working solution. The same practice was operated for the other three peptide solutions. All reagents were loaded into the opaque 96-well plate due to the instability of the substrate to light, and the reaction was then monitored by the FLUOstar OPTIMA Microplate Reader (BMG LABTECH, Germany) in the following 30 min to detect the fluorescence of the digested substrate.

*Blank group: 20 μl PBS,180 μl substrate (50 μM) and 10 μl HCl (1mM)

Positive control group: 20 µl PBS,180 µl substrate (50 µM) and 10 µl Trypsin (1µg/ml)

Trypsin (10 µl of a 0.1 µM stock solution in 1 mM HCl) was added to the wells of a micro-titre plate containing 180 µl substrate (Phe-Pro-Arg-NHMec, obtained from Sigma/Aldrich, Poole, Dorset, UK) (50 µM) and 20 µl Lividin-AW in concentrations of 1–1000 µM in 10 mM phosphate buffer, pH 7.4, containing 2.7 mM KCl and 137 mM NaCl (final volume 210 µl). Each determination was carried out in triplicate. The rate of hydrolysis of the substrate was monitored continuously at 37 ℃, by measuring the rate of increase of fluorescence due to the production of 7-amino-4-methylcoumarin (NH2Mec) at 460 nm (excitation 360 nm) in a CYTOFLUOR® multi-well plate reader Series 4000 spectrofluorimeter.

2.11 Chymotrypsin inhibition assay

Inhibitory activity assays on the synthetic peptide replicate and its various P1-site-substituted variants against chymotrypsin were performed the same as detailed for the trypsin inhibition assay, except that the target protease was chymotrypsin and the fluorogenic substrate utilised was Succinyl-Ala-Ala-Pro-Phe-NHMec (obtained from Bachem, UK).

2.12 Trypsin cleavage

Both trypsin and peptide stock solution were prepared as 1mg/ml in PBS, and their working solutions (200 µg/ml) were five-fold-diluted from stock. In the cleavage process, 50µl of trypsin working solution together with 950µl peptide working solution were incubated at 37℃ for 20min and 90µl of this mixture solution was added into 10µl TFA/H_2O (10% v/v) to terminate reactions at 0min, 1min, 2min, 5min, 10min, 20min. Each sample at different time points was subjected to analysis on a Perseptive Biosystems DE MALDI-TOF instrument.

CHAPTER 3

A Combined Molecular Cloning and Mass Spectrometric Method to Identify a Novel Peptide from the Skin Secretion of *Odorrana hejiangensis :* Characterization and Design of Analogues

3.1 Introduction

Odorrana, also known as odorous frogs, is a genus of frogs belonging to the Ranidae family. They are distributed in East Asia and surrounding areas and generally, a remarkably pointed snout is a typical feature for those frogs and they are found to live in fast-flowing mountain streams. According to the Antimicrobial Peptide Database (APD), 121 antimicrobial peptides from *Odorrana* species have been reported and divided into several peptide families such as odorranains (L. Chen et al. 2007) brevinins (Quan et al. 2008), nigrocins (J. Li et al. 2007) and esculentins (X. Yang et al. 2011).

Naturally-occurring antimicrobial peptides are sensitive to proteolysis and the host proteases in infected areas could result in the proteolytic degradation of AMPs (Mahlapuu et al. 2016). Peptide modifications such as N-acetylation, C-amidation or disulphide bond formation are commonly utilised to increase the proteolytic resistance of AMPs (Rink et al. 2010, Falanga et al. 2017). The disulphide bond is a typical functional group in many peptides, and it is usually formed via the coupling of two thiol groups provided by cysteine residues. In the modification of peptides, disulphide bonds play a significant role in peptide folding and stability (Sevier, Kaiser 2002, T. Liu et al. 2016). Additionally, a disulphide bond links two parts of the peptide and around this bridge, hydrophobic residues will bind to each other by hydrophobic interactions, which can increase the stability of peptides, because water molecules always break up the secondary structure via amide-amide hydrogen bonds (G. Wang 2012).

Positive charge plays a vital role in the bioactivity of antimicrobial peptides, and it is common to introduce cationic amino acid residues into these to strengthen their activity (Bahar, Ren 2013). The Tat peptide is derived from the HIV-1 Tat protein, and it has been shown to mediate various cellular delivery processes (Brooks et al. 2005). This short

linear sequence contains two lysine and six arginine residues (RKKRRQRRR), which provides a concentrated positive charge for its transduction ability. In a study in 2004 (Santra et al. 2004), this short linear sequence was conjugated to FITC-silica nanoparticles (FSNPs) for bioimaging purposes. TATp–FSNPs were prepared by a microemulsion system and studied for labelling of human lung adenocarcinoma cells (A-549) *in vitro*. The cells were efficiently labelled with TATp–FSNPs, unlike with FSNPs alone which showed no effective labelling. TATp-modified nanoparticles have also been investigated for their capability to deliver diagnostic and therapeutic agents across the blood-brain barrier.

In this study, the novel peptide QUB-1568, was isolated from the skin secretion of *Odorrana hejiangensis*. The structure of the peptide was obtained via "shotgun" cloning using 3'-Rapid amplification of cDNA ends (3'-RACE) and characterised by MS/MS sequencing. A synthetic replicate of the peptide was subjected to functional assays to evaluate its bioactivities. Since no anticancer activities were observed, an analogue in conjunction with TATq was designed to enhance the efficacy. Also, in addition, a disulphide bond was also introduced to obtain another analogue with improved stability. Both analogues were chemically synthesised, and their bioactivities were evaluated.

3.2 Methods

3.2.1 Specimen Biodata and Secretion Acquisition

Eight specimens of *O. hejiangensis* (6–8cm snout-to-vent length, sex undetermined) were collected in the field in China. The frogs were kept in a vivarium at 25^{o}C under a 12 h/12 h day/night cycle and were fed crickets three times per week. Their skin secretions were harvested after the frogs had been maintained under these conditions for around 4 months. The collection of the skin secretion was detailed in section 2.1.1.

3.2.2 Molecular Cloning of QUB-1568 Precursor-Encoding cDNA

The whole procedure employed was described in section 2.1. Polyadenylated mRNA isolation was performed using magnetic oligo-dT beads and subsequently reverse transcribed. The cDNA was subjected to 3'-RACE procedures to obtain full-length prepro-antimicrobial peptide nucleic acid sequence data using a SMART-RACE kit. Briefly, the 3'-RACE reactions employed a nested universal primer (NUP) and a degenerate sense primer (S1: 5'-GAWYYAYYHRAGCCYAAADATG-3') which was designed to a highly conserved domain of the 5'-untranslated region of previously characterised antimicrobial peptide cDNAs from *Rana* species. PCR products were gel-purified, cloned using a pGEM-T vector system and sequenced using an ABI 3100 automated sequencer. The 3'-RACE was facilitated by a nested universal primer (NUP) and the degenerate sense primer

3.2.3 Identification and Structural Analysis of Peptides in Skin Secretion

As detailed in section 2.2, a further 10 mg of lyophilised skin secretion were dissolved and subjected to reversed phase HPLC, and eluted fractions were collected at 1 min intervals. Then each fraction was further analysed by use of a MALDI-TOF mass spectrometer in positive detection mode using CHCA as the matrix. Fractions with peptide molecular masses coincident with the mature peptides predicted from the cloned cDNA were then infused into an LCQ Fleet ion-trap electrospray mass spectrometer followed by trapping of suitable ions for MS/MS fragmentation. The physicochemical properties of the peptides, such as the number of amino acids, molecular mass, theoretical pI, net charge and grand average of hydropathicity, were computed by ProtParam and the helical wheel projections were constructed via use of RZ Lab.

3.2.4 Solid-Phase Peptide Synthesis

Following the confirmation of primary structures of the cloned cDNA-encoded peptides, the wild-type peptides and their site-substituted analogues were chemically-synthesised by an automated solid phase peptide synthesiser. After cleavage from the synthesis resin and side-chain deprotection, the peptides were purified by reversed phase HPLC and both molecular masses and MS/MS fragmentation profiles were employed to confirm the purity and authenticity of their structures.

3.2.5 Circular Dichroism (CD) Analysis

A CD spectrometer was employed to perform the analysis of peptide secondary structures. Each peptide was dissolved in 10 mM ammonium acetate and 10mM ammonium acetate with 50% TFE, respectively. All CD spectra were obtained at 20C from 250 nm to 190 nm at a scanning speed of 100 nm/min. More details are listed in section 2.5.

3.2.6 Minimal Inhibitory Concentration Assays

Six microorganisms were used for minimal inhibitory concentrations (MICs) assay: *Staphylococcus aureus*, *Escherichia coli*, *Candida albicans*, Methicillin-resistant *Staphylococcus aureus* (MRSA), *Pseudomonas aeruginosa* and *Enterococcus faecalis*. Broth and agar dilution methods were employed to determine MICs at culture growth of $\geqslant 10^5$ colony forming units (cfu)/mL of bacteria and peptide concentrations were applied from 512-1 μM. Peptide solutions with growth cultures were incubated in 96-well plates for 18 h at 37 ℃. Following this, the growth of the microorganisms was measured using a microplate reader at 550 nm.

3.2.7 Membrane permeability assay

As described in section 2.7, peptide solutions and microbial cultures were prepared. Each well of the sample groups in a black 96 well plate contained a volume of 50 μL of

bacterial suspension and 50 µL of peptide solution. Each well of the negative control group was constituted by an amount of 50 µL of bacterial suspension and 40 µL of 5% TSB. The positive control group was established by using 70% isopropanol-permeabilised bacterial cells and was made by a volume of 50 µL of permeabilised bacterial cell suspension and 40 µL of 5% TSB. Ten microliter of SYTOX green nucleic acid stain was added to each well to a final concentration of 5 µM. Meanwhile, the background fluorescence was measured using a volume of 90 µL 5% TSB and 10 µL SYTOX green nucleic acid stain at the same concentration. The black plate was incubated for 2 h at 37 ◦C in the dark. The fluorescent intensity of each well was recorded using an ELISA plate reader with excitation at 485 nm and emission at 528nm.

3.2.8 Haemolysis Assay

As detailed in section 2.8, a suspension of horse red blood cells (4%, v/v) was incubated with peptides of the concentration range of 1 µM to 512 µM at 37 ℃ for 2 h. PBS together with cells served as a negative control and 2.0% of Triton X-100™ mixed with cells were taken as a positive control. Then haemolysis detection was assessed at 550 nm by a microplate reader.

3.2.9 Anti-cancer assay

The human breast cancer cell line (MB435s), human prostate cancer cell line (PC3), the human lung cancer cell line (H157), human neurospongioma cell line (U251MG) and human breast cancer cell line (MCF-7) were used for the anti-cancer assay. MTT cell viability assay was employed to evaluate the cancer cell viability. Following the MTT assay, the absorbance was detected by a Synergy HT plate reader at 570nm. (Described in section 2.9)

3.3 Results

3.3.1 Molecular cloning and sequencing analysis

From the skin-derived cDNA library of *O. hejiangensis*, a cDNA encoding the biosynthetic precursor of a putative novel bioactive peptide named QUB-1568 was consistently and repeatedly cloned using the 3'-RACE approach (Figure 3.1). The open-reading frame of this cloned precursor consisted of 64 amino acid residues, which included a 22 amino acid residues signal peptide and a mature peptide of 17 amino residues. The putative peptide sequence was preceded by two consecutive basic amino acids, Lys-Arg (KR), which represented a typical cleavage site. At the C-terminal, a glycine (G) residue was located as an amide donor.

A bioactive peptide named QUB-1568 was cloned from the skin secretion of the Hejiang Odorous Frog, *Odorrana hejiangensis*, the sequence consisted of 15 amino acids with C-terminal amidation. On the basis of the NCBI (the National Centre for Biotechnological Information)-BLAST analysis, the novel peptide was found to be identical in primary structure to the C-terminal part of kukunorisin-1 and displayed 87% identity with preprokukunorin-1 from *Rana kukunoris* (Figure 3.2).

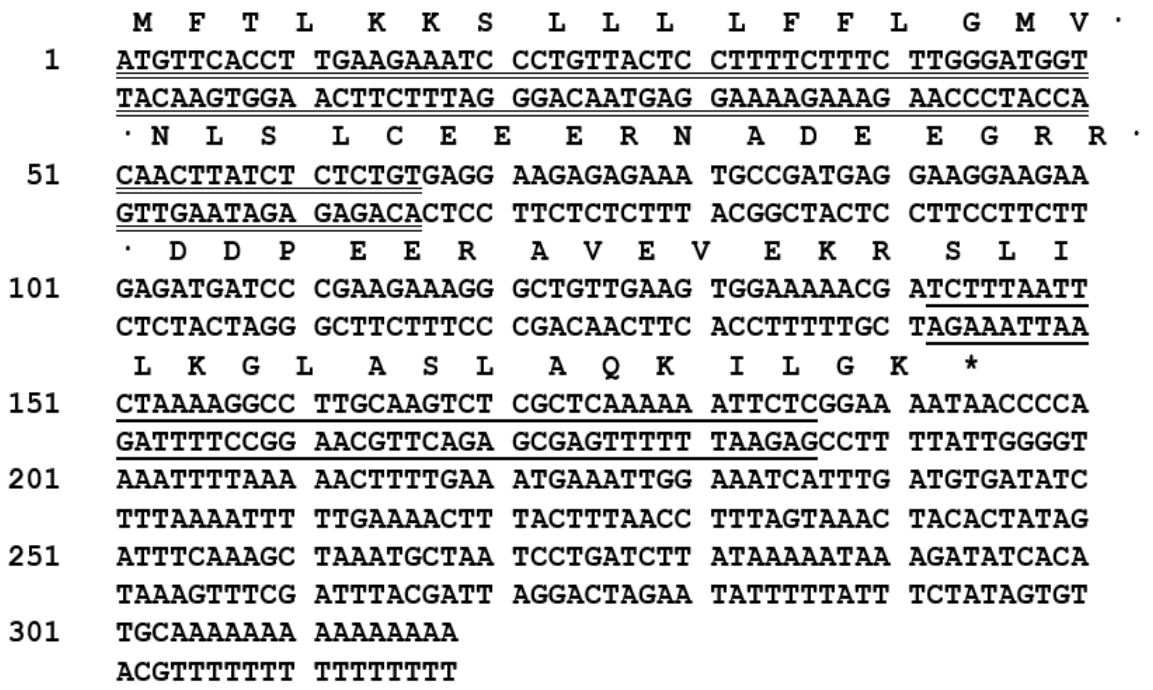

Figure 3.1 Nucleotide and translated open-reading frame amino acid sequence of cloned cDNA encoding the biosynthetic precursor of the putative bioactive peptide, QUB 1568, from the skin of the frog, *Odorrana hejiangensis*. The putative signal peptide is double-underlined, the mature active peptide is single-underlined, and the stop codon is indicated by an asterisk.

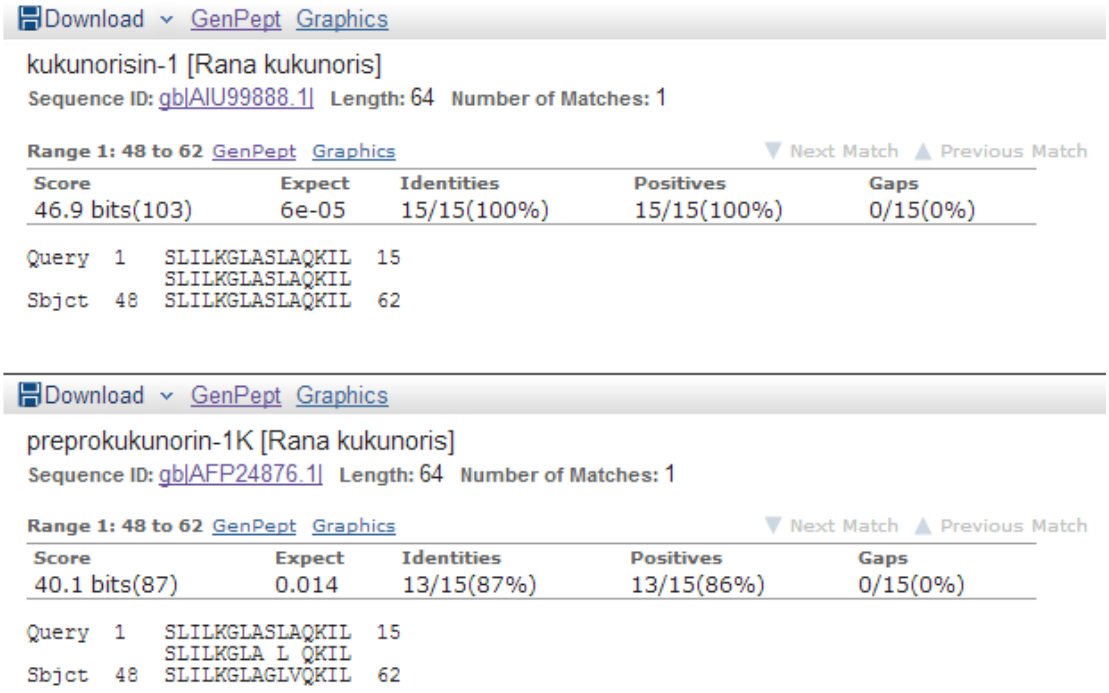

Figure 3.2 NCBI-BLAST analyses of the mature peptide of the QUB 1568 biosynthetic precursor-encoding cDNA. QUB-1568 showed 100% identity with part of kukunorisin-1 (S_{48}-L_{62}) and 87% identical to preprokukunorin-1K, both sequences come from the same species, *Rana kukunoris*.

3.3.2 Identification and structural characterisation of peptide QUB 1568

The skin secretion from the *O. hejiangensis* was solvent-extracted and then fractionated by a gradient reverse-phase HPLC using a C5 column, 240 min fractions were collected automatically at 1 min intervals. Each chromatographic fraction was subjected to mass identification by MALDI-TOF mass spectrometry. By comparing the computed molecular mass of the putative peptide QUB-1568 with the results presented by MALDI-TOF MS, the elution location of the peptide in HPLC fractions was confirmed (Figure **3.3**). MS/MS fragmentation sequencing of the peptide confirmed its structural characterisation and the data are shown in Table 3.1.

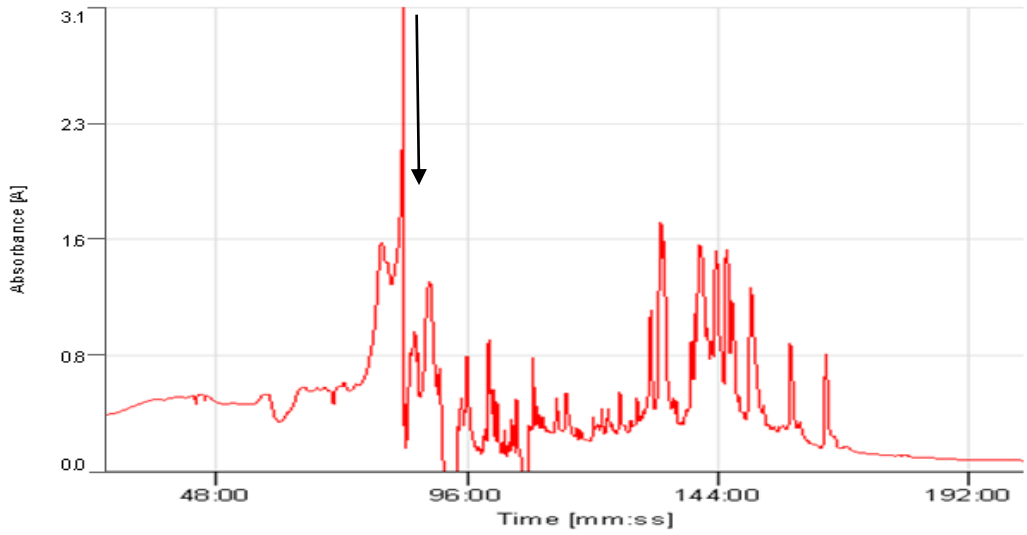

Figure 3.3 Region of reverse-phase HPLC chromatogram of the skin of the Hejiang Odorous frog, *Odorrana hejiangensis*. The elution position/retention time of the putative mature peptide is indicated with an arrow.

Table 3.1 Predicted b- and y-ion series (singly and doubly charged) of QUB-1568 through a molecular cloning peptides database. Observed fragment ions in MS/MS spectra were indicated in colour.

#1	b(1+)	b(2+)	Seq.	y(1+)	y(2+)	#2
1	88.03931	44.52329	S			15
2	201.12338	101.06533	L	1479.99858	740.50293	14
3	314.20745	157.60736	I	1366.91451	683.96089	13
4	427.29152	214.14940	L	1253.83044	627.41886	12
5	555.38649	278.19688	K	1140.74637	570.87682	11
6	612.40796	306.70762	G	1012.65140	506.82934	10
7	725.49203	363.24965	L	955.62993	478.31860	9
8	796.52915	398.76821	A	842.54586	421.77657	8
9	883.56118	442.28423	S	771.50874	386.25801	7
10	996.64525	498.82626	L	684.47671	342.74199	6
11	1067.68237	534.34482	A	571.39264	286.19996	5
12	1195.74095	598.37411	Q	500.35552	250.68140	4
13	1323.83592	662.42160	K	372.29694	186.65211	3
14	1436.91999	718.96363	I	244.20197	122.60462	2
15			L-Amidated	131.11790	66.06259	1

3.3.3 Peptide synthesis

Two analogues of QUB-1568 were synthesized by SPPS, one of the peptides was named QUB-1774, whose sequence had two additional cysteine residues one on each of the C- and N- terminals of QUB-1568, respectively, and another was named QUB-2889, whose N-terminal was attached to a Tat peptide sequence (RKKRRQRRR). Their sequences are shown in Table 3.2. After modification, QUB-1774 lost a net positive charge, while its hydropathicity slightly increased. In the case of QUB-2889, its net positive charge increased remarkably, while the GRAVY was reduced to a minus figure (Table 3.3).

Table 3.2 The peptide sequences of QUB-1568 and its two analogues: QUB-1774 and QUB-2889. The modifications of the newly designed peptides are highlighted.

NAME	SEQUENCE
QUB-1568	SLILKGLASLAQKIL-NH2
QUB-1774	CSLILKGLASLAQKILC
QUB-2889	RKKRRQRRRSLILKGLASLAQKIL-NH2

Table 3.3 Physicochemical properties of QUB-1568 and its two analogues: QUB-1774 and QUB-2889, grand average of hydropathicity (GRAVY).

	Number of amino acids	**Molecular Weight**	**Net charge**	**GRAVY**	**Theoretical PI**
QUB-1568	15	1568.98	+3	1.220	10.00
QUB-1774	17	1774.25	+2	1.371	8.90
QUB-2889	22	2889.58	+11	-0.833	12.70

3.3.4 Secondary structure analysis of peptide

The helical wheel projections of QUB-1568 and its two analogues are shown in Figure 3.4. Both QUB-1568 and QUB-1774 have perfect amphipathic conformations with the hydrophobic residues on one side and hydrophilic, polar residues on another side. In the case of QUB-2889, there is not a clear division, although hydrophobic residues are mostly located on one side, the positively charged lysine residues are found throughout the helix. Additionally, in all three plots, there is a hydrophobic leucine always located at the hydrophilic side of the helix.

The secondary structures of each peptide were determined by circular dichroism (CD). All the peptides showed two spectral absorptions at 208 and 222 nm that indicated typical-helical structures in the membrane-mimetic environment, in which the two designed peptides presented higher peaks than the original peptide (Figure 3.5 A), while they all exhibited random coil structures in 10mM ammonium acetate solution (Figure 3.5 B).

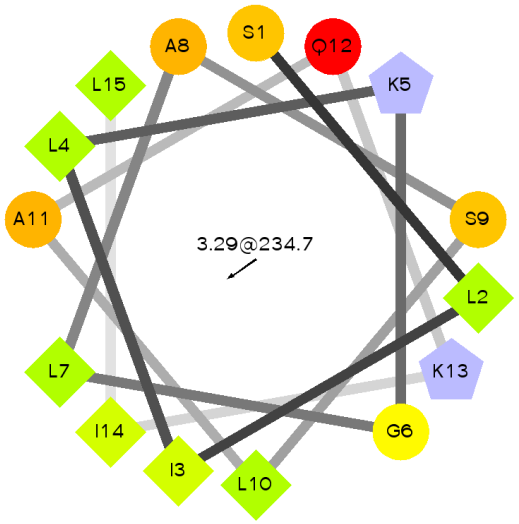

(A)

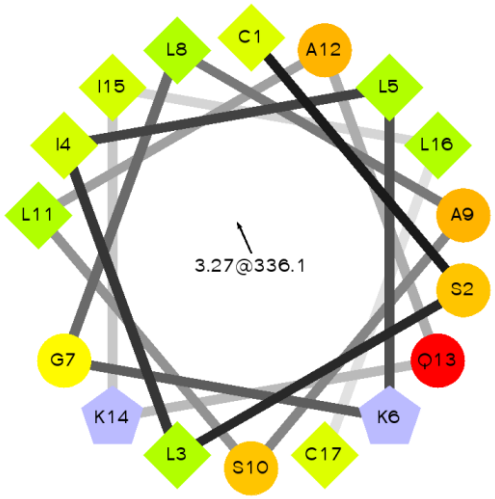

(B)

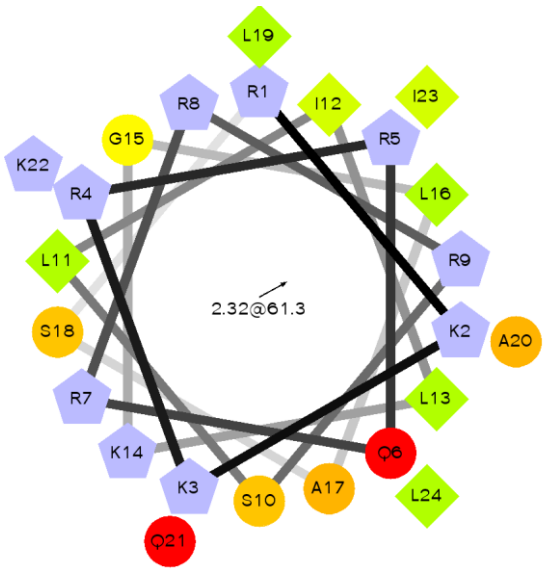

(C)

Figure 3.4 Helical wheel projections for (A) QUB-1568, (B) QUB-1774 and (C) QUB-2889. Hydrophilic residues: circles; hydrophobic residues: diamonds; potentially negatively charged: triangles; and potentially positively charged: pentagons. The most hydrophobic residue is green, and the amount of green decreasing proportionally to the hydrophobicity, with zero hydrophobicity coded as yellow. Hydrophilic residues are coded red with pure red being the most hydrophilic (uncharged) residue, and the amount of red decreasing proportionally to the hydrophilicity. The potentially charged residues are light blue. The arrows indicate the direction of the hydrophobic moment (HM), the small number represents the HM magnitude, and the bigger number represents the HM Angle.

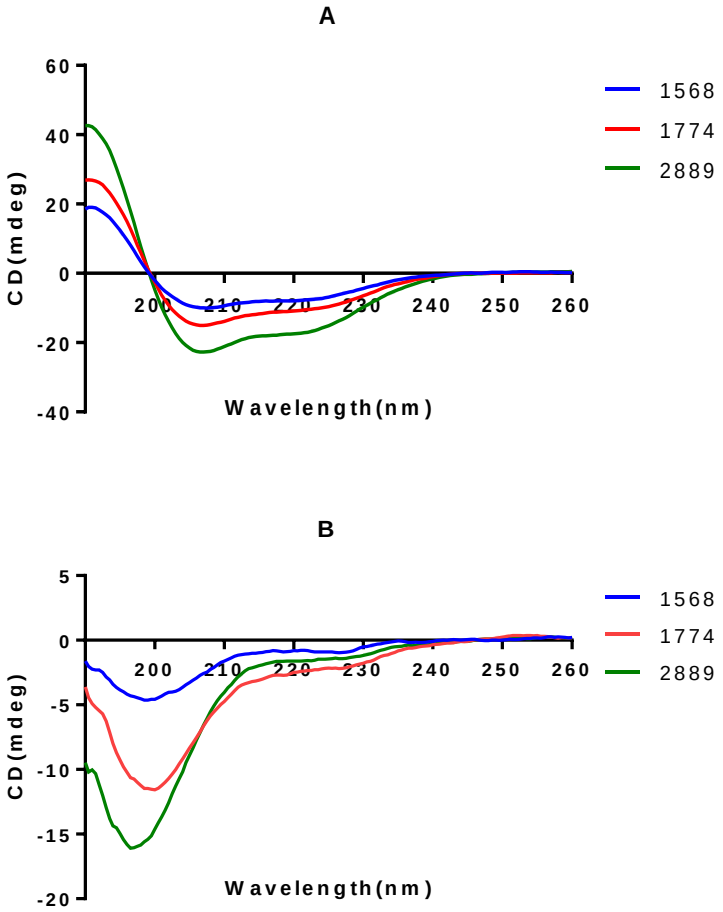

Figure 3.5 Circular dichroism (CD) spectra of QUB-1568 and its analogues (100μM) (A) in 50% 2,2,2-trifluoroethanol (TFE)/10mM ammonium water solution, (B) in 10mM ammonium acetate water solution.

3.3.5 Antimicrobial activity of QUB-1568 and two designed analogues.

QUB-1568 was found to have a broad spectrum antimicrobial activity against Gram+ve, and Gram-ve bacteria, and even against the pathogenic yeast and drug resistant bacteria. Also, its best activity was against Gram+ve bacteria and yeast. Compared to QUB-1568, the synthetic analogue QUB-1774 had lower bioactivity against all the tested bacteria (except *E.coli*) and no inhibition of *Enterococcus faecalis* and *Pseudomonas aeruginosa*, while QUB-2889 showed a significant improvement in antimicrobial activity against all the tested microbes. Data are shown in Table 3.4.

Table 3.4 Minimum inhibitory concentrations (MICs) determined for six different test microorganisms.

Peptide	Minimum Inhibitory Concentration (μM)					
	S.aureus	*E.coli*	*C.albicans*	*MRSA*	*E.faecalis*	*P.aeruginosa*
QUB-1568	8	32	4	16	64	128
QUB-1774	32	32	64	64	512	512
QUB-2889	2	1	1	4	8	2

3.3.6 *S.aureus* membrane permeabilisation test

Besides its antimicrobial activity, QUB-1568 was able to permeate the membrane of *S.aureus* at a concentration of 32μM, and more impressively, QUB-1774 and QUB-2889 were found to possess cell-membrane permeabilisation at their MIC values, which were 32μM and 2μM, respectively. Each assay was carried out individually over three experiments with three replicates for each concentration.

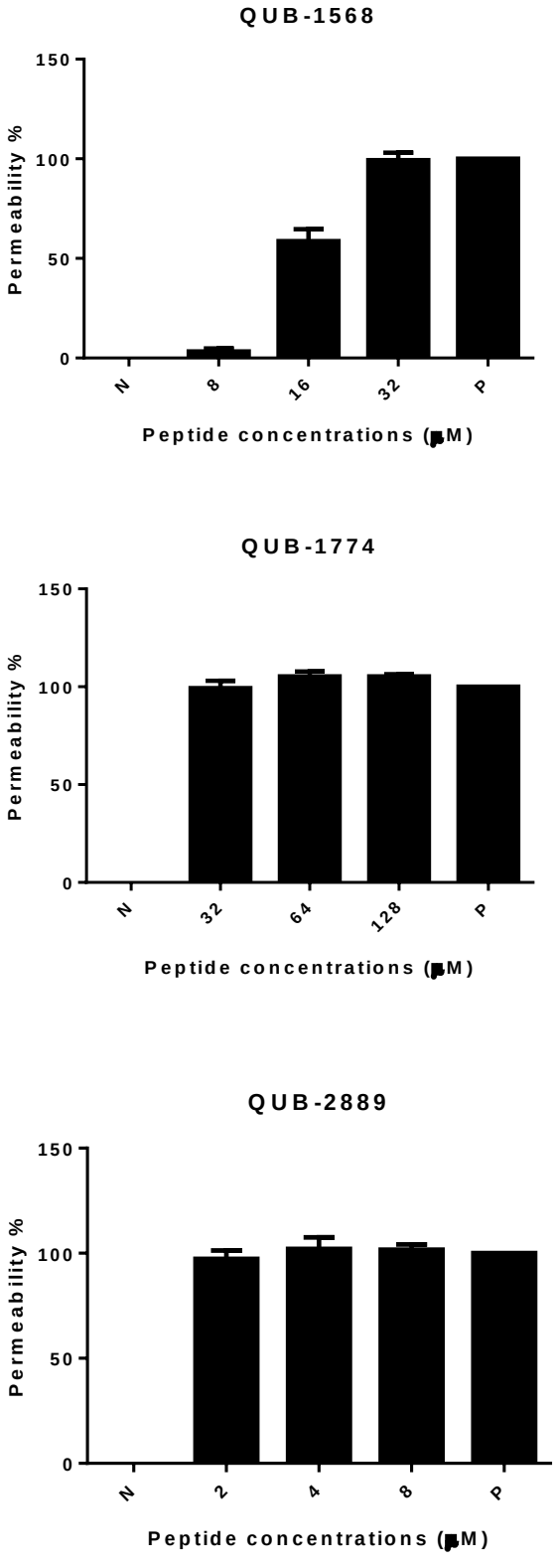

Figure 3.6 Cell-membrane permeability effects of QUB-1568 and it two analogues on *S.aureus*, peptide concentrations corresponding to 1×MIC, 2× MIC and 4 ×MIC. P:

positive control, incubation of *S. aureus* with 70% isopropyl alcohol. N: negative control was represented as the vehicle only. Data represent means ± SD of 3 replicates.

3.3.7 Haemolytic activity assay

As shown in Figure 3.6, QUB-1568 has apparent lower cytotoxicity (only 20% haemolysis at 128 μM) than the other modified analogue and the two analogues showed similar haemolysis against horse blood cells when the concentration was less than or equal to 16 μM. After this point, the cytotoxicity of QUB-2889 increased rapidly and all the blood cells were lysed at a concentration of 128 μM, while the activity of QUB-1774 grew steadily and reached 100% at a concentration of 256 μM. Noticeably, QUB-1568 does not lyse all the blood cells even at its highest concentration. The EC_{50} values in Table 3.5 can also reflect the haemolytic activity directly, and both modified peptides possess relatively high cytotoxicity at an antimicrobial level. Contrary, QUB-1568 has a relatively low haemolytic activity.

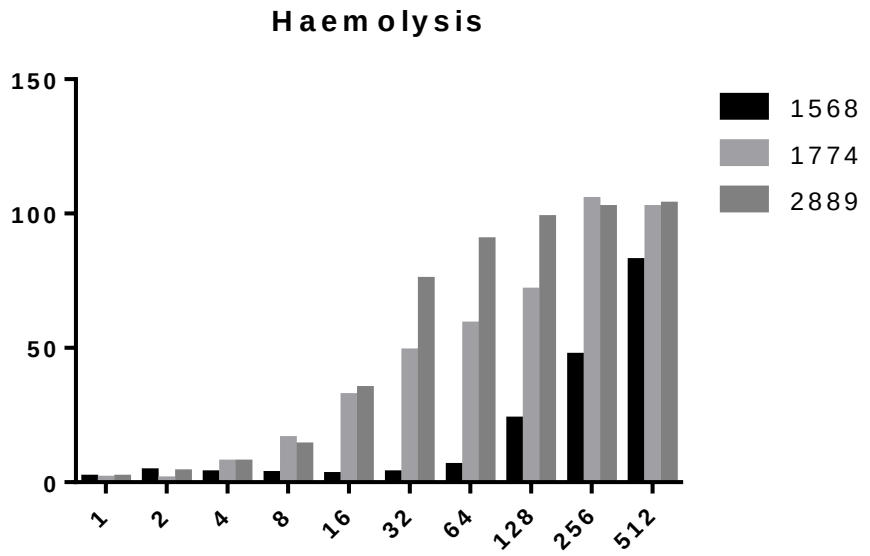

Figure 3.7 The haemolytic activity of QUB-1568, 1774 and 2889 at concentrations from 1 to 512 μM. The positive control is 1% Triton X-100. Data represent means ± SD of 3 replicates.

Table 3.5 Relative haemolysis of QUB-1568, QUB-1774 and QUB-2889. The 100% haemolysis was induced by 1% Triton X-100.

Peptide sequence	Cytotoxicity on Horse Erythrocytes
	EC_{50} (μM)
QUB-1568	187.05
QUB-1774	48.51
QUB-2889	23.53

3.3.8 Cell culture

Using the cell culture and MTT assay described in Methods section 2.7, QUB-2889 showed bioactivity against all the tested cancer cells, which is an excellent improvement

of anticancer activity. Besides, it demonstrated the most anti-cancer effectiveness against non-small lung cancer cell line H157. Similar to QUB-1568, no significant activity was observed for QUB-1774 among these five cell lines (Table 3.6).

Table 3.6 The IC_{50} concentrations of QUB-1568 and its analogues against the human breast cancer cell line (MB435s), human prostate cancer cell line (PC3), the human lung cancer cell line (H157), human glioblastoma cell line (U251MG) and human breast cancer cell line (MCF-7).

Peptide sequence	**IC_{50} (μM)**				
	PC-3	*H157*	*MB435S*	*U251MG*	*MCF-7*
QUB-1568	46.34	41.36	62.94	47.25	71.43
QUB-1774	52.16	37.57	45.33	34.03	55.84
QUB-2889	5.489	2.917	5.01	6.342	7.209

3.4 Discussion

QUB-1568 can be considered as a novel peptide since the BLAST analysis showed the primary sequence of QUB-1568 had 100% identity with the C-terminal part of the sequence of kukunorisin-1(S48-L62) from *Rana* species, while kukunorisin-1 is still unpublished and other BLAST results are of hypothetical proteins. Besides, according to the sequence alignments among QUB-1568 and some previously identified *Odorrana* peptides belong to different peptide families (Table 3.7), QUB-1568 shows no sequence similarities with all three peptides, suggesting that QUB-1568 may represent a new peptide family.

Table 3.7 Sequence alignments of QUB-1568, Odorranain-HP (L. Chen et al. 2007), Brevinin-1HSa (Conlon, Kolodziejek et al. 2008) and Nigrocin-2ISa (Iwakoshi-Ukena et

al. 2011). The QUB-1568 sequence is shorter than all other peptides, and it does not contain cysteine residue as these other peptides do.

NAME	SEQUENCE	PEPTIDE FAMILY	SOURCE
Odorranain-HP	GLLRASSVWGRKYYVDLAGCAKA	Odorranain	*Odorrana grahami*
Brevinin-1HSa	FLPAVLRVAAKIVPTVFCAISKKC	Brevinin	*Odorrana hosii*
Nigrocin-2ISa	GIFSTVFKAGKGIVCGLTGLC	Nigrocin	*Odorrana ishikawae*
QUB-1568	SLILKGLASLAQKIL-NH2	-	*Odorrna heijiangensis*

The synthetic duplicate of QUB-1568 showed a broad-spectrum activity against both bacteria and fungi, in which more potent inhibition was exhibited towards Gram-positive bacteria and the pathogenic yeast. It seems that this peptide has better interactions with relatively less cationic membranes since comparing to Gram-negative bacteria, Gram-positive bacteria have less negative charges, and the cell surface of fungi are neutral in potential (Malanovic, Lohner 2016b).

To investigate how a disulphide bond affects peptide function and also increase the stability of QUB-1568, two Cysteines were added into its N- and C-terminus respectively. Naturally, the newly designed analogue was found to have weaker antimicrobial activity but higher toxicity than the original peptide. Frequently, the increased hydrophobicity and net charge bring stronger bioactivities, whereas in this case, a slight increase of hydrophobicity did not improve peptide antimicrobial activity, while the decreased net charge exhibited noticeable impact on peptide antimicrobial activity. The inhibitory of QUB-1774 against five microbes weakened (except for *E.coli*), especially, the effect on

E.faecalis, *P.aeruginosa* were abolished. An exception was observed, the MIC value for *E.coli* was unchanged after peptide design, it can be suggested that Gram-positive bacteria and yeast are sensitive to the small change of peptide net charge, and hydrophobicity have more impact on Gram-negative bacteria. The different cell structures of these three microbes is a contributing factor to this result, and Gram-negative bacteria had an outer membrane that others do not have, higher hydrophobicity makes the peptide insert deeper into the core portion of the cell membrane (Giuliani et al. 2008). The newly designed peptide presented more α-helical content than the original peptide, suggesting that the presence of a disulphide bond increased the amphiphilicity of peptide, as amphiphilicity and helicity are essential properties for peptide-membrane interactions, and this can be proven by the increased cytotoxicity of QUB-1774. Although no significant anti-cancer activity was observed among the five tested cell lines, the IC_{50} concentrations were slighted improved, and it might be supposed that higher hydrophobicity of peptide can strengthen its bioactivity towards cancer cells to some extent, but it is not the critical factor. Whereas, to directly prove that the new peptide has a more stable structure, further peptide stability assays should be performed.

Basically, at the initial adsorption between peptide and membrane, the cationic peptide will interact with the anionic membrane constituent, similar to bacteria cell membranes, neoplastic cells have electronegative membranes due to the appearance of negatively charged lipids (Riedl et al. 2011). Hence, this cationic sequence was attached to the N-terminal of QUB-1568 to increase its anti-cancer activity. This modification makes the net charge of the peptide increase from 3 to 11, which is higher than the average upper limit of net charge for AMPs. Besides, the CD spectra showed QUB-2889 had more α-helical structure than the original peptide, which means it has better amphiphilicity. Because of the increase of positive charge and amphiphilicity, the designed peptide

QUB-2889 showed a significant improvement of antimicrobial activity, at the same time, its haemolysis activity was also dramatically increased but still higher than its antimicrobial level. Actually, after modification, the hydrophobicity of QUB-2889 decreased to a negative value, which will bring weaker activity under normal circumstances; however, it did not make a difference due to the extreme high net charge. Also, the peptide inhibition towards Gram-negative bacteria was remarkably enhanced, this can be explained since Gram-negative bacteria membrane contains more negative charges than other tested microbes do. Combine with the antimicrobial activity of the other two peptides, and it is evident that the inhibitory on Gram- bacteria is mainly influenced by positive charges.

The test of membrane permeability is a practical approach to investigate the action modes of antimicrobial peptides, in the current study, the two modified peptides showed total membrane permeabilisation at their MICs. Especially, QUB-2889 with an impressively low active concentration of 2μM directly disrupt the *S.aureus* cell membrane integrity. Due to the low active concentration and potent activity, non-pore formation mechanisms can be considered such as interaction with intracellular anionic ligands causing their leakage, or resulting in segregation of differently charged lipids (Mattila et al. 2008), et al. While both QUB-1568 and QUB-1774 achieve 100% membrane permeability at concentrations of 32μM, and it seems like they induce a pore formation mechanism.

Moreover, the anti-cancer activity of QUB-2889 was improved as well, because the neoplastic cell membrane contains anionic lipids making the membrane sensitive to cationic AMPs. It can be assumed that this designed peptide interacts with and disrupts the cancer cell membrane just like for the antimicrobial activity. Besides, the short TAT peptide has been reported to successfully take part in many cellular processes including the mediation of molecules to pass the blood-brain barrier, this is also an essential point

for cancer therapies. In the treatment of brain tumours, chemotherapy has questionable effectiveness since most drugs cannot pass through the blood-brain barrier (Deeken, Löscher 2007). It can be considered as a potential way to combine with TAT sequence to promote the effectiveness of drugs for brain cancers. Among the five cancer cell lines QUB-2889 showed the highest potency against human non-small lung cancer cell line (H157). Non-small lung cancer cells are undifferentiated malignant neoplasms, they are large and flattened, which may provide a bigger surface for peptide-membrane interactions. Further investigations on the action modes of QUB-2889 should be done to find whether QUB-2889 can kill the cancer cells via non-membrane related pathway.

In conclusion, the newly discovered novel peptide QUB-1568 was an antimicrobial peptide with potent broad-spectrum antimicrobial activity and relatively low cytotoxicity. Two analogues were designed to investigate the structure-activity relationships. It is apparent from the results that with a small difference of net charge of the peptide, its hydrophobicity has more impact on Gram-negative bacteria than Gram-positive bacteria and yeast. However, hydrophobicity did not make a difference under an extreme positive condition. Furthermore, the addition of a Tat sequence has successfully improved the peptide bioactivity towards all tested cancer cells. Due to the excellent antimicrobial activity of the designed peptide, more functional experiments (e.g. biofilm assays, membrane permeability assays, etc.) can be done to explore the potential of QUB-2889.

CHAPTER 4

Identification, Characterisation and modification of the Antimicrobial Peptide, QUB-3025, from the Skin Secretion of *Phyllomedusa coelestis*.

4.1 Introduction

Antimicrobial peptides (AMPs) exist as defenders to protect their host from invasion by bacteria, virus, fungi and other threats, and they are widely spread among mammals, amphibians, insects, plants, etc. (Bahar, Ren 2013). For example, cathelicidins are an antimicrobial peptide family that constitute a vital part of mammalian innate immune defence (Zanetti 2004), and one of the other groups of host defence peptides (HDPs), defensins, contain numbers of cysteine residues and are found not only in animals, but also in plants (Pearce et al. 2008). Cecropins, which were isolated from insects, play a crucial role in insect cell-free immunity (Lauwers et al. 2009).

Phyllomedusa is a genus of tree frog of the subfamily Phyllomedusinae, and are distributed in Central and South America, with around 30 species belonging to this genus (Amano 2016). After years of exploration, *Phyllomedusa* is considered as a rich source of bioactive peptides, and more than 80 antimicrobial peptides have been discovered in species of this genus (de Azevedo Calderon et al. 2011). Specifically, these peptides are divided into several families like dermaseptins, phylloseptins, plasticins, dermatoxins, etc. (Nicolas, El Amri 2009).

Dermaseptin was first found in the skin of Neobatrachian South American arboreal frogs *Phyllomedusa* and all of the peptides of the dermaseptin family have been isolated from the skins of this frog genus (Amiche et al. 1999). Generally, dermaseptins consist of 27-34 amino acid residues with a common motif sequence (A (A/V) GKAAL (G/N)) in the middle and a conserved tryptophan residue at the third position. The intrinsic lysine residues provide positive charges which contribute to the cationicity of dermaseptins; also, a great majority of dermaseptins can potentially adopt an amphipathic helical

formation in aqueous solution or at the surface of the bacterial membrane (Zairi et al. 2009).

According to previous studies, dermaseptins share similar N-terminals while varying a lot in their C-terminals (Nicolas, El Amri 2009). The relationship between bioactivity and structures of dermaseptins has been deeply investigated. Taking the most-studied dermaseptin, dermaseptin-B2 (containing 33 residues), as an example, by detection of interactions between SDS micelles and dermaseptin B2 analogues, the N-terminal 1−11 segment was proven to be indispensable for antimicrobial activity while the remaining region also showed influence on the activity (Lequin et al. 2003). Furthermore, another study, which focused on the active mechanism of dermaseptin B2, demonstrated that the C-terminal truncated analogue, [1-23]- dermaseptin B2, showed no antimicrobial activity since it did not penetrate and disturb the hydrophobic core of the bilayer like the full length dermaseptin B2 (Galanth et al. 2008).

Here, the isolation of a novel antimicrobial peptide precursor from the skin secretion of *Phyllomedusa coelestis*, is described, using molecular cloning combined with mass spectrometry. An analogue with a shorter sequence was designed, which preserved conserved sequences while reducing the sequence length. Both peptides were identified and evaluated in antimicrobial, anti-cancer and haemolytic assays; hence, the critical role of the conserved sequence can be told by comparing the obtained results.

4.2 Methods

4.2.1 Specimen Biodata and Secretion Acquisition

Eight specimens of *Phyllomedusa coelestis* (6–8cm snout-to-vent length, sex undetermined) were collected commercially in the field in Peru. The frogs were kept in a vivarium at 25 C under a 12 h/12 h day/night cycle and were fed crickets three times

per week. Their skin secretions were harvested after the frogs had been maintained under these conditions for around 4 months. The method of skin secretion collection was detailed in section 2.1.

4.2.2 Molecular Cloning of QUB-3025 Precursor-Encoding cDNA

Five mg of the lyophilised skin secretion were dissolved in 1 mL of cell lysis/binding buffer. Magnetic oligo-dT beads were used to isolate the polyadenylated mRNA following the procedure described by the manufacturer. To acquire full-length prepropeptide nucleic acid sequence data, a SMART-RACE kit was employed with a nested universal primer (NUP) and a degenerate primer pool (5´-ACTTTCYGAWTTRYAAGMCCAAABATG-3´) designed to a segment of the 5´-untranslated region of phylloxin cDNA from *Phyllomedusa bicolor*. PCR products were analysed by DNA-gel electrophoresis, purified and cloned using a pGEM®-T Easy vector system and the selected samples were sequenced using an ABI 3100 automated sequencer. The Blast Alignment Search Tool (BLAST) of the National Center for Biotechnology Information (NCBI) was used to study the similarities of the novel amino acid sequences with the known sequences in the BLASTp database. Alignments were established to compare the novel sequences with the two identified sequences.

4.2.3 Identification and Structural Analysis of Peptides in Skin Secretion

As detailed in section 2.2, a further 10 mg of lyophilised skin secretion were dissolved and subjected to reversed phase HPLC, and eluted fractions were collected at 1 min intervals. Then each fraction was further analysed by use of a MALDI-TOF mass spectrometer in positive detection mode using CHCA as the matrix. Fractions with peptide molecular masses coincident with the mature peptides predicted from the cloned

cDNA were then infused into an LCQ Fleet ion-trap electrospray mass spectrometer followed by trapping of suitable ions for MS/MS fragmentation. The physicochemical properties of the peptides, such as the number of amino acids, molecular mass, theoretical pI, net charge and grand average of hydropathicity, were computed by ProtParam and the helical wheel projections were constructed using RZ Lab.

4.2.4 Solid-Phase Peptide Synthesis

Following the confirmation of primary structure of the cloned cDNA-encoded peptide, the wild-type peptide and its truncated analogue, were chemically-synthesised by an automated solid phase peptide synthesiser. After cleavage from the synthesis resin and side-chain deprotection, the peptides were purified by reversed phase HPLC and both molecular masses and MS/MS fragmentation profiles were employed to confirm the purity and authenticity of their structures.

4.2.5 Circular Dichroism (CD) Analysis

A CD spectrometer was employed to perform the analysis of peptide secondary structures. Each peptide was dissolved in 10 mM ammonium acetate and 10mM ammonium acetate with 50% TFE, respectively. All CD spectra were obtained at 20C from 250 nm to 190 nm at a scanning speed of 100 nm/min. More details were given in section 2.5.

4.2.6 Minimal Inhibitory Concentration Assays

Six microorganisms were used for minimal inhibitory concentration (MICs) assays: *Staphylococcus aureus*, *Escherichia coli*, *Candida albicans*, Methicillin-resistant *Staphylococcus aureus* (MRSA), *Pseudomonas aeruginosa* and *Enterococcus faecalis*. Also, two well-known antibiotics – ampicillin and norfloaxin, together with the bioactive peptide melittin, were also tested for comparison. Broth and agar dilution methods were employed to determine MICs at culture growth of $\geqslant 10^5$ colony forming units (cfu)/mL

of bacteria. Peptides and cultures were added into 96-well plates, and the plates were incubated at 37℃, 18h. Following this, the growth of the microorganisms was measured using a microplate reader at 550 nm.

4.2.7 Membrane permeability assay

As described in section 2.7., peptide solutions and bacterial cultures were prepared in advance. Each well of the sample groups in a black 96 well plate contained a volume of 50 μL of bacterial suspension and 50 μL of peptide solution. Each well of the negative control group was constituted by an amount of 50 μL of bacterial suspension and 40 μL of 5% TSB. The positive control group was established by using 70% isopropanol-permeabilised bacterial cells and was made by a volume of 50 μL of permeabilised bacterial cell suspension and 40 μL of 5% TSB. Ten microliter of SYTOX green nucleic acid stain was added to each well to a final concentration of 5 μM. Meanwhile, the background fluorescence was measured using a volume of 90 μL 5% TSB and 10 μL SYTOX green nucleic acid stain at the same concentration. The black plate was incubated for 2 h at 37 ◦C in the dark. The fluorescent intensity of each well was recorded using an ELISA plate reader with excitation at 485 nm and emission at 528nm.

4.2.8 Haemolysis Assay

A suspension of horse red blood cells (4%, v/v) was incubated with peptides in the concentration range of 1 μM to 512 μM at 37 ℃ for 2 h. PBS together with cells served as a negative control and 2.0% of Triton X-100™ mixed with cells were taken as a positive control. Haemolysis was then assessed at 550 nm by a microplate reader.

4.2.9 Anti-cancer assay

The human breast cancer cell line (MB435s), human prostate cancer cell line (PC3), the human lung cancer cell line (H157), human neurospongioma cell line (U251MG) and

human breast cancer cell line (MCF-7) were used in the anti-cancer assays. MTT cell viability assay was employed to evaluate the cancer cell viability. Following the MTT assay, the absorbance was detected by a Synergy HT plate reader at 570nm. (details given in section 2.9)

4.3 Results

4.3.1 Molecular cloning and sequencing analysis

From the skin-derived cDNA library of *Phyllomedusa coelestis*, a cDNA encoding the biosynthetic precursor of a putative novel bioactive peptide named QUB-3025 was consistently and repeatedly cloned. The open-reading frame of this cloned precursor consisted of 77 amino acid residues, which included a 22 amino acid residue signal peptide and a mature peptide of 28 amino residues. The putative peptide sequence was preceded by two successive basic amino acids, Lys-Arg (KR), which represented a typical cleavage site. At the C-terminal, a glycine (G) residue was located as an amide donor (Figure 4.1). The NCBI-BLAST (Figure 4.2) indicated this novel peptide has a highly conserved sequence with the dermaseptin family peptides, dermaseptin-2 (DStar02), dermaseptin-1 (DStormo01) and dermadistinctin-L (DDL).

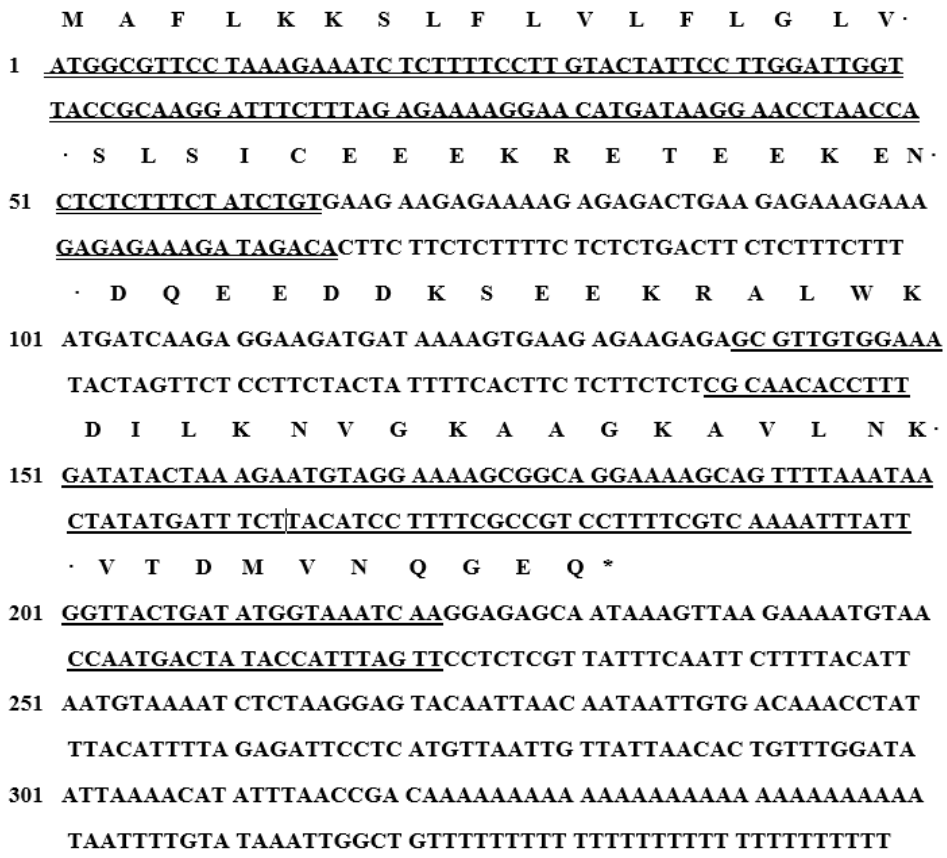

Figure 4.1 The open-reading frame the biosynthetic precursor of QUB-3025. The putative signal peptide is double-underlined, the mature peptide is single-underlined, and an asterisk indicates the stop codon.

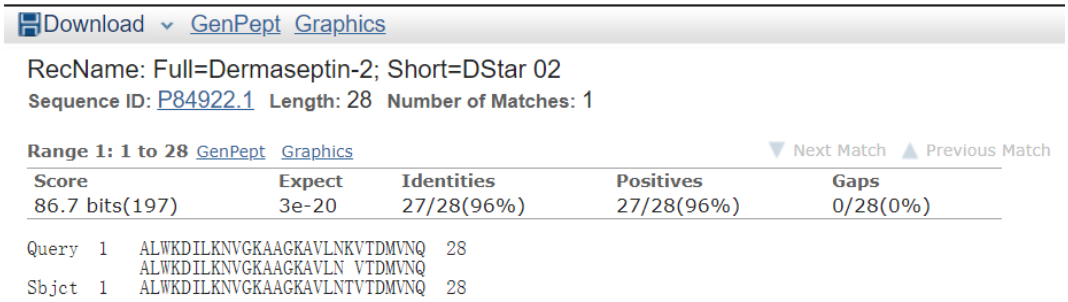

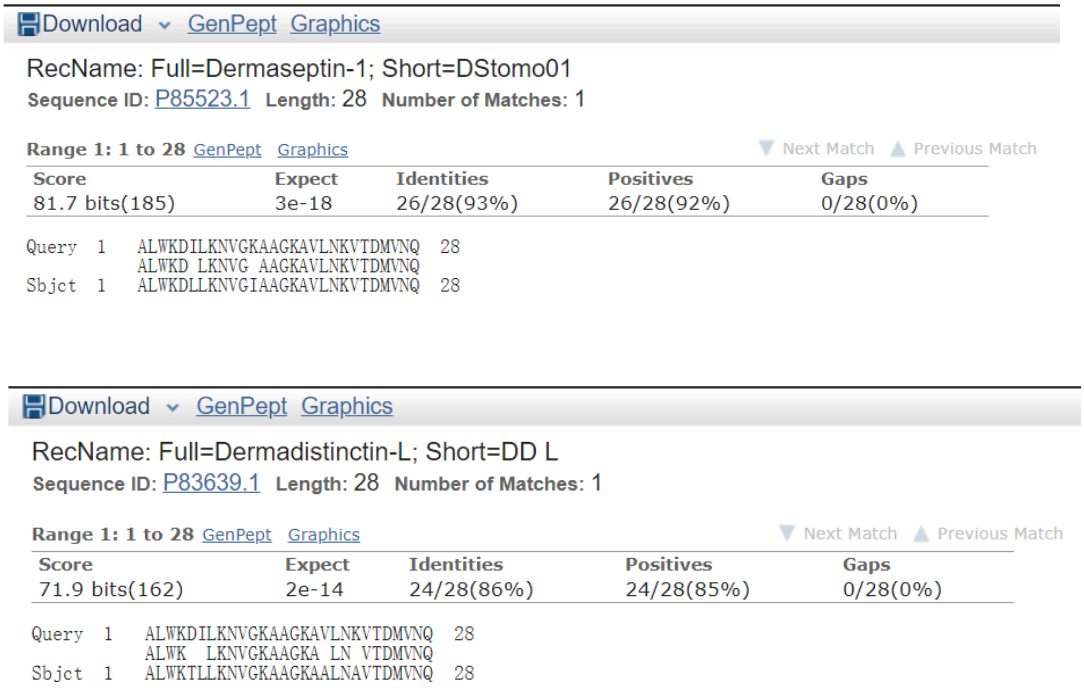

Figure 4.2 The results of NCBI-BLAST. QUB-3025 shows high sequence identities with dermaseptin-2 (96%), demaseptin-1 (93%) and dermadistinctin-L (86%).

4.3.2 Identification and structural characterisation of peptides

The crude skin secretion was dissolved and fractioned by reversed-phase high-performance liquid chromatography (RP-HPLC) and each fraction was analyzed by MALDI-TOF MS. After comparison of the computed and the identified molecular masses of QUB-3025, the elution site of the peptide was confirmed (Figure 4.3). The peptide structure was characterized by MS/MS fragmentation sequencing (Table 4.1).

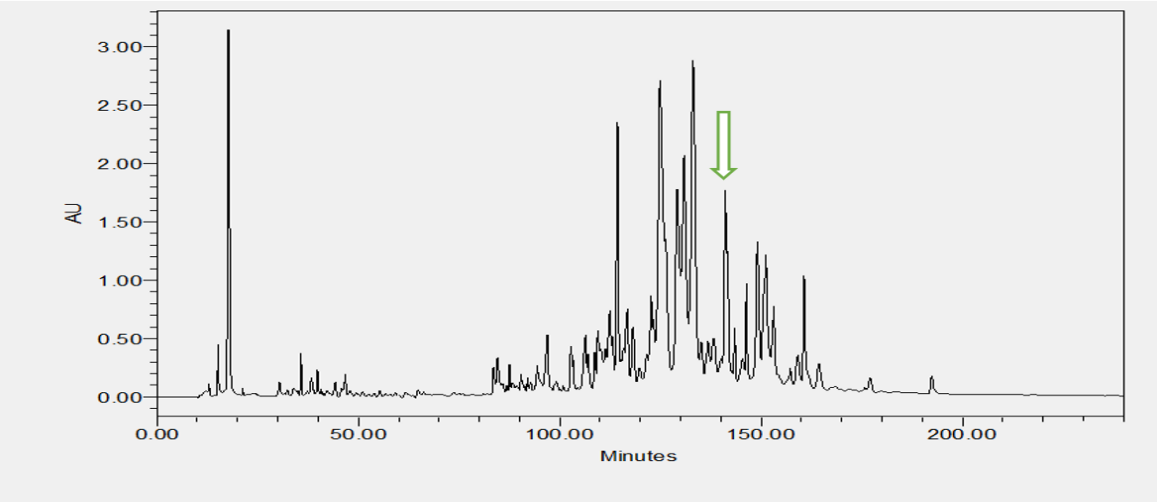

Figure 4.3 The reverse-phase HPLC chromatogram of the skin secretion from *Phyllomedusa coelestis.* The elution position of QUB3025 is indicated with an arrow. The components were monitored at a wavelength of 214 nm. The Y-axis shows the relative absorbance at 214 nm, and the X-axis shows the retention time in minutes.

Table 4.1 Predicted b- and y-ion series of QUB-3025 through a molecular cloning peptides database.

#1	b(1+)	b(2+)	Seq.	y(1+)	y(2+)	#2
1	72.04440	36.52584	A			28
2	185.12847	93.06787	L	2952.68171	1476.84449	27
3	371.20779	186.10753	W	2839.59764	1420.30246	26
4	499.30276	250.15502	K	2653.51832	1327.26280	25
5	614.32971	307.66849	D	2525.42335	1263.21531	24
6	727.41378	364.21053	I	2410.39640	1205.70184	23
7	840.49785	420.75256	L	2297.31233	1149.15980	22
8	968.59282	484.80005	K	2184.22826	1092.61777	21
9	1082.63575	541.82151	N	2056.13329	1028.57028	20
10	1181.70417	591.35572	V	1942.09036	971.54882	19
11	1238.72564	619.86646	G	1843.02194	922.01461	18
12	1366.82061	683.91394	K	1786.00047	893.50387	17
13	1437.85773	719.43250	A	1657.90550	829.45639	16
14	1508.89485	754.95106	A	1586.86838	793.93783	15
15	1565.91632	783.46180	G	1515.83126	758.41927	14
16	1694.01129	847.50928	K	1458.80979	729.90853	13
17	1765.04841	883.02784	A	1330.71482	665.86105	12
18	1864.11683	932.56205	V	1259.67770	630.34249	11
19	1977.20090	989.10409	L	1160.60928	580.80828	10
20	2091.24383	1046.12555	N	1047.52521	524.26624	9
21	2219.33880	1110.17304	K	933.48228	467.24478	8

22	2318.40722	1159.70725	V	805.38731	403.19729	7
23	2419.45490	1210.23109	T	706.31889	353.66308	6
24	2534.48185	1267.74456	D	605.27121	303.13924	5
25	2665.52235	1333.26481	M	490.24426	245.62577	4
26	2764.59077	1382.79902	V	359.20376	180.10552	3
27	2878.63370	1439.82049	N	260.13534	130.57131	2
28			Q-Amidated	146.09241	73.54984	1

4.3.3 Peptide synthesis

The synthetic replicate of QUB-3025 and its truncated analogue, named QUB-1994, were synthesised from their C-terminals by SPPS. After cleavage, the peptides were lyophilised, then subjected to functional assays. Their sequences are shown in Table 4.2. Using the computer calculations by ProtParam, several physiochemical properties of the peptides were obtained (Table 4.3). The new truncated analogue peptide contained 19 amino acids, which is nine fewer than QUB-3025. They have the same number of positive charges, which is four and the hydropathicity of peptide increased after modification.

Table 4.2 The peptide sequences of QUB-3025 and its analogue: QUB-1994. The modified peptide QUB-1994 is a truncated analogue of the original peptide and the removed part of sequence is highlighted.

NAME	SEQUENCE
QUB-3025	ALWKDILKNVGKAAGKAVLNKVTDMVNQ-NH_2
QUB-1994	ALWKDILKNVGKAAGKAVL-NH_2

Table 4.3 Physicochemical properties of the peptides computed by ProtParam. Grand average of hydropathicity (GRAVY).

	Number of amino acids	Molecular Weight	Net charge	GRAVY	Theoretical PI
QUB-3025	28	3024.59	+4	-0.039	9.83
QUB-1994	19	1994.43	+4	0.379	10.00

4.3.4 Secondary structure analysis

The helical wheel of QUB-3025 (Figure 4.4 A) lacks a clear separation of hydrophobic and hydrophilic residues, and amino acid types are just spread randomly around the helix. The situation is better for QUB-1994 (Figure 4.4 B), where most residues are divided into two faces of the helix by their hydropathicity. Compared to QUB-1994, QUB-3025 contains more hydrophilic residues including two charged residues (K21, D24) and one most hydrophilic residue (Q28) on its hydrophobic side, and another two less hydrophilic residues (N20, N27). The secondary structures of the two peptides were determined by circular dichroism (CD) in 10mM ammonium acetate/water solution and 50% 2,2,2-trifluoroethanol (TFE) in 10mM ammonium acetate water solution, respectively. In the membrane-mimetic medium (TFE solution), QUB-3025 was induced to form a typical α-helical conformation, while it had two spectral absorptions at 204 and 217 nm, which meant it adopts a random-coil and β-sheet structure in ammonium acetate solution. As for QUB-1994, it showed a random-coil structure in 2, 2, 2-trifluoroethanol (TFE)/10mM ammonium water solution (Figure 4.4 C, D).

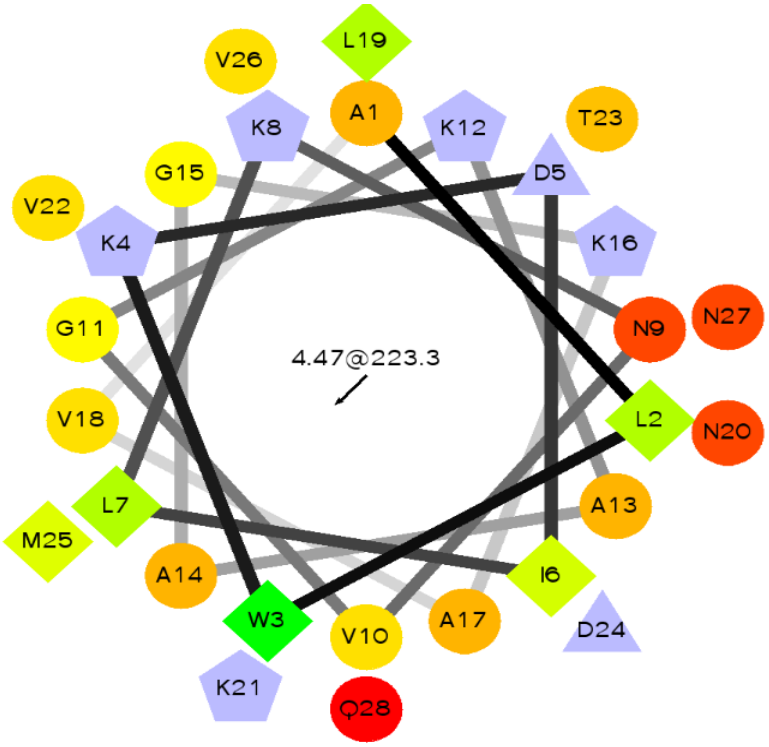
L19
V26
A1
K8
K12
T23
G15
D5
V22
K4
K16
N9
N27
G11
4.47@223.3
V18
L2
N20
L7
A13
M25
A14
I6
W3
V10
A17
D24
K21
Q28

(A)

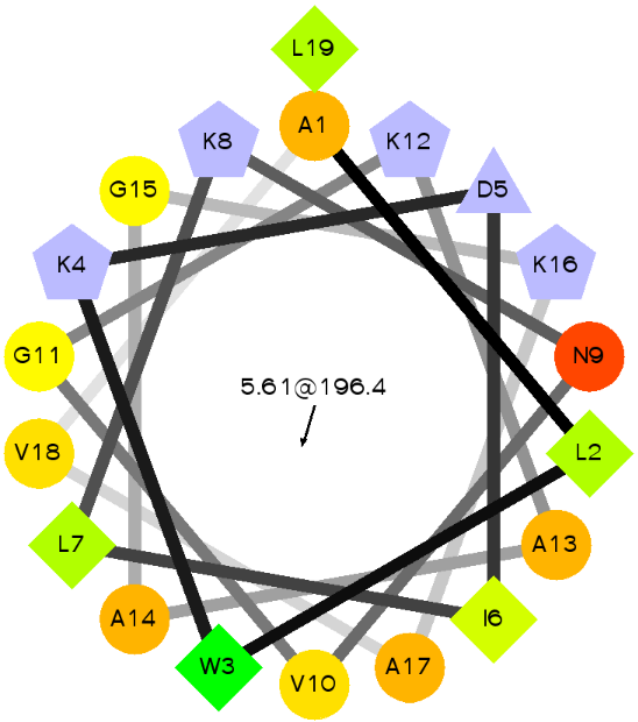
L19
A1
K8
K12
G15
D5
K4
K16
N9
G11
5.61@196.4
V18
L2
L7
A13
A14
I6
W3
V10
A17

(B)

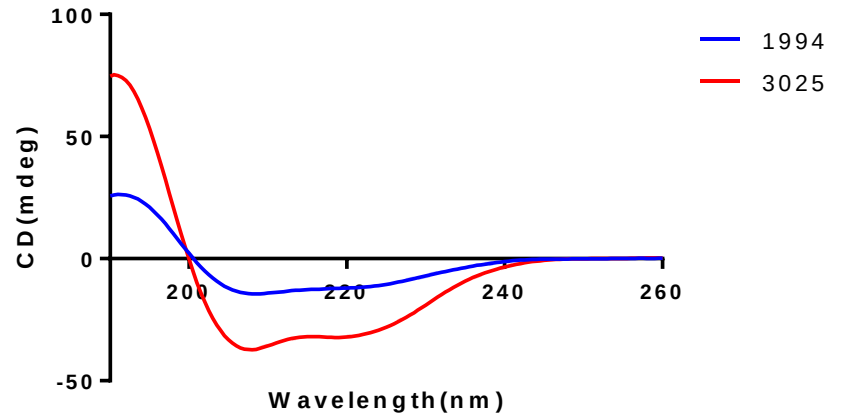

(C)

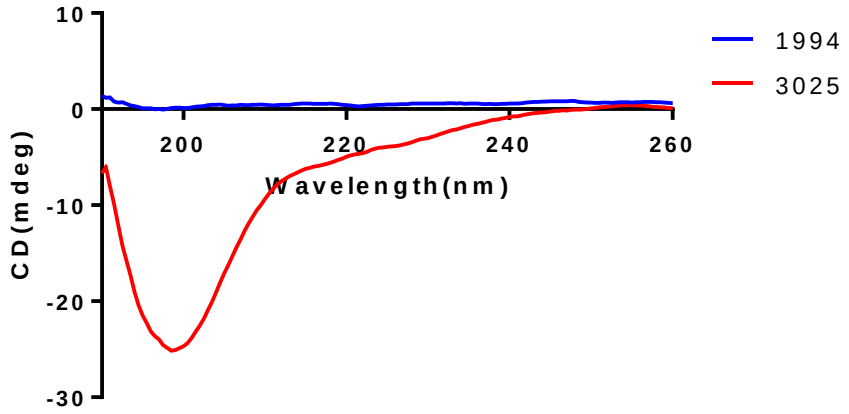

(D)

Figure 4.4 Helical wheel projections for (A) QUB-1568, (B) QUB-1774 and (C) QUB-2889. The potentially charged residues are light blue. The arrows indicate the direction of the hydrophobic moment (HM), the small number represents the HM magnitude, and the bigger number means the HM Angle. CD spectra recorded for QUB-3025 and QUB-1994 (100Mm) in 50% 2,2,2-trifluoroethanol (TFE)/10mM ammonium water solution(C) and in 10mM ammonium acetate water solution(D).

4.3.5 Antimicrobial assays

The synthetic replicate of QUB-3025 showed a broad spectrum antimicrobial activity towards Gram +ve bacteria as well as yeast. However, and when tested with *Escherichia coli* (*E.coli*), antibiotic resistant *Pseudomonas aeruginosa* (*P.aeruginosa*) and methicillin-resistant *Staphylococcus aureus* (MRSA), it was inferior to one of the most commonly used antibiotics: Ampicillin (Table 4.4). Interestingly, except for improvement of antibacterial activity against *E.coli*, the shorter designed peptide showed identical MICs to QUB-3025.

Table 4.4 Minimum inhibitory concentrations (MICs) determined for six different test microorganisms with natural peptide QUB-3025 and structurally-modified peptide QUB-1994. The blank control was established by the culture medium, and the positive control was represented growth culture. ND: not detected.

	Minimum Inhibitory Concentration (μM)					
	S.aureus	*E.coli*	*C.albicans*	*MRSA*	*E.faecalis*	*P.aeruginosa*
QUB-3025	4	4	8	16	128	32
QUB-1994	4	2	8	16	128	32
Norfloxacin	3.132	0.391	ND	0.4	12.8	0.8
Ampicillin	0.179	22.896	ND	ND	0.8	ND

4.3.6 *E.coli* membrane permeability assay

Following antimicrobial activity detection, QUB-3025 and its designed analogue were subjected to membrane permeability tests on the Gram-negative bacterium, *E.coli*. Both were found capable of increasing membrane permeability. For QUB-3025, the

permeability enhanced along with peptide concentration, while QUB-1994 showed membrane permeabilisation at its MIC. Each test was carried out individually over three experiments with three replicates for each concentration (Figure 4.5).

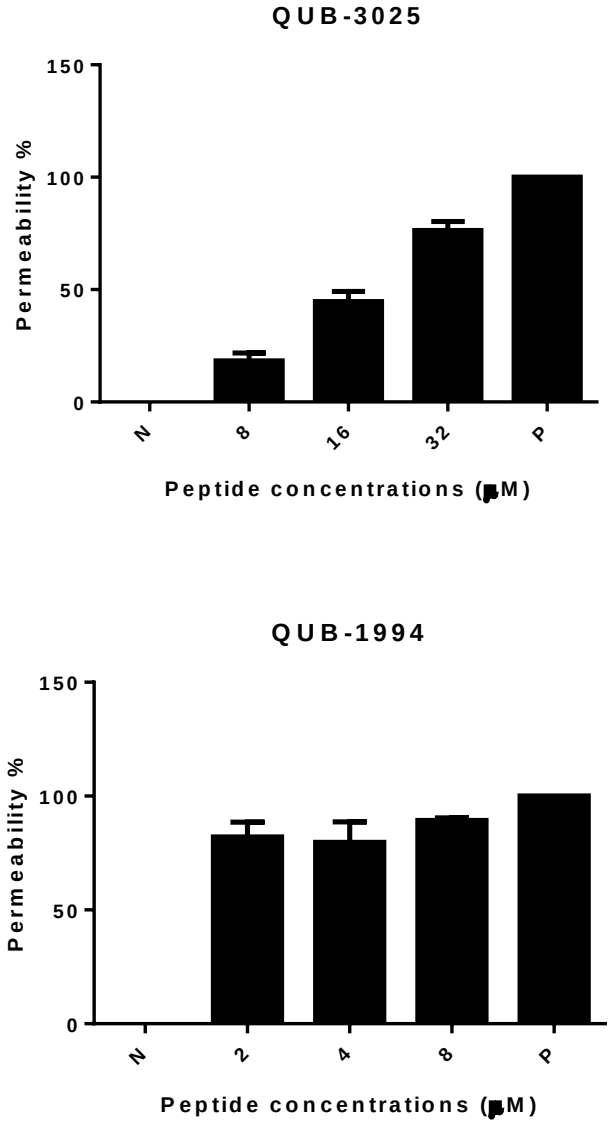

Figure 4.5 Cell-membrane permeability effects of QUB-3025 and QUB-1994 on *E.coli*, peptide concentrations corresponding to 1×MIC, 2× MIC and 4 ×MIC. P: positive control, incubation of *E.coli* with 70% isopropyl alcohol. N: negative control was represented as the vehicle only. Data represent means ± SD of 3 replicates.

4.3.7 Haemolysis assay

Following the evaluation of the haemolytic activity against horse red blood cells, both QUB-3025 and QUB-1994 showed haemolytic EC_{50} values at the level of 10^3 μM which is higher than Ampicillin (10^5 μM); however, they all showed relatively low haemolytic effects at their MICs. Besides, the haemolytic activity of melittin was much stronger than that of both and was also higher than its MICs (Table 4.5).

Table 4.5 Relative haemolysis for QUB-3025, QUB-1994, ampicillin and norfloxacin. The 100% haemolysis was induced by 1% Triton X-100.

NAME	EC_{50} (μM)
QUB-3025	1.971×10^3
QU8-1994	1.553×10^3
Ampicillin	> 512
Norfloxacin	> 512

1.7.1 Anti-cancer assay

Unfortunately, both QUB-3025 and QUB-1994 showed no significant anti-cancer activity against all tested cell lines (Figure 4.6). The human breast cancer cell line (MB435s), human prostate cancer cell line (PC3), the human lung cancer cell line (H157), human neurospongioma cell line (U251MG) and human breast cancer cell line (MCF-7) were all subjected to the MTT cell viability assay.

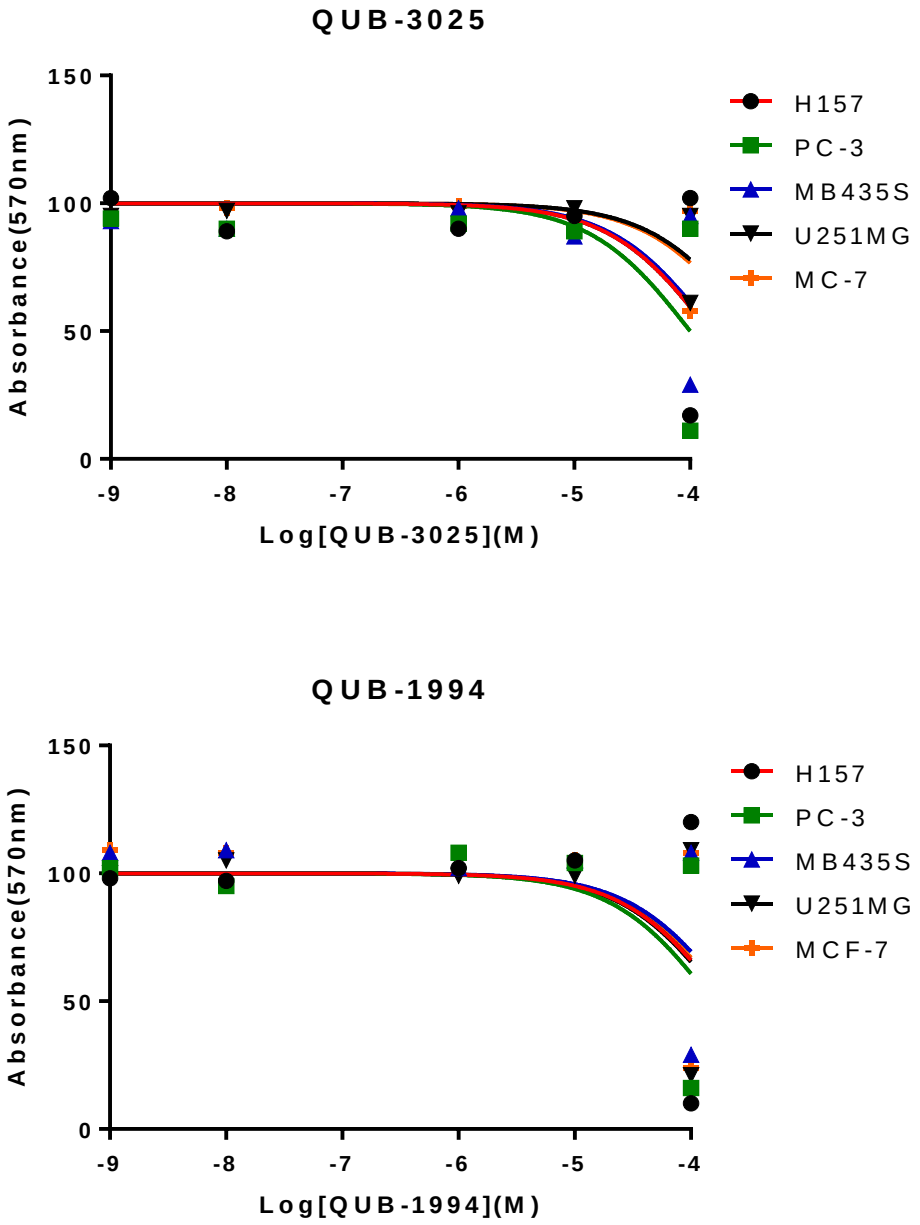

Figure 4.6 The concentration-absorbance curves showed anti-cancer effects of QUB-3025 and QUB-1994 against PC-3, H157, MB435S, U251MG and MCF-7 cell lines.

4.4 Discussion

In this study, a novel bioactive peptide named QUB-3025 was isolated and characterised from the defensive skin secretion of *Phyllomedusa coelestis*, it was a process including the combination of molecular cloning, high-performance liquid chromatography analysis

and tandem mass spectrometry technology. It turned out that QUB-3025 is a typical dermaseptin peptide which consists of 28 amino acids with the basic sequence (-GKAAG-) as well as the conserved Tryptophan residue. Based on the sequence feature of dermaseptin, a shorter analogue of QUB-3025 was designed to determine the importance of conserved sequence. As listed in Table 4.6, most dermaseptins possess broad-spectrum antimicrobial activities, and do not have haemolytic activity at MICs, compare to other dermaseptin peptides, QUB-3025 showed an antimicrobial activity in average level; however, it showed little haemolysis which is a significant advantage for peptide clinical development.

Table 4.6 Comparisons of bioactivities among QUB-3025, Dermaseptin-B4 (DRS-B4) (Charpentier et al. 1998), Dermadistinctin-L (DDL) (Batista et al. 1999), Dermadistinctin-L1 (DRS-L1) and Dermaseptin-B2 (van Zoggel et al. 2012, Galanth et al. 2008). "ND" means not detected, "-" indicates no data found.

		QUB-3025	DRS-B4	DDL	DRS-L1	DRS-B2
MIC(μM)	S.	4	3.0	1.3	>128	0.7
	E.	4	5.0	2.5	8	0.8
Haemolysis(μM)		>128	-	≥12.5	>100	>50
Anticancer		ND	-	-	HepG2 cells	PC-3 cells

Dermaseptins are a family of cationic peptides, most of them were found to possess potent antimicrobial activity due to the amphipathic helical structure they adapt at the bacteria membrane, which is essential reason for their selective bacteria membrane disruptive action (Pierre et al. 2000). The fluorescent emission analysis of the NBD-labelled dermaseptin-S1 (Pouny et al. 1992) revealed the binding affinities between S1 and different small unilamellar vesicles (SUV). S1 was found to aggregate on the acidic

SUV as membrane-bound monomers, self-associated and then penetrate into the hydrophobic pocket of the membrane, while none of this happened at the presence of zwitterionic SUV and the alpha-helical conformation could help dermaseptin bind to the acidic SUV membrane tightly and disrupt the membrane with carpet mode (Amiche et al. 2008).

The synthetic replicates of QUB-3025 and its shorter analogue QUB-1994 were subjected to antimicrobial tests against six pathogens, and interestingly, they exhibited identical MICs towards almost all tested microorganisms with only one exception, the Gram-negative bacterium *E.coli*. The newly designed peptide showed even better inhibitory activity (MIC=2 μM) against *E.coli* than the original peptide did (MIC=4 μM), and this can be explained by their differences in properties and secondary structures. As the predicted helical wheels showed, QUB-1994 showed better amphipathicity than QUB-3025 due to a more definite division of hydrophobic side and hydrophilic side. Compare to QUB-1994, QUB-3025 contains more hydrophilic residues K21, D24, Q28 (the most hydrophilic), N20, N27, which can also be proven by the hydrophobicity change, QUB-1994 showed a distinct increase of GRAVY. Regarding the mechanisms, both peptides were membrane-disruptors; however it took higher concentrations for QUB-3025 to destroy the *E.coli* cell membrane and QUB-1994 was capable of membrane permeabilisation at MIC. Thus, it is reasonable to speculate that QUB-1994 acts in "carpet mode" while QUB-3025 acts in "toroidal mode". Typically, the net charge of an AMP is considered as the most effective factor for antimicrobial activity; however, in this situation, it can be suggested that the increased hydrophobicity brings more effective membrane permeabilization, which is responsible for the stronger activity. The results may also indicate that shortening the C-terminal, but keeping the conserved sequence, would not significantly alter the antimicrobial activity of dermaseptins.

In the antimicrobial test, two commonly used antibiotics were also applied for comparison. Ampicillin (Delcour 2009), belongs to beta-lactam antibiotics, has been utilised to against many infectious diseases, like respiratory tract infections, urinary tract infections, meningitis, salmonellosis, and endocarditis. It is capable of penetrating Gram-positive and some Gram-negative bacteria, and irreversibly inhibiting of the enzyme transpeptidase which is vital in bacterial cell wall synthesis, thus, result in bacteriolytic. As for Norfloxacin (Shen, Pernet 1985), it is a type of synthetic fluoroquinolone antibiotics, which is effective against urinary tract infections, gynaecological infections, inflammation of the prostate gland, gonorrhoea and bladder infection. Its activity is achieved by inhibiting the necessary enzymes for bacterial DNA separation via binding to the substrate DNA, thereby inhibiting cell division.

Compare to the two antibiotics, QUB-3025 possess more broad-spectrum activity even against the pathogenic yeast, *C.albicans*. Since these two antibiotics tend to achieve their antibacterial activity by inhibiting specific enzymes that are important to some cellular processes, while these enzymes are different in prokaryotic bacteria and eukaryotic fungi. For AMPs, they are most membrane-active, and cell membrane can be found both in bacteria and fungi, cationic AMPs can bind to the polysaccharides from the fungal cell wall and then disrupt the cell membrane to accomplish the antifungal activity (K. Wang et al. 2016). More detailed, QUB-3025 showed great inhibitory of *E.coli* that even not inferior to ampicillin did, which is related to not only the cell structure of *E.coli* but also antimicrobial mechanisms of both ampicillin and QUB-3025. *E.coli* belongs to Gram-negative bacteria, which means it has the anionic outer membrane and relatively thin cell wall (peptidoglycan layers), this confirmation may make it hard for ampicillin to penetrate outer membrane and target the enzyme transpeptidase to inhibit cell wall synthesis. In contrary, cationic AMPs will attractively bind to the anionic outer

membrane, and it is easier for penetration with the relatively thin cell wall. This explanation can also be applied to illustrate why ampicillin showed better inhibitory towards *S.aureus* than QUB-3025 did. Gram-positive bacteria have a thicker cell wall but no outer membrane, inhibiting the cell membrane synthesis would be more effective than penetrating the thick peptidoglycan layers and then interacting with the cell membrane. In terms of the potent antimicrobial activities, both ampicillin and QUB-3025 showed little haemolytic activity towards horse erythrocytes.

To date, several antimicrobial dermaseptins were also reported to possess anticancer activity. Dermaseptin B2 (Drs B2), isolated from the skin secretions of the Amazonian tree frog *Phyllomedusa bicolor*, was found to have excellent antitumor activity against several cell lines such as prostate cancer cells PC-3 and LNCaP, liver cancer cells DU-145, breast cancer cells MDA-MB-231 and lymphoma cancer cells Raji. The antitumor mechanism of Drs B2 against human prostate cancer cell line PC-3 was suggested to be membrane-related necrosis involving a carpet-like manner (van Zoggel et al. 2012). Dermaseptin L1 (Conlon et al. 2007) is another ACP identified from the lemur leaf frog *Hylomantis lemur*, and it showed selectively growth inhibitory against the human hepatoma-derived HepG2 cells (with IC50=45μM). The recently characterised Dermaseptin-PH, isolated from the South American Orange-Legged Leaf Frog, also showed potent activity against five cell lines (H157, MCF-7, U251MG, MDA-MB-435S, and PC-3). However, no significant anticancer activity was detected for QUB-3025 and its designed analogue. As shown of the sequence alignments table 4.7, peptides from different sources and with different length all exhibit the conserved third W and the sequence -V(A)GKAAL(G)-. Moreover, the ACP sequences contain glutamic acid residues that QUB-3025 does not have. Since glutamic acid has been involved in anticancer therapies whether by itself or by conjugating with other drugs (Dutta et al.

2013), it can be conjectured that glutamic acid residues play an important role for the anticancer activity of dermaseptins. A further investigation like residue substitution can be done to verify this conjecture.

Table 4.7 Sequence alignments among QUB-3025, dermaseptin PH, dermaseptin B2 and dermaseptin L1. The conserved residues among three peptides are yelllow hilighted, while gluttamic acids that only occur in ACPs are gray highlighted.

NAME	SEQUENCE	Number
QUB-3025	ALWKDILKNVGKAAGKAVLNKVTDMVNQ-NH_2	28
Drs PH	ALWKEVLKNAGKAALNEINNLV-NH_2	22
Drs L1	GLWSKIKEAAKAAGKAALNAVTGLVNQGDQPS	32
Drs B2	GLWSKIKEVGKEAAKAAAKAAGKAALGAVSEAV-NH_2	33

To sum up, the newly identified bioactive peptide named QUB-3025, from the skin secretions of *Phyllomedusa coelestis*, showed high sequence homology to the dermaseptin peptide family. QUB-3025 was proven to be an antimicrobial peptide with a broad-spectrum activity that even bears comparison with one of the most commonly used antibiotics, ampicillin. Interestingly, compared to QUB-3025, its shorter analogue showed little change in antimicrobial activity, which may suggest the C-terminal sequence of dermaseptin has little contribution to antimicrobial activity. Besides, weak haemolytic activity was found for both peptides, which provides enormous potential for them to become clinical drugs.

CHAPTER 5

A novel Kunitz-like trypsin inhibitor isolated from the defensive skin secretion of the Odorous frog: *Odorrana versabilis*.

5.1 Introduction

Protease inhibitors (PIs) are pervasive molecules in organisms, and they are commonly involved in potential drug design for the treatment of cancer, hypertension, inflammation, diabetes and protozoan infections (McKerrow et al. 2008). In 2004, based on similarities detectable at the level of amino acid sequence, Neil D. Rawlings and his colleagues (Rawlings et al. 2004) identified 48 protease inhibitor families, and according to the MEROPS database, there are now 99 families of inhibitors (https://www.ebi.ac.uk/merops/cgi-bin/family_index?type=I). In many studies, however, researchers also like to classify protease inhibitors through their catalytic types, thus, inhibitors can be classified as serine-, cysteine-, aspartic and metallopeptidase inhibitors (Krowarsch et al. 2003).

Skin secretions from amphibians are an abundant source of multi-functional bioactive peptides and these peptides are useful agents for hydration, regulating and strengthening defensive mechanisms and consequently, they are expected to possess great pharmaceutical potential like protease inhibitors, neural stimulation, immunomodulatory, antimicrobial, anticancer, etc. (Całkosiński et al. 2009). Over the past decades, many different kinds of trypsin inhibitors have been identified from amphibian secretions, and according to the similarities of structural domains, sequences, reactive sites and mechanisms, these inhibitors can be classified as different types (e.g. Kazal-, Bowman-Birk and Kunitz-type) (Proaño-Bolaños et al. 2017). Kazal-type inhibitors have been isolated from phyllomedusine frogs (R. Li et al. 2012), such as the Splendid leaf frog (Proaño-Bolaños et al. 2017), Bowman-Birk inhibitors from *Odorrrana* frogs (M. Wang et al. 2012), and Kunitz-type inhibitors from the tomato frog (Conlon, Kim 2000) and ranid frogs (X. Chen et al. 2016). Kunitz-type inhibitors are a type of serine protease inhibitor which generally consist of 50 to 60 amino acid residues and are stabilized by a

disulphide bond-rich structure and a highly exposed P1 active site residue for interacting with proteases (trypsin mostly) is usually arginine or lysine. Therefore, this family of inhibitors are traditionally considered as trypsin inhibitors (Smith et al. 2016, J. Li et al. 2008).

Over the past decades, many different types of protease inhibitors have been identified from amphibian secretions and these inhibitors with low molecular weights and potent inhibitory activity, were thought to be potential candidates for novel peptide drugs (Krowarsch et al. 2003). Odorous frogs are distributed in East Asia and surrounding areas and their skin secretions have been well-studied with several trypsin inhibitors from these species having been reported (J. Li et al. 2008, Wu et al. 2017, M. Wang et al. 2012). As a member of the *Odorrana* genus, *Odorrana versabilis* was chosen as a research object which has a great potential to provide novel and functional protease inhibitors.

In this study, the cloning of skin-derived cDNAs and identification and structural characterisation of a novel peptide with potent trypsin inhibitory activity, are described. According to bioinformatic analysis, this peptide is a member of the Kunitz-type inhibitor family with a canonical Kunitz-type reactive centre. Meanwhile, a P1-substituted analogue was also synthesised and evaluated.

5.2 Methods

5.2.1 Specimen Biodata and Secretion Acquisition

Eight specimens of *O. versabilis* (6–8cm snout-to-vent length, sex undetermined) were collected in the field in China. The frogs were kept in a vivarium at 25℃ under a 12 h/12 h day/night cycle and were fed crickets three times per week. Their skin secretions were harvested after the frogs had been maintained under these conditions for around 4 months. The dorsal skin surface was stimulated by gentle transdermal electrical stimulation (6V

DC; 4 ms pulse-width; 50 Hz) through platinum electrodes for two periods of 20s. The resultant viscous white secretion was washed from the skin with deionised water, snap-frozen in liquid nitrogen and finally lyophilised and stored at -20 ℃ before analysis. All procedures were subjected to ethical approval and carried out under appropriate UK animal research personal and project licenses.

5.2.2 Molecular Cloning of Kunitzin-OV Precursor-Encoding cDNA from a Skin Secretion-Derived cDNA Library of *O. versabilis*

The isolation of pure mRNA from crude skin secretion was achieved by utilizing a magnetic oligo-dT bead kit which could bind polyadenylated mRNA in the cell lysis buffer supplied with the kit. Reverse transcription and synthesis of first-strand cDNA was followed by a 3'-RACE reaction to isolate target antimicrobial peptide precursor nucleic acid sequence data with a SMART-RACE kit. 3'-RACE was facilitated by a nested universal primer (NUP) (supplied by the kit) and a sense primer (REry-3: 5'-GAWYYAYYHRAGCCYAAADATG-3') which was designed to a highly conserved domain of the 5'-untranslated region of previously characterized antimicrobial peptide cDNAs from *Rana* species. The PCR cycling procedure included an initial denaturation step at 94 ℃ maintained for 90 s, then 35 thermal cycles which involved 60 s at 94 ℃ for denaturation, primer annealing for 30s at 58℃, and 180 s for the extension at 72℃. The PCR products were purified by gel electrophoresis and cloned using a pGEM-T vector system. The DNA sequences of clones were obtained by use of an ABI 3100 automated capillary sequencer.

5.2.3 Identification and Structural Analysis of Peptides in Skin Secretion

A further 10 mg of lyophilised skin secretion was dissolved in 1.5 mL of 0.05/99.95 (v/v) trifluoroacetic acid (TFA) /water and then clarified by centrifugation. The supernatant (1 mL) was then subjected to reversed phase HPLC using a Waters gradient reverse phase HPLC system, fitted with an analytical column (Jupiter, C5, 300 Å, 5μm, 4.6 mm×250 mm, Phenomenex, Macclesfield, Cheshire, UK). Column elution was achieved with a gradient formed from 0.05/99.95 (v/v) TFA/water to 0.05/29.95/70.00 (v/v/v) TFA/water/acetonitrile in 240 min at a flow rate of 1 mL/min, and the effluent was monitored by UV absorbance at 214 nm 280 nm. The eluted fractions were collected at 1 min intervals. The molecular masses of peptides in each fraction were further analysed by use of a MALDI-TOF mass spectrometer (Voyager DE, PerSeptive Biosystems, Foster City, CA, USA) in positive detection mode using α-cyano-4-hydroxycinnamic Acid (CHCA) as the matrix. Fractions with peptide molecular masses coincident with those of the mature peptides predicted from the cloned cDNA were then infused into an LCQ Fleet ion-trap electrospray mass spectrometer (Thermo Fisher Scientific, San Francisco, CA, USA) followed by trapping of suitable ions for MS/MS fragmentation.

5.2.4 Solid-Phase Peptide Synthesis

Following the confirmation of primary structures of the cloned cDNA-encoded peptides, the wild-type peptide and its truncated analogue were chemically-synthesised by an automated solid phase peptide synthesiser (Protein Technologies, Tucson, AZ, USA). After cleavage from the synthesis resin and side-chain deprotection, the peptides were purified by reversed phase HPLC and both molecular masses and MS/MS fragmentation profiles were employed to confirm the purity and authenticity of their structures. The

physicochemical properties of the peptides, such as the number of amino acids, molecular mass, theoretical pI, net charge and grand average of hydropathicity, were computed using ProtParam.

5.2.5 Minimal Inhibitory Concentration Assays

Antimicrobial activity of the peptides was monitored by determination of minimal inhibitory concentrations (MICs) using standard model microorganisms: the Gram-positive bacterium, *Staphylococcus aureus* (NCTC 10788), the Gram-negative bacterium, *Escherichia coli* (NCTC 10418) and the yeast, *Candida albicans* (NCPF 1467). The peptides were initially dissolved in physiological PBS to yield stock solutions of 5.12 × 104 μM. MICs were determined within the peptide concentration range of 1μM to 512μM, obtained through dilution of the stock solutions in PBS. The assays were carried in 96-well microtitre plates, and the respective concentrations of peptides and controls were inoculated with microorganism cultures (5×10^5 CFU/mL). The plates were incubated for 18 h at 37℃ in a humidified atmosphere. Following this, the growth of the microorganisms was determined by measuring the optical density of the culture at 550 nm using a microplate reader (EL808, Biolise BioTek, Winooski, VT, USA).

5.2.6 Haemolysis Assay

A suspension of horse red blood cells (4%, v/v) (TCS Biosciences, Botolph Claydon, Buckingham, UK) was incubated with peptides of the concentration range of 1 μM to 512 μM at 37 ℃ for 2 h. PBS together with cells served as a negative control and 2.0% of Triton X-100™ (Sigma-Aldrich) mixed with cells were taken as a positive control. Then haemolysis detection was assessed at 550 nm by a microplate reader.

5.2.7 Trypsin inhibition assay

Trypsin (10 µl of a 0.1 µM stock solution in 1mMHCl) was added to the wells of a micro-titre plate containing substrate (Phe-Pro-Arg-NHMec, obtained from Sigma/Aldrich, Poole, Dorset, UK) (50 µM) and either reconstituted chromatographic fraction (33%), in the first instance or, subsequently, synthetic peptide replicates (10-1000 µM) in 10 mM phosphate buffer, pH 7.4, containing 2.7 mM KCl and 137 mM NaCl (final volume 210 µl). Each determination was carried out in triplicate. The rate of hydrolysis of the substrate was monitored continuously at 37 ℃, by measuring the rate of increase of fluorescence due to the production of 7-amino-4-methylcoumarin (NH_2Mec) at 460 nm (excitation 360 nm) in aFluoStar OPTIMA plate reader.

5.2.8 Chymotrypsin inhibition assay

Inhibitory activity assays on synthetic peptide replicate and their various P1-site-substituted variants against chymotrypsin, were performed the same as detailed for the trypsin inhibition assay 3.7, except that the target protease was chymotrypsin and the fluorogenic substrate utilised was Succinyl-Ala-Ala-Pro-Phe-NHMec obtained from Bachem, UK.

5.2.9 Trypsin cleavage of inhibitor peptides

1 mg of trypsin and 1 mg of synthetic Kunitzin-OV were incubated in 1 ml of sodium phosphate buffer, at room temperature for 2 h. Samples (20 µl) were removed at 0, 1, 2, 5, 10, 20 min, respectively, into 0.05% (v/v) trifluoroacetic acid/water to terminate reactions. One µl of each sample from different time points was subjected to analysis on a MALDI-TOF instrument.

5.3 Results

5.3.1 Molecular cloning and sequencing analysis of Kunitzin-OV

From the skin-derived cDNA library of *Odorrana versabilis*, the cDNA encoding the biosynthetic precursor of a putative novel bioactive peptide named Kunitzin-OV was consistently and repeatedly cloned. The open-reading frame of this cloned precursor consisted of 63 amino acid residues, which included a 22 amino acid residues signal peptide and a mature peptide of 13 amino residues. The putative peptide sequence was preceded by two successive basic amino acids, Lys-Arg (KR), which represented a typical cleavage site. A single disulphide bond (Cys 8-3) was located at the C-terminal (Figure 5.1). From the NCBI -BLAST analysis, the novel peptide showed 71% identity with ishikawain-2 from *Odorrana ishikawae* and 100% identity of a kunitzin precursor (Figure 5.2).

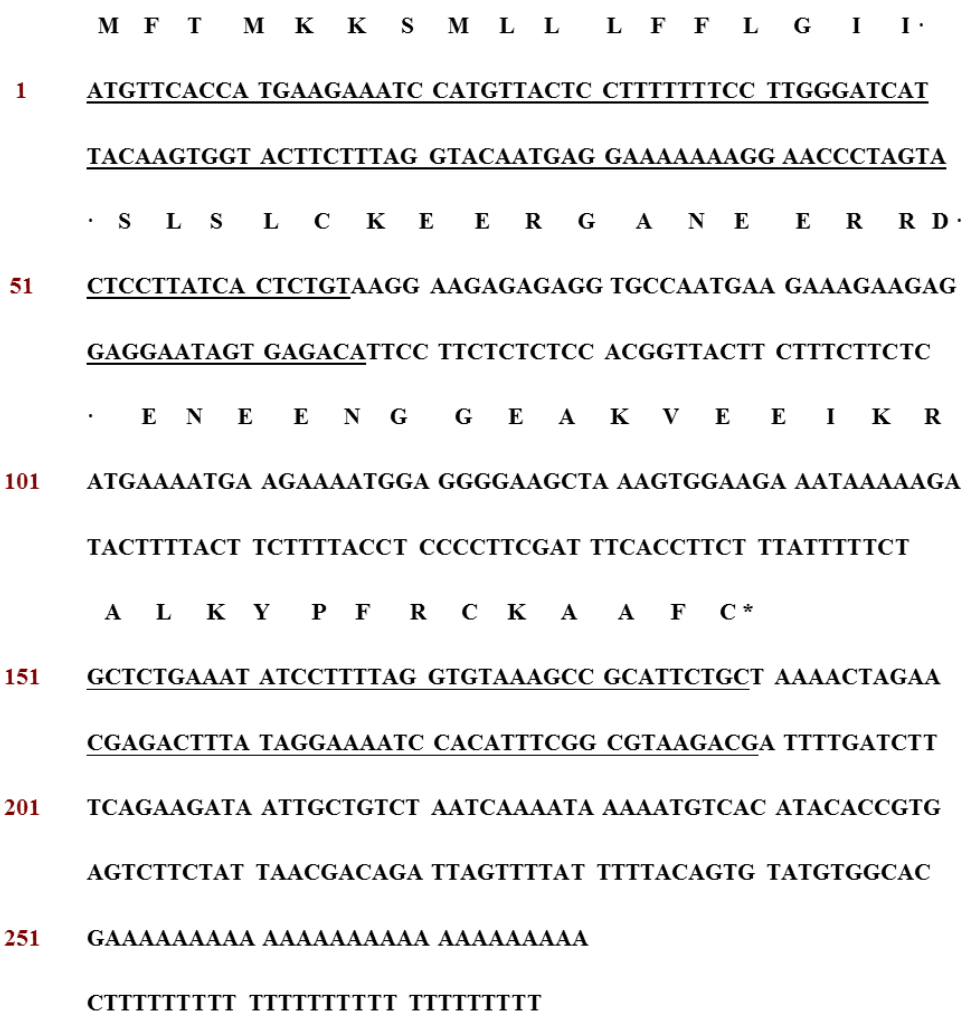

Figure 5.1 The open-reading frame the biosynthetic precursor of Kunitzin-OV. The putative signal peptide is double-underlined, the mature peptide is single-underlined, and an asterisk indicates the stop codon.

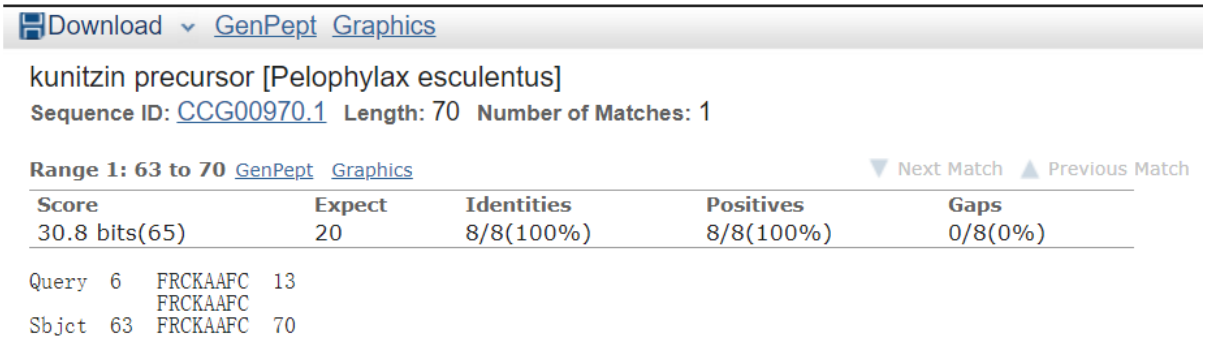

Figure 5.2 NCBI-BLAST analyses of the mature peptide of the Kunitzin-OV biosynthetic precursor-encoding cDNA.

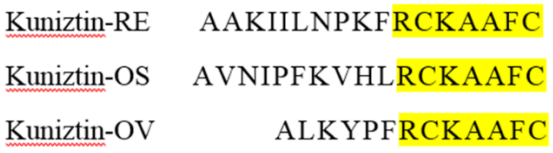

Figure 5.3 The primary structure of the novel Kunitzin-OV from *O. versabilis* skin secretion compared with other kunitzins. Fully conserved residues are highlighted.

5.3.2 Identification and structural characterisation of peptides

By using a gradient reverse-phase HPLC as described, each fraction was identified by MALDI-TOF MS. After comparison of the computed and the determined molecular masses of Kunitzin-OV, the elution site of the peptide was confirmed (Figure 5.4). The peptide structure was characterised by MS/MS fragmentation sequencing (Figure 5.5).

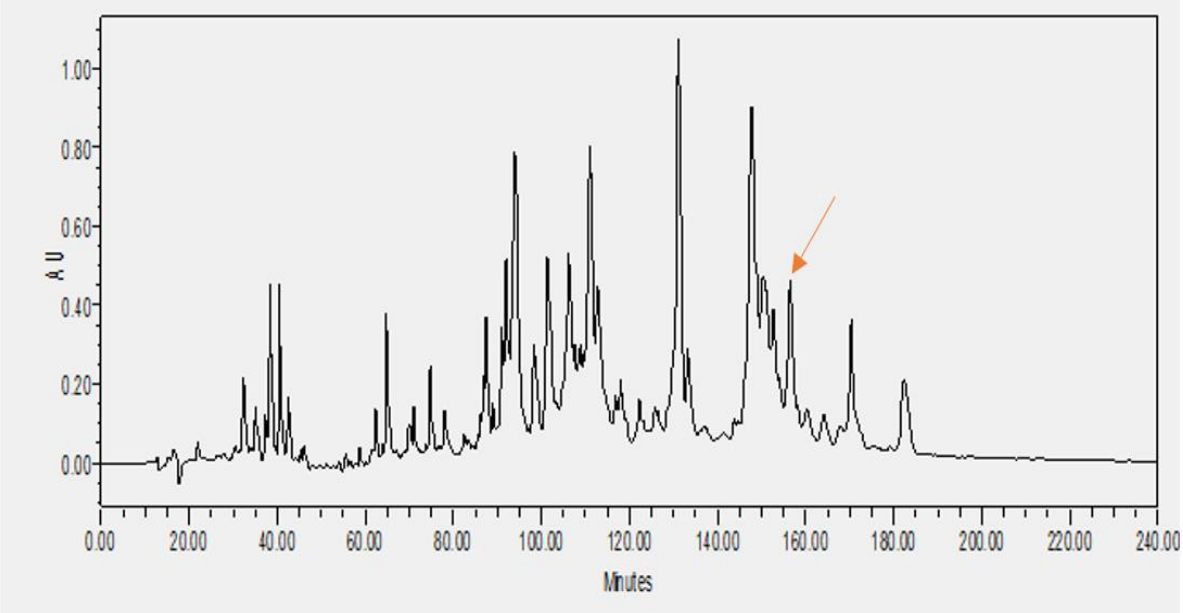

Figure 5.4 The reverse-phase HPLC chromatogram of the skin secretion of *Odorrana versabilis*, the elution position is indicated with an arrow. The components were monitored at a wavelength of 214 nm.

Table 5.1 Predicted b- and y-ion series (singly and doubly charged) of QUB-1568 through a molecular cloning peptides database. Observed fragment ions in MS/MS spectra were indicated in colour.

#1	b(1+)	b(2+)	Seq.	y(1+)	y(2+)	#2
1	72.04444	36.02222	A			13
2	185.12850	92.56425	L	1446.73850	723.36925	12
3	313.22346	156.61173	K	1333.65444	666.82722	11
4	476.28679	238.143395	Y	1205.559484	602.779742	10
5	573.33955	286.669775	P	1042.49615	521.248075	9
6	720.40797	360.203985	F	945.44338	472.72169	8
7	876.50908	438.25454	R	798.37497	399.187485	7
8	979.51826	489.75913	C	642.27386	321.13693	6
9	1107.61323	553.806615	K	539.26467	269.632335	5
10	1178.65034	589.32517	A	411.16971	205.584855	4
11	1249.68745	624.843725	A	340.13260	170.0663	3
12	1396.75587	698.377935	F	269.09549	134.547745	2
13	1499.76505	749.882525	C	122.02707	61.013535	1

5.3.3 Peptide synthesis

A replicate of Kunitzin-OV and its modified analogue were synthesised from C-terminus to N-terminus, by SPPS. The lysine-9 residue was substituted by a phenylalanine. Their sequences are shown in Table 5.2.

Table 5.2 The peptide sequences of Kunitzin-OV and its analogue. The substituted residue is in bold.

NAME	***SEQUENCE***
KUNITZIN-OV	ALKYPFRC**K**AAFC
KUNITZIN-OV VARIANT	ALKYPFRC**F**AAFC

5.3.4 Antimicrobial/ Haemolysis assays

The physicochemical properties of the peptides, such as the number of amino acids, molecular mass, theoretical pI, net charge and grand average of hydropathicity, were computed by ProtParam and are listed in Table 5.3. No significant antimicrobial activities were observed for Kunitzin-OV and its variant, while the previously discovered trypsin inhibitor, Kunitzin-RE (X. Chen et al. 2016), which had the identical C-terminal disulphide bond as Kunitzin-OV, did inhibit *E. coli.* (Table 5.4). Both peptides showed little haemolytic activity (less than 10%) even at concentrations up to 512 μM.

Table 5.3 Physicochemical properties of Kunitzin-OV and Kunitzin-RE (X. Chen et al. 2016), the grand average of hydropathicity (GRAVY).

	Number of amino acids	Molecular Weight	Net charge	GRAVY	Theoretical PI
Kunitzin-OV	13	1517.87	+3	0.354	9.39
Kunitzin-RE	17	1894.37	+4	0.547	9.85

Table 5.4 Minimum inhibitory concentrations (MICs) determined for three different test microorganisms with natural peptide Kunitzin-OV, Kunitzin-OV variant, the previously discovered trypsin inhibitor Kunitzin-RE and its variant (X. Chen et al. 2016). The blank control was established by the culture medium, and the positive control was represented growth culture.

peptides	Sequence	Minimum Inhibitory Concentration (μM)		
		S.aureus	*E.coli*	*C.albicans*
Kunitzin-OV	**ALKYPFRCKAAFC**	512	512	512
Kunitzin-OV Variant	**ALKYPFRCFAAFC**	512	512	512
Kunitzin-RE	**AAKIILNPKFRCKAAFC**	512	30	512
Kunitzin-RE Variant	**AAKIILNPKFRCFAAFC**	512	160	512

5.3.5 Trypsin inhibition and peptide cleavage

Kunitzin-OV displayed a trypsin inhibitory activity with a Ki value of 3.042 μM. With a Lys-9 residue occupying the P1 position, no chymotrypsin activity was observed. Whereas, when Lys-9 at P1 position was substituted by Phe (F), trypsin inhibitory activity totally disappeared, and a chymotrypsin optimised inhibitory activity was obtained, with a Ki value of 2.874 μM. The data of Kunitzin-RE and its variant are also shown for comparison. (Table 5.5)

The synthetic replicate of Kunitzin-OV and its variant were subjected to trypsin cleavage assay. The obtained fragments are presented in Table 5.6 and each shows that the catabolites are cleaved through typical trypsin cleavage sites.

Table 5.5 Inhibitor constants for QUB-1518 and its P1 site substituted variant against trypsin and chymotrypsin. P1 positions are bold. *N.I. =No inhibition.

	Peptide	***Ki (μM) (trypsin)***	***Ki (μM) (chymotrypsin)***
Kunitzin-OV	ALKYPFRC**K**AAFC	3.042	N.I.*
Kunitzin-OV Variant	ALKYPFRC**F**AAFC	N.I.	2.0874
Kunitzin-RE	AAKIILNPKFRC**K**AAFC	5.56	N.I.
Kunitzin-RE Variant	AAKIILNPKFRC**F**AAFC	48.37	17.5

Table 5.6 Fragments of Kunitzin-OV (A) and Kunitzin-RE (B) after incubating with trypsin. Each catabolite was detected by MALDI-TOF MS, and the observed molecular masses was compared to the computed values.

Cleavage fragments	Molecular weight (g/mol)	
	Calculated	Observed
ALKYPFRCKAAFC	1517.86	1521.71
ALKYPFR	894.07	896.66
YPFR	581.66	583.58
ALKYPFRCK	1125.39	1128.48
YPFRCK	812.98	815.24

（A）

Cleavage fragments	Molecular weight (g/mol)	
	Calculated	Observed
AAKIILNPKFRCKAAFC	1894.39	1894.85
IILNPKFRCKAAFC	1624.06	1625.23
AAKIILNPKFR	1270.58	1271.22
IILNPKFR	1000.25	1000.67
AAKIILNPK	967.21	968.05

（B）

5.4 Discussion

Odorous frogs are distributed in East Asia and surrounding areas, and they are named because of their smelly skin secretion which plays a fundamental role in defensive systems (X. Yang et al. 2011). To date, hundreds of functional peptides have been isolated from *Odorrana* skin secretion, not only many potent antimicrobial peptides but

also trypsin inhibitors. A small trypsin inhibitor OGTI was identified from *Odorrana grahami* (*with Ki value of* 0.4 μM) in 2008 (J. Li et al. 2008). A potent Bowman Birk-type trypsin inhibitor (with *a Ki* value of 388 ± 28 nM) was originally isolated from the skin of the Hejiang Odorous Frog, *Odorrana hejiangensis* (M. Wang et al. 2012). Additionally, a new class of protease inhibitor with trypsin inhibition (with a *Ki* of 5.56 mM) was reported in the skin secretion of *Odorrana schmackeri* (X. Chen et al. 2016).

In this study, a novel peptide was isolated from the skin secretion of the Chinese Bamboo Leaf Odorous frog, *Odorrana versabilis*, and it is a short peptide composed of 13 amino acids residues which contain a single disulphide bond (-CKAAFC-) located at the C-terminal between Cys8 and Cys13. The primary sequence of this novel peptide was subjected to homology searches using NCBI-BLAST, and it presented 100% identity to a kunitzin precursor. The name Kunitzin was originally reported for two trypsin inhibitors, Kunitzin-RE and Kunitzin-OS, from *Rana esculenta* and *Odorrana schmackeri* respectively (X. Chen et al. 2016). Based on the comparison of structure homology, the six-residue disulphide bond of the novel peptide is identical to the C-terminal loop of the previously reported kunitzins, while their amino acid residues are arranged in different order at the N-terminal. Besides, the novel peptide in this study was determined to possess the ability to inhibit trypsin as kunitzins do; as a result, this novel trypsin inhibitor was named Kunitzin-OV.

In the antimicrobial assay, Kunitzin-OV exhibited no significant inhibition against either Gram bacteria or yeast, which was quite different with the results obtained from the test on Kunitzin-RE, as this reported peptide possessed a narrow-spectrum antimicrobial activity against the Gram-negative bacterium *E.coli*. The results just corresponded to the physicochemical properties of these two peptides, Kunitzin-RE contains one more net

charge and a higher GRAVY index than Kunitzin-OV, in which more positive charge brings better electrostatic attraction between cationic peptide and anionic bacteria membrane surface, and higher hydrophobicity promotes the peptide to permeate the bacteria bilayer and interact with the hydrophobic tail (Bahar, Ren 2013). Moreover, these results also suggested that the disulphide bond (-CKAAFC-) is not a decisive factor for antimicrobial activity, as Chen (X. Chen et al. 2016) and his colleagues also synthesised this single loop alone to test its antimicrobial properties, and no activity was observed against all tested microbes. In 1995, Sonohara and his partners (Sonohara et al. 1995) investigated the differences between the surface of *S.aureus* and *E.coli* via electrophoretic mobility measurements, and they found that *E. coli* had a more negatively charged and less soft surface than that of *S. aureus*. Meanwhile, *C.albicans* is a potentially pathogenic yeast, it is a eukaryotic organism and has different cell wall components than bacteria. These may explain why Kunitzin-RE only showed limited activity against *E.coli*.

Table 5.7 Comparison of the reactive site (highlighted) of kunitzin-OV with different kind of Kunitz-type protease inhibitors. The reactive sites are highlighted.

NAME	Number of amino acids	REACTIVE SITE	SOURCE
Kunitzin-OV	13	-F R C K A A F-	This study
VKTO1_HAPHA	55	-G R C K A S F-	UniProtKB - D2Y2Q6
VKTCT_OPHHA	58	-G F C K A Y I-	UniProtKB - B6RLX2
BPT1_BOVIN	58	-G P C K A R I-	UniProtKB - P00974
CSTI_BOMMO	55	-G P C K G S F-	UniProtKB - P81902
SPIT2_HUMAN	51	-G P C R A S F-	UniProtKB - O43291

domain 2			
AMBP_HUMAN domain 2	51	-G P C R A F I-	UniProtKB - P02760
VKT_OXYSC	51	-G P C R A A I-	UniProtKB - B7S4N9

In a further investigation, Kunitzin-OV was subjected to protease inhibitor assay, and it showed inhibition of trypsin with a *Ki* value of 3.042 μM and no inhibitory activity towards chymotrypsin which is about the same as Kunitzin-RE (inhibition of trypsin with *Ki*=5.56 μM). Based on the bioinformatics analysis, the C-terminal disulphide-bridged loop of Kunitzin-OV displayed a high degree of similarity to the reactive centre of several Kunitz-type inhibitors from different sources (Table 5.7), the P1 position of all these inhibitors are occupied by either a K (Lys) or an R (Arg) residue. Since the sequence of Kunitzin-OV is quite short, and it does not contain the conserved G (Gly) residue at the P4 position as the other Kunitz-type inhibitors do, we suggested it as a novel and non-typical Kunitz-type trypsin inhibitor from amphibian skin secretions. Kunitzin-OV is not the only example, except for the other two kuniztins mentioned above, OGTI (J. Li et al. 2008) is also a trypsin inhibitor (AVNIPFKVHFRCKAAFC) from *Odorrana grahami* that belongs to this type, and it has the identical reaction loop of kunitzins. Furthermore, the Ishikawain-2 from *Odorrana ishikawae*, which also contains the C-terminal six-residue loop, was first considered as an antimicrobial peptide, but no antimicrobial activity was found after testing (Sonohara et al. 1995). We thought it is highly likely to be a member of this particular kind of trypsin inhibitor, but surely further research is needed to prove it.

By replacing Lys-9 with Phe, the site-substituted analogue showed an optimised chymotrypsin inhibitory activity (with *Ki* value of 2.0874μM), while the inhibitory

activity towards trypsin was totally inhibited. Generally, kunitz-type inhibitors achieve their inhibition through a standard mechanism (canonical inhibition), they interact with the target via a tight and non-covalent bond, which is just like enzyme-substrate complex. Without any changes of conformation, the inhibitors block the active site of the serine protease, and an antiparallel β-sheet is formed between the enzyme and its inhibitor. The so-called protease-binding loop refers to an extended, solvent-exposed and convex fragment that has charge of protease inhibitory activity, and the location of the reactive site (P1-P'1 peptide bond) is in the most exposed part of this loop. Crossing from P3 to P'3 position, the protease-binding loop is highly complementary to the concave enzyme active site (Krowarsch et al. 2003). Thus, in this study, -RCKAAF- is the trypsin-bonding loop and the reactive site (K-A) is complementary to the trypsin active site, once the Lys-9 (P1 position) was substituted by Phe, the trypsin inhibitory activity vanished. It also suggested that the variant contains the reactive site (K-F) which works for the inhibition of chymotrypsin. Apparently, it is natural selection that a Lys residue occupied the P1 position of kunitzins to regulate the inhibitory activity towards trypsin.

In the case of Kunitzin-RE, the result is slightly different, weak inhibition of trypsin (*Ki*=48.37μM) was still observed for the substituted analogue. Combine with the data obtained from trypsin cleavage, each segment of both Kunitzin-OV and Kunitzin-RE was cleavage by trypsin via typical cleavage site Lys and Arg, the difference was the C-terminal function loop of Kunitzin-OV was catabolized via Lys-9 while this did not happen to Kunitzin-RE. Considering to the N-terminal structure of both peptides, it can be assumed that the Lys close to the most exposed region of the protease-binding loop is also associated with trypsin inhibitory activity and could protect the functional disulphide loop from cleavage, in this way, the inhibitory activity may be more stable and effective. Actually, it has been described that association energy can be influenced by residues

around the protease-binding loop and even from a distant region and these residues can still contact enzyme (Ascenzi et al. 2003).

On the basis of the catabolites obtained in the trypsin cleavage assay, Kunitzin-OV was catabolized by trypsin through the classical cleavage sites Lys and Arg. These data may imply that Kunitzin-OV achieves its inhibition by competing with the substrate for the active site of the trypsin. Besides, the functional loop was cleaved via the Lys-9 residue at the very end of the incubation, which means this sequence was catabolized in a highly-ordered way and the inhibitory reaction would continue until the loop was cleaved. As above-mentioned, addition of a Lys or Arg residue around the loop may be an efficient way to protect the P1 position from cleavage, although further research needs to be done to prove this.

Kunitzin-OV is a novel peptide isolated from the defensive skin of the Odorous frog, *Odorrana versabilis.* It is considered as a non-typical Kunitz-like trypsin inhibitor with a highly conserved reactive site (K-A) and quite a short sequence. However, its protease-binding loop was catabolized by trypsin during the trypsin cleavage test, and further modification should be done to improve its stability.

Chapter 6

General Discussion

6.1 Structure/Activity relationships of AMPs

Due to their broad-spectrum effects and low drug resistance induction, naturally-occurring antimicrobial peptides are regarded as potential alternatives to drug resistance-inducing antibiotics (Jenssen et al. 2006). However, as nothing is perfect, to keep the balance between strong antimicrobial activity and cytotoxicity of these naturally-occurring potent peptides, rational peptide modification is required (Porto et al. 2012). The activities of AMPs are closely related to their physiochemical properties including length, net charge, amphipathicity, hydrophobicity and helicity (Alessandro et al. 2000), and reasonable adjustment of these characteristics can optimise the activities of AMPs. Apparently, it is not easy, but a comprehensive work due to a simple change of an amino residue could entirely change the peptide properties, thus alter the peptide activity.

In this study two newly isolated antimicrobial peptides together with their modified analogues were employed in a series of functional assays, and the results showed the modifications of sequence could bring different activities. Firstly, the sequence length can influence the peptide haemolytic activity to some extent. Compared to QUB-1568, its more extended analogues shower higher haemolysis; similarly, QUB-3025 also showed higher EC_{50} values against horse erythrocytes than did its shorter analogue and these results can be verified by previous studies in which long sequence tended to interact with the neutral membranes of blood cells (Niidome et al. 2005).

Moreover, the increased helicity and positive charges also contribute to the higher haemolysis. Margitta Dathe et al.(Dathe et al. 1996) have discovered the correlation between peptide helicity and bioactivity. In their study, the KLAL peptide together with its D-amino acid substituted analogue were subjected to different charged membranes to

detect their binding affinity. The results showed peptides with higher helicity possessed better interaction with the low charged membrane surface.

Besides, the net charge is crucial for the binding process, and the more positive charge usually brings more potent antibacterial activity; however, there is a threshold, as too much positive charge also result in greater toxic effects. For instance, L-V13K is a cationic antimicrobial peptide (with net charge +7). A series of V13K analogues with different net charge was designed to investigate the correlation between net charge and biological activities of AMPs. The results indicated that a low level of net charge (<+4) blocked entirely the bioactivities of those designed peptides, on the contrary, a high level of net charge (+9 and +10) enhanced their antimicrobial activity but also led to a significant increase of cytotoxicity towards human erythrocytes (Jiang et al. 2008).

In addition, in certain conditions, action modes of antimicrobial peptides are closely related to their hydrophobicity. Following the membrane permeability assay, it can be shown that when the net charges are at similar levels, compared to original peptides (QUB-1568 and QUB-3025), peptides (QUB-1774 and QUB-1994) with higher hydrophobicity could permeate bacteria cell membranes at a lower concentration. Also, it has been proven earlier that the enhancement of hydrophobicity made it easier for the α-helical peptide to interact with membrane hydrophobic cores of both zwitterionic phospholipids and erythrocytes. Furthermore, the action mode was changed when hydrophobicity remarkably increased (Tachi et al. 2002). However, when the positive charge significantly increased, even hydrophobicity decreased, peptide (QUB-2889) could still permeate the bacteria membrane at a low concentration, and its haemolysis also increased.

It is suggested that net charge plays a most key role among all these peptide properties. When the net charge is significantly increased or extremely high, it becomes the main influential factor for peptide activity, even though hydrophobicity decreases, both antimicrobial activity and cytotoxicity will remain strong, and peptide can still permeate the cell membrane effectively. On the other hand, when only one positive charge was removed, the antimicrobial activity of peptide (QUB-1774) weakened. Hence, increasing the net charge within a reasonable range is a practical approach to improve the selective peptide effects towards pathogenic cells, at the same time, peptide helicity should be controlled at a relatively low level to lower the cytotoxicity. Other factors like hydrophobicity can also be adjusted to improve the peptide selectivity and change the action modes.

6.2 Bacteria resistance against AMPs

As is well known, due to the membrane-active mechanisms, the relatively low possibility for bacteria to generate resistance is one of the most important reasons for AMPs serving as potential candidates for antibiotics. However, along with increasing numbers of studies focusing on AMPs, their diverse non-membranous actions, such as inhibition of protein synthesis (Srinivas et al. 2010) and binding to the minor groove of DNA (Brogden 2005) have also been reported, and these antibiotic-like actions are possible contributing factors for AMP resistance. Besides, the defensive mechanisms can also protect the invading bacteria from these naturally-occurring peptides. Hence, it is necessary to investigate the bacterial defensive actions for AMP therapeutic development.

6.2.1 Biofilm

Bacteria cells are capable of adhering on any surface and producing an extracellular matrix of polysaccharide biopolymer, proteins or DNA that surround the cells (López et

al. 2010). This complex is termed a biofilm, which makes it difficult for AMPs to get into bacterial cells and results in limited activity. The extracellular component of biofilm can protect the bacterial cells from cationic AMPs by electrostatic repulsion. Accordingly, only 33 peptides with anti-biofilm activity are listed in The Antimicrobial Peptide Database http://aps.unmc.edu/AP/database/antiA.php. Human cationic host defence peptide LL-37 was found to possess a potent inhibitory activity on biofilm formation of *Pseudomonas aeruginosa*, and the effective concentration was even much higher than its minimal inhibitory concentration of bacterial growth. It was revealed that LL-37 was capable of reducing the cell attachment, stimulating twitching motility, and affecting two major quorum sensing systems (Las and Rhl), leading to the downregulation of genes essential for biofilm development (Overhage et al. 2008).

To combine AMPs with chelating agents which are able to influence the stability of the biofilm is also an effective way to enhance the inhibition against bacterial biofilm. Temporin 1Tb (TB) is an antimicrobial peptide derived from the skin of the European common frog, which was able to inhibit the biofilm formation of *Staphylococcus epidermidis*, while the combination of ethylenediaminetetra-acetic acid (EDTA) with TB bought significant improvement on the anti-biofilm activity, EDTA/TB combination showed potent killing effect against the biofilms and no haemolysis at eradicating concentrations (Maisetta et al. 2016).

6.2.2 Proteolysis

Since naturally-occurring antimicrobial peptides are sensitive to proteolysis, the host proteases at infected areas could result in the proteolytic degradation of AMPs and many bacteria have been found to have the ability to secret AMP-lytic proteases, which is also an obstacle for AMPs to serve as clinical drugs (Mahlapuu et al. 2016). Scott N. Dean et al. demonstrated that the D-isomer of LL-37 possessed equivalent ability against the

biofilm formation of *P.aeruginosa* as LL-37 did, in which the D-isomer was even more effective than the original peptide during the *in vivo* test. The trypsin resistance of D-isomer might be the contributing factor to its higher *in vivo* potency (Dean et al. 2011). Similarly, M33-D treated mice showed 100% survival over *in vivo* anti-MRSA test, while no survival was obtained for M33-L, moreover, M33-D was highly stable to bacterial proteolysis, while the contrary result was observed for M33-L (Falciani et al. 2012). It is apparent that the application of D-forms of AMPs is an effective way to reduce the proteolytic sensitivity.

6.2.3 Membrane modification

The electrostatic attraction between anionic bacteria membrane and cationic peptides is a crucial factor for AMPs to achieve their activity; thus, bacteria with modified surface positive charges are less sensitive to AMPs. For instance, the d-alanylation of teichoic acids in Gram-positive bacteria results in a decrease of net charge, which is effective resistance to AMPs (Simanski et al. 2013). Correspondingly, the Gram-negative bacteria *Porphyromonas gingivalis* are capable of modifying the outer membrane-embedded lipopolysaccharides to protect against AMPs (Jain, Darveau 2010). However, D-GL13K, the D-isomer of salivary protein-derived peptide GL13K, was proven to be effective against charge modified Gram-negative bacteria, due to its ability to kill *P. gingivalis* and gingipain protease-negative strains (Bechinger, Gorr 2017).

Although diverse types of bacterial defensive mechanisms against AMPs exist, it not as strong as antibiotic resistance and simple modification of peptide, like D-peptide synthesis can be applied to avoid some resistance. Due to the general structure of bacteria cell membranes, it is challenging to develop complete resistance; furthermore, a single AMP can employ several mechanisms to achieve its antimicrobial activity, which also contributes to relatively low bacterial resistance.

6.3 Combination use of AMPs and antibiotics

Besides AMPs themselves, the combination of AMPs and antibiotics is also proven to be a potential strategy for better effect and lower bacteria resistance. Three antimicrobial peptides nisin Z, pediocin PA-1/AcH and colistin, alone or combined with several antibiotics, were subjected to antimicrobial test against *Pseudomonas fluorescens* and its antibiotic-resistant variants. The results revealed the synergistic effect of antimicrobial peptide and antibiotics towards antibiotic-resistant variants, which provided a positive strategy for reducing bacteria resistance (Naghmouchi et al. 2012).

Besides, the combination of AMPs with different secondary structures also brings surprises. Both α-helical magainin 2 and cyclic β-sheet tachyplesin I are membrane-permeated peptides, the combination of these two peptides demonstrated remarkable improvement of antibacterial activity compared to individual peptides, while the haemolysis remained unchanged. Kobayashi et al. also revealed the crucial role of the tachyplesin I cyclic structure for synergism (Kobayashi et al. 2001). These results are meaningful for AMP therapeutic development.

6.4 Development of therapeutic AMPs

Due to their rapid action, broad-spectrum of activity and low possibility of resistance, AMPs have been studied a lot and are regarded as a potential novel category of drug (Mahlapuu et al. 2016). However, the clinical development of AMPs involves several challenges like weak *in vivo* efficacy (Myhrman et al. 2013), low metabolic stability (Vlieghe et al. 2010), high production cost (Bray 2003), and also limited data about safety profiles (Mahlapuu et al. 2016). Thus, only a few AMPs have been applied in clinical use. For instance, polymixins (Velkov et al. 2013), which are natural compounds produced by Gram-positive bacteria, are employed as a last resort in the treatment of

infections caused by Gram-negative "superbugs" *Pseudomonas aeruginosa* or carbapenemase-producing Enterobacteriaceae.

Although the number of antimicrobial peptide drugs is limited, there are still hundreds of AMPs being currently investigated, and under clinical development, several examples are listed in Table 6.1. Magainins, from skin secretions of African clawed frogs (*Xenopodinae*, *Pipidae*), possess broad-spectrum activity against bacteria and are capable of disruption of bacterial cell membrane permeability (Flamm et al. 2016). Accordingly, pexiganan, which is a synthetic analogue of magainin II composed of 22 amino acids (Flamm et al. 2016), was developed as topical cream in phase three clinical trial for the treatment of mild diabetic foot infection (Lipsky et al. 2008). Furthermore, many mammalian AMPs such as omiganan (Jenssen et al. 2006), hLF1-11 (van der Velden, Walter JFM et al. 2009) and iseganan (Bellm et al. 2002) were also subjected to clinical evaluation for various infectious diseases.

Table 6.1 Examples of AMPs under clinical trial.

Name	Source	Clinical phase	Indication	Administration	Clinical trial identifier
Pexiganan (MSI-78)	Analog of magainin II (skin secretion of African clawed frog)	III	Infected diabetic foot ulcers	Topical cream	NCT01590758
Omiganan	Derived from indolicidin (bovine)	III	Catheter infections	Topical gel	NCT00231153
hLF1-11	Derived from lactoferricin (human)	I/II	Bacteraemia and fungal infections in immunocompromized haematopoetic stem cell	Intravenous treatment (in saline)	NCT00509938

			transplant recipients		
Iseganan (IB-367)	Derived from protegrin 1 (porcine leukocytes)	III	Oral mucositis in patients receiving radiotherapy for head and neck malignancy	Oral solution	NCT00022373

6.5 Conclusions and prospects

Antimicrobial peptides are regarded as a novel class of natural antibiotics that could be applied efficiently in the clinic; nevertheless, the production of AMPs is still facing several challenges. The chemical synthesis of AMPs is uneconomical since these peptides often are made up of more than 10 amino acids and most of their active concentrations are at micromolar level, requiring a relatively large quantity of peptide to achieve the effective concentration (Kozlov et al. 2008). Consequently, the cost of AMPs would cost more in comparison with the equally active amount of conventional antibiotics (Kozlov et al. 2008). This problem may be solved by the employment of bacterial expression systems (mainly in *Escherichia coli*) which is a widely used way in protein and peptide drugs manufacture (Schmidt 2004). In addition, the structural nature and biological activity of AMPs can also bring difficulties for production. The linear structure and high cationic feature of these compounds lead to instability, and this is why they are easy to degrade by bacterial proteases (Vlieghe et al. 2010). Furthermore, the production capacity would decline to a large extent because their highly antibacterial activity is lethal for host cells (Piers, Brown et al. 1993). To solve these obstacles, AMPs were subjected to combine with carrier protein or stabilising segments prior to bacteria expression (Pazgier, Lubkowski 2006, Morin et al. 2006).

Currently, the application of nanoparticles is considered as an innovative way to boost the development of therapeutic peptides, since those nanostructured carriers are able to deliver peptides to specific targets, release the peptide at a desired time and also enhance the stability of peptides (L. Zhang et al. 2010). Moreover, lipids and polymers, which are biocompatible and biodegradable, are suitable materials for nanostructured carriers (Mahlapuu et al. 2016). For example, LLKKK18, the18-mer analogue of LL-37, was an effective anti-mycobacterial peptide (Nagaoka et al. 2005). By encapsulating LLKKK18 into self-assembling Hyaluronic Acid (HA) nanogels, not only the anti-mycobacterial activity and proteolytic stability were enhanced, but the cytotoxicity was also reduced. Besides, the macrophage-internalised HA successfully delivered the peptide to infected macrophages, which improved the peptide specificity (Silva et al. 2016). Moreover, nanoparticles have been employed to improve the anti-biofilm activity of peptides (d'Angelo et al. 2015), while the efficacy of AMPs could also be enhanced by loading into nanomaterials which contain antimicrobial activity (Umerska et al. 2016).

In conclusion, AMPs provide a new option for the therapy of infectious disease due to their rapid action, broad-spectrum activity and low possibility of bacterial resistance. Their activities are closely related to the physical properties and structures, and their action modes also vary in different environments and situations. To date, the clinical use of AMPs faces many challenges; however, various coping strategies are also under development, and there are already several AMPs undergoing clinical trials. It is expected for some of these potent peptides to become therapeutic drugs in the near future.

References

BAIRLEY, R., 2009. *Cancer chemotherapy: basic science to the clinic.* John Wiley & Sons.

ALESSANDRO, T., LUCA, S. and ANNA, G., 2000. Amphipathic, α ‐ helical antimicrobial peptides. *Peptide Science*, vol. 55, no. 1, pp. 4-30. Available from: https://doi.org/10.1002/1097-0282(2000)55:13.0.CO;2-M ISSN 0006-3525. DOI AID-BIP30>3.0.CO;2-M.

ALVES, R.R.N., VIEIRA, W.L.S., SANTANA, G.G., VIEIRA, K.S. and Montenegro, Paulo Fernando Guedes Pereira., 2013. Herpetofauna used in traditional folk medicine: conservation implications. In: *Animals in Traditional Folk Medicine*Springer, pp. 109-133.

AMANO, M., 2016. *Subchapter 2D - Sauvagine.* Y. TAKEI, H. ANDO and K. TSUTSUI eds., San Diego: Academic Press Available from: http://www.sciencedirect.com/science/article/pii/B9780128010280001124 ISBN 9780-128010280. DOI //doi.org/10.1016/B978-0-12-801028-0.00112-4.

AMICHE, M., LADRAM, A. and NICOLAS, P., 2008. A consistent nomenclature of antimicrobial peptides isolated from frogs of the subfamily Phyllomedusinae. *Peptides*, vol. 29, no. 11, pp. 2074-2082.

AMICHE, M., SEON, A.A., PIERRE, T.N. and NICOLAS, P., 1999. The dermaseptin precursors: a protein family with a common preproregion and a variable C ‐ terminal antimicrobial domain. *FEBS Letters*, vol. 456, no. 3, pp. 352-356.

ANAN'EVA, N.B., UTESHEV, V.K., ORLOVA, N.L. and GAKHOVA, E.N., 2015. Strategies for Conservation of Endangered Amphibian and Reptile Species. *Izvestiia Akademii Nauk.Seriia Biologicheskaia*, no. 5, pp. 509-517.

ANUNTHAWAN, T., DE LA FUENTE-N��EZ, C., HANCOCK, R.E. and KLAYNONGSRUANG, S., 2015. Cationic amphipathic peptides KT2 and RT2 are taken up into bacterial cells and kill planktonic and biofilm bacteria. *Biochimica Et Biophysica Acta (BBA)-Biomembranes*, vol. 1848, no. 6, pp. 1352-1358.

ASCENZI, P., BOCEDI, A., BOLOGNESI, M., SPALLAROSSA, A., COLETTA, M., CRISTOFARO, R. and MENEGATTI, E., 2003. The bovine basic pancreatic trypsin inhibitor (Kunitz inhibitor): a milestone protein. *Current Protein and Peptide Science*, vol. 4, no. 3, pp. 231-251.

BAHAR, A.A. and REN, D., 2013. Antimicrobial peptides. *Pharmaceuticals*, vol. 6, no. 12, pp. 1543-1575.

BAIRD, D., 1965. Paleozoic lepospondyl amphibians. *American Zoologist*, vol. 5, no. 2, pp. 287-294.

BATISTA, C.V.F., ROSENDO DA SILVA, L., SEBBEN, A., SCALONI, A., FERRARA, L., PAIVA, G.R., OLAMENDI–PORTUGAL, T., POSSANI, L.D.and BLOCH, C., 1999. *Antimicrobial peptides from the Brazilian frog Phyllomedusa distincta1*. Available from: http://www.sciencedirect.com/science/article/pii/S0196978199000509 ISBN 0196-9781. DOI //doi.org/10.1016/S0196-9781(99)00050-9.

BECHINGER, B. and GORR, S., 2017. Antimicrobial peptides: mechanisms of action and resistance. *Journal of Dental Research*, vol. 96, no. 3, pp. 254-260.

BELLM, L., GILES, F.J., REDMAN, R. and YAZJI, S., 2002. Iseganan HCl: a novel antimicrobial agent. *Expert Opinion on Investigational Drugs*, vol. 11, no. 8, pp. 1161-1170.

BERGER, L., SPEARE, R., DASZAK, P., GREEN, D.E., CUNNINGHAM, A.A., GOGGIN, C.L., SLOCOMBE, R., RAGAN, M.A., HYATT, A.D. and MCDONALD, K.R., 1998. Chytridiomycosis causes amphibian mortality associated with population declines in the rain forests of Australia and Central America. *Proceedings of the National Academy of Sciences*, vol. 95, no. 15, pp. 9031-9036.

BIAN, W., MENG, B., LI, X., WANG, S., CAO, X., LIU, N., YANG, M., TANG, J., WANG, Y. and YANG, X., 2018. OA-GL21, a novel bioactive peptide from Odorrana andersonii, accelerated the healing of skin wounds. *Bioscience Reports*, pp. BSR20180215.

BLABER, M., ZHANG, X.J. and MATTHEWS, B.W., 1993. Structural basis of amino acid alpha helix propensity. *Science*, vol. 260, no. 5114, pp. 1637-1640.

BOWDISH, D.M., DAVIDSON, D.J., LAU, Y.E., LEE, K., SCOTT, M.G. and HANCOCK, R.E., 2005. Impact of LL‐37 on anti‐infective immunity. *Journal of Leukocyte Biology*, vol. 77, no. 4, pp. 451-459.

BRAY, B.L., 2003. Large-scale manufacture of peptide therapeutics by chemical synthesis. *Nature Reviews Drug Discovery*, vol. 2, no. 7, pp. 587.

BROGDEN, K.A., 2005. Antimicrobial peptides: pore formers or metabolic inhibitors in bacteria?. *Nature Reviews Microbiology*, vol. 3, no. 3, pp. 238.

BROOKS, H., LEBLEU, B.and VIVÈS, E., 2005. *Tat peptide-mediated cellular delivery: back to basics.* Available from:

http://www.sciencedirect.com/science/article/pii/S0169409X04002741 ISBN 0169-409X. DOI //doi.org/10.1016/j.addr.2004.12.001.

BUTCHART, S.H., AKÇAKAYA, H.R., CHANSON, J., BAILLIE, J.E., COLLEN, B., QUADER, S., TURNER, W.R., AMIN, R., STUART, S.N. and HILTON-TAYLOR, C., 2007. Improvements to the red list index. *PloS One*, vol. 2, no. 1, pp. e140.

CAŁKOSIŃSKI, I., ZASADOWSKI, A., BRONOWICKA-SZYDEŁKO, A., DZIERZBA, K., SEWERYN, E., DOBRZYŃSKI, M. and GAMIAN, A., 2009. Amphibian skin secretions as a new source of antibiotics and biologically active substances. *Postepy Higieny i Medycyny Doswiadczalnej (Online)*, vol. 63, pp. 537-548.

CHAN, D.I., HUNTER, H.N., TACK, B.F. and VOGEL, H.J., 2008. Human macrophage inflammatory protein 3α: protein and peptide nuclear magnetic resonance solution structures, dimerization, dynamics, and anti-infective properties. *Antimicrobial Agents and Chemotherapy*, vol. 52, no. 3, pp. 883-894.

CHAN, D.I., PRENNER, E.J. and VOGEL, H.J., 2006. Tryptophan-and arginine-rich antimicrobial peptides: structures and mechanisms of action. *Biochimica Et Biophysica Acta (BBA)-Biomembranes*, vol. 1758, no. 9, pp. 1184-1202.

CHARPENTIER, S., AMICHE, M., MESTER, J., VOUILLE, V., LE CAER, J., NICOLAS, P. and DELFOUR, A., 1998. Structure, synthesis, and molecular cloning of dermaseptins B, a family of skin peptide antibiotics. *Journal of Biological Chemistry*, vol. 273, no. 24, pp. 14690-14697.

CHEN, L., LI, Y., LI, J., XU, X., LAI, R. and ZOU, Q., 2007. An antimicrobial peptide with antimicrobial activity against Helicobacter pylori. *Peptides*, vol. 28, no. 8, pp. 1527-1531.

CHEN, T., ZHOU, M., GAGLIARDO, R., WALKER, B. and SHAW, C., 2006. Elements of the granular gland peptidome and transcriptome persist in air-dried skin of the South American orange-legged leaf frog, Phyllomedusa hypocondrialis. *Peptides*, vol. 27, no. 9, pp. 2129-2136.

CHEN, X., WANG, H., SHEN, Y., WANG, L., ZHOU, M., CHEN, T. and SHAW, C., 2016. Kunitzins: prototypes of a new class of protease inhibitor from the skin secretions of European and Asian frogs. *Biochemical and Biophysical Research Communications*, vol. 477, no. 2, pp. 302-309.

CHEN, Y., GUARNIERI, M.T., VASIL, A.I., VASIL, M.L., MANT, C.T. and HODGES, R.S., 2007. Role of peptide hydrophobicity in the mechanism of action of α-helical antimicrobial peptides. *Antimicrobial Agents and Chemotherapy*, vol. 51, no. 4, pp. 1398-1406.

CHIVASSO, P., BRUNO, V.D., MARSICO, R., ANNAIAH, A.S., CURTIS, A., ZEBELE, C., ANGELINI, G.D., BRYAN, A.J. and RAJAKARUNA, C., 2018. Effectiveness and safety of aprotinin use in thoracic aortic surgery. *Journal of Cardiothoracic and Vascular Anesthesia*, vol. 32, no. 1, pp. 170-177.

CONLON, J.M. and KIM, J.B., 2000. A protease inhibitor of the Kunitz family from skin secretions of the tomato frog, Dyscophus guineti (Microhylidae). *Biochemical and Biophysical Research Communications*, vol. 279, no. 3, pp. 961-964.

CONLON, J.M. and LEPRINCE, J., 2010. Identification and analysis of bioactive peptides in amphibian skin secretions. In: *Peptidomics*Springer, pp. 145-157.

CONLON, J.M., MECHKARSKA, M., RADOSAVLJEVIC, G., ATTOUB, S., KING, J.D., LUKIC, M.L.and MCCLEAN, S., 2014. *A family of antimicrobial and immunomodulatory peptides related to the frenatins from skin secretions of the Orinoco*

lime frog Sphaenorhynchus lacteus (Hylidae). Available from: http://www.sciencedirect.com/science/article/pii/S0196978114001053 ISBN 0196-9781. DOI //doi.org/10.1016/j.peptides.2014.03.020.

CONLON, J.M., WOODHAMS, D.C., RAZA, H., COQUET, L., LEPRINCE, J., JOUENNE, T., VAUDRY, H.and ROLLINS-SMITH, L.A., 2007. *Peptides with differential cytolytic activity from skin secretions of the lemur leaf frog Hylomantis lemur (Hylidae: Phyllomedusinae).* Available from: http://www.sciencedirect.com/science/article/pii/S0041010107001626 ISBN 0041-0101. DOI //doi.org/10.1016/j.toxicon.2007.04.017.

D'ANGELO, I., CASCIARO, B., MIRO, A., QUAGLIA, F., MANGONI, M.L. and UNGARO, F., 2015. Overcoming barriers in Pseudomonas aeruginosa lung infections: engineered nanoparticles for local delivery of a cationic antimicrobial peptide. *Colloids and Surfaces B: Biointerfaces*, vol. 135, pp. 717-725.

DATHE, M., SCHÜMANN, M., WIEPRECHT, T., WINKLER, A., BEYERMANN, M., KRAUSE, E., MATSUZAKI, K., MURASE, O. and BIENERT, M., 1996. Peptide helicity and membrane surface charge modulate the balance of electrostatic and hydrophobic interactions with lipid bilayers and biological membranes. *Biochemistry*, vol. 35, no. 38, pp. 12612-12622.

DE AZEVEDO CALDERON, L., Alexandre de Almeida, E Silva, CIANCAGLINI, P. and STÁBELI, R.G., 2011. Antimicrobial peptides from Phyllomedusa frogs: from biomolecular diversity to potential nanotechnologic medical applications. *Amino Acids*, vol. 40, no. 1, pp. 29-49.

DE CARO, G., ENDEAN, R., ERSPAMER, V. and ROSEGHINI, M., 1968. Occurrence of caerulein in extracts of the skin of Hyla caerulea and other Australian hylids. *British Journal of Pharmacology and Chemotherapy*, vol. 33, no. 1, pp. 48-58.

DEAN, S.N., BISHOP, B.M. and VAN HOEK, M.L., 2011. Susceptibility of Pseudomonas aeruginosa biofilm to alpha-helical peptides: D-enantiomer of LL-37. *Frontiers in Microbiology*, vol. 2, pp. 128.

DEEKEN, J.F. and LÖSCHER, W., 2007. The blood-brain barrier and cancer: transporters, treatment, and Trojan horses. *Clinical Cancer Research*, vol. 13, no. 6, pp. 1663-1674.

DENNISON, S.R., WALLACE, J., HARRIS, F. and PHOENIX, D.A., 2005. Amphiphilic α-helical antimicrobial peptides and their structure/function relationships. *Protein and Peptide Letters*, vol. 12, no. 1, pp. 31-39.

D'ORAZIO, J., JARRETT, S., AMARO-ORTIZ, A. and SCOTT, T., 2013. UV radiation and the skin. *International Journal of Molecular Sciences*, vol. 14, no. 6, pp. 12222-12248.

DOYLE, J., BRINKWORTH, C.S., WEGENER, K.L., CARVER, J.A., LLEWELLYN, L.E., OLVER, I.N., BOWIE, J.H., WABNITZ, P.A. and TYLER, M.J., 2003. nNOS inhibition, antimicrobial and anticancer activity of the amphibian skin peptide, citropin 1.1 and synthetic modifications. *The FEBS Journal*, vol. 270, no. 6, pp. 1141-1153.

DUELLMAN, W.E. and TRUEB, L., 1994. *Biology of amphibians.* JHU press.

DUTTA, S., RAY, S. and NAGARAJAN, K., 2013. Glutamic acid as anticancer agent: An overview. *Saudi Pharmaceutical Journal*, vol. 21, no. 4, pp. 337-343.

EISENBERG, D., WEISS, R.M. and TERWILLIGER, T.C., 1982. The helical hydrophobic moment: a measure of the amphiphilicity of a helix. *Nature*, vol. 299, no. 5881, pp. 371.

EPAND, R.M. and EPAND, R.F., 2011. Bacterial membrane lipids in the action of antimicrobial agents. *Journal of Peptide Science*, vol. 17, no. 5, pp. 298-305.

ESCRIBÁ, P.V., GONZÁLEZ‐ROS, J.M., GOÑI, F.M., KINNUNEN, P.K., VIGH, L., SÁNCHEZ‐MAGRANER, L., FERNÁNDEZ, A.M., BUSQUETS, X., HORVÁTH, I. and BARCELÓ‐COBLIJN, G., 2008. Membranes: a meeting point for lipids, proteins and therapies. *Journal of Cellular and Molecular Medicine*, vol. 12, no. 3, pp. 829-875.

FALANGA, A., NIGRO, E., DE BIASI, M.G., DANIELE, A., MORELLI, G., GALDIERO, S. and SCUDIERO, O., 2017. Cyclic peptides as novel therapeutic microbicides: Engineering of human defensin mimetics. *Molecules*, vol. 22, no. 7, pp. 1217.

FALCIANI, C., LOZZI, L., POLLINI, S., LUCA, V., CARNICELLI, V., BRUNETTI, J., LELLI, B., BINDI, S., SCALI, S. and DI GIULIO, A., 2012. Isomerization of an antimicrobial peptide broadens antimicrobial spectrum to gram-positive bacterial pathogens. *PLoS One*, vol. 7, no. 10, pp. e46259.

FLAMM, R.K., RHOMBERG, P.R., FARRELL, D.J.and JONES, R.N., 2016. *In vitro spectrum of pexiganan activity; bactericidal action and resistance selection tested against pathogens with elevated MIC values to topical agents.* Available from: http://www.sciencedirect.com/science/article/pii/S0732889316301729 ISBN 0732-8893. DOI //doi.org/10.1016/j.diagmicrobio.2016.06.012.

FORD, H.L. and PARDEE, A.B., 1999. Cancer and the cell cycle. *Journal of Cellular Biochemistry*, vol. 75, no. S32, pp. 166-172.

FRIEDRICH, T., KRÖGER, B., BIALOJAN, S., LEMAIRE, H.G., HÖFFKEN, H.W., REUSCHENBACH, P., OTTE, M. and DODT, J., 1993. A Kazal-type inhibitor with thrombin specificity from Rhodnius prolixus. *Journal of Biological Chemistry*, vol. 268, no. 22, pp. 16216-16222.

FROST, D.R., 2015. No title. *Amphibian Species of the World: An Online Reference.Version 6.0.Electronic Database.American Museum of Natural History, New York, USA*.

GALANTH, C., ABBASSI, F., LEQUIN, O., AYALA-SANMARTIN, J., LADRAM, A., NICOLAS, P. and AMICHE, M., 2008. Mechanism of Antibacterial Action of Dermaseptin B2: Interplay between Helix− Hinge− Helix Structure and Membrane Curvature Strain. *Biochemistry*, vol. 48, no. 2, pp. 313-327.

GASCON, C., 2007. *Amphibian conservation action plan: proceedings IUCN/SSC Amphibian Conservation Summit 2005*. IUCn.

GASPAR, D., VEIGA, A.S. and CASTANHO, M.A., 2013. From antimicrobial to anticancer peptides. A review. *Frontiers in Microbiology*, vol. 4, pp. 294.

GAZIT, E., BOMAN, A., BOMAN, H.G. and SHAI, Y., 1995. Interaction of the mammalian antibacterial peptide cecropin P1 with phospholipid vesicles. *Biochemistry*, vol. 34, no. 36, pp. 11479-11488.

GIULIANI, A., PIRRI, G., BOZZI, A., DI GIULIO, A., ASCHI, M. and RINALDI, A.C., 2008. Antimicrobial peptides: natural templates for synthetic membrane-active compounds. *Cellular and Molecular Life Sciences*, vol. 65, no. 16, pp. 2450-2460.

HANEY, E.F., NAZMI, K., LAU, F., BOLSCHER, J.G.M.and VOGEL, H.J., 2009. *Novel lactoferrampin antimicrobial peptides derived from human lactoferrin.* Available from: http://www.sciencedirect.com/science/article/pii/S0300908408001259 ISBN 0300-9084. DOI //doi.org/10.1016/j.biochi.2008.04.013.

HOCKING, D.J. and BABBITT, K.J., 2014. Amphibian contributions to ecosystem services. *Herpetological Conservation and Biology*.

HOFFMANN, M., HILTON-TAYLOR, C., ANGULO, A., BÖHM, M., BROOKS, T.M., BUTCHART, S.H., CARPENTER, K.E., CHANSON, J., COLLEN, B. and COX, N.A., 2010. The impact of conservation on the status of the world's vertebrates. *Science*, pp. 1194442.

HONG, Z., CHAN, K. and YEUNG, H.W., 1992. Simultaneous determination of bufadienolides in the traditional Chinese medicine preparation, Liu‐Shen‐Wan, by liquid chromatography. *Journal of Pharmacy and Pharmacology*, vol. 44, no. 12, pp. 1023-1026.

HOSKIN, D.W. and RAMAMOORTHY, A., 2008. Studies on anticancer activities of antimicrobial peptides. *Biochimica Et Biophysica Acta (BBA)-Biomembranes*, vol. 1778, no. 2, pp. 357-375.

IWAKOSHI-UKENA, E., UKENA, K., OKIMOTO, A., SOGA, M., OKADA, G., SANO, N., FUJII, T., SUGAWARA, Y. and SUMIDA, M., 2011. Identification and characterization of antimicrobial peptides from the skin of the endangered frog Odorrana ishikawae. *Peptides*, vol. 32, no. 4, pp. 670-676.

IWASAKI, T., ISHIBASHI, J., TANAKA, H., SATO, M., ASAOKA, A., TAYLOR, D. and YAMAKAWA, M., 2009. Selective cancer cell cytotoxicity of enantiomeric 9-mer

peptides derived from beetle defensins depends on negatively charged phosphatidylserine on the cell surface. *Peptides*, vol. 30, no. 4, pp. 660-668.

JAIN, S. and DARVEAU, R.P., 2010. Contribution of Porphyromonas gingivalis lipopolysaccharide to periodontitis. *Periodontology 2000*, vol. 54, no. 1, pp. 53-70.

JENSSEN, H., HAMILL, P. and HANCOCK, R.E., 2006. Peptide antimicrobial agents. *Clinical Microbiology Reviews*, vol. 19, no. 3, pp. 491-511.

JIANG, Z., VASIL, A.I., HALE, J.D., HANCOCK, R.E., VASIL, M.L. and HODGES, R.S., 2008. Effects of net charge and the number of positively charged residues on the biological activity of amphipathic α ‐ helical cationic antimicrobial peptides. *Peptide Science*, vol. 90, no. 3, pp. 369-383.

KANG, S., JI, H. and LEE, B., 2012. Anticancer activity of undecapeptide analogues derived from antimicrobial peptide, Brevinin-1EMa. *Archives of Pharmacal Research*, vol. 35, no. 5, pp. 791-799.

KIM, S., KIM, S.S., BANG, Y., KIM, S. and LEE, B.J., 2003. In vitro activities of native and designed peptide antibiotics against drug sensitive and resistant tumor cell lines. *Peptides*, vol. 24, no. 7, pp. 945-953.

KO, W.S., PARK, T.Y., PARK, C., KIM, Y.H., YOON, H.J., LEE, S.Y., HONG, S.H., CHOI, B.T., LEE, Y.T. and CHOI, Y.H., 2005. Induction of apoptosis by Chan Su, a traditional Chinese medicine, in human bladder carcinoma T24 cells. *Oncology Reports*, vol. 14, no. 2, pp. 475-480.

KOBAYASHI, S., HIRAKURA, Y. and MATSUZAKI, K., 2001. Bacteria-selective synergism between the antimicrobial peptides α-helical magainin 2 and cyclic β-sheet tachyplesin I: toward cocktail therapy. *Biochemistry*, vol. 40, no. 48, pp. 14330-14335.

KONDEJEWSKI, L.H., JELOKHANI-NIARAKI, M., FARMER, S.W., LIX, B., KAY, C.M., SYKES, B.D., HANCOCK, R.E. and HODGES, R.S., 1999. Dissociation of antimicrobial and hemolytic activities in cyclic peptide diastereomers by systematic alterations in amphipathicity. *Journal of Biological Chemistry*, vol. 274, no. 19, pp. 13181-13192.

KÖNIG, E., BININDA-EMONDS, O.R.P.and SHAW, C., 2015. *The diversity and evolution of anuran skin peptides.* Available from: http://www.sciencedirect.com/science/article/pii/S0196978114003295 ISBN 0196-9781. DOI //doi.org/10.1016/j.peptides.2014.11.003.

KOZLOV, S.A., VASSILEVSKI, A.A. and GRISHIN, E.V., 2008. Antimicrobial peptide precursor structures suggest effective production strategies. *Recent Patents on Inflammation & Allergy Drug Discovery*, vol. 2, no. 1, pp. 58-63.

KROWARSCH, D., CIERPICKI, T., JELEN, F. and OTLEWSKI, J., 2003. Canonical protein inhibitors of serine proteases. *Cellular and Molecular Life Sciences CMLS*, vol. 60, no. 11, pp. 2427-2444.

KUMAR, P., KIZHAKKEDATHU, J.N. and STRAUS, S.K., 2018. Antimicrobial Peptides: Diversity, Mechanism of Action and Strategies to Improve the Activity and Biocompatibility In Vivo. *Biomolecules*, vol. 8, no. 1, pp. 4.

KUNITZ, M.J. and NORTHROP, J.H., 1936. Isolation from beef pancreas of crystalline trypsinogen, trypsin, a trypsin inhibitor, and an inhibitor-trypsin compound. *The Journal of General Physiology*, vol. 19, no. 6, pp. 991-1007.

LADNER, R.C. and LEY, A.C., 2006. No title. *Kunitz Domain Peptides*.

LADRAM, A. and NICOLAS, P., 2016. Antimicrobial peptides from frog skin: biodiversity and therapeutic promises. *Front.Biosci*, vol. 21, pp. 1341-1371.

LAI, R., ZHENG, Y., SHEN, J., LIU, G., LIU, H., LEE, W., TANG, S. and ZHANG, Y., 2002. Antimicrobial peptides from skin secretions of Chinese red belly toad Bombina maxima. *Peptides*, vol. 23, no. 3, pp. 427-435.

LAUWERS, A., TWYFFELS, L., SOIN, R., WAUQUIER, C., KRUYS, V. and GUEYDAN, C., 2009. Post-transcriptional regulation of genes encoding anti-microbial peptides in Drosophila. *Journal of Biological Chemistry*.

LAVER, D.R., 1994. The barrel-stave model as applied to alamethicin and its analogs reevaluated. *Biophysical Journal*, vol. 66, no. 2, pp. 355-359.

LEE, J.K., GOPAL, R., PARK, S., KO, H.S., KIM, Y., HAHM, K. and PARK, Y., 2013. A proline-hinge alters the characteristics of the amphipathic α-helical AMPs. *PLoS One*, vol. 8, no. 7, pp. e67597.

LEHMANN, A., 2008. Ecallantide (DX-88), a plasma kallikrein inhibitor for the treatment of hereditary angioedema and the prevention of blood loss in on-pump cardiothoracic surgery. *Expert Opinion on Biological Therapy*, vol. 8, no. 8, pp. 1187-1199.

LEONTIADOU, H., MARK, A.E. and MARRINK, S.J., 2006. Antimicrobial peptides in action. *Journal of the American Chemical Society*, vol. 128, no. 37, pp. 12156-12161.

LEQUIN, O., BRUSTON, F., CONVERT, O., CHASSAING, G. and NICOLAS, P., 2003. Helical structure of dermaseptin B2 in a membrane-mimetic environment. *Biochemistry*, vol. 42, no. 34, pp. 10311-10323.

LI, C., HASHIMI, S.M., CAO, S., MELLICK, A.S., DUAN, W., GOOD, D. and WEI, M.Q., 2013. The mechanisms of chansu in inducing efficient apoptosis in colon cancer cells. *Evidence-Based Complementary and Alternative Medicine*, vol. 2013.

LI, J., WU, J., WANG, Y., XU, X., LIU, T., LAI, R. and ZHU, H., 2008. A small trypsin inhibitor from the frog of Odorrana grahami. *Biochimie*, vol. 90, no. 9, pp. 1356-1361.

LI, J., XU, X., XU, C., ZHOU, W., ZHANG, K., YU, H., ZHANG, Y., ZHENG, Y., REES, H.H. and LAI, R., 2007. Anti-infection peptidomics of amphibian skin. *Molecular & Cellular Proteomics*, vol. 6, no. 5, pp. 882-894.

LI, R., WANG, H., JIANG, Y., YU, Y., WANG, L., ZHOU, M., ZHANG, Y., CHEN, T. and SHAW, C., 2012. A novel Kazal-type trypsin inhibitor from the skin secretion of the Central American red-eyed leaf frog, Agalychnis callidryas. *Biochimie*, vol. 94, no. 6, pp. 1376-1381.

LIPSKY, B.A., HOLROYD, K.J. and ZASLOFF, M., 2008. Topical versus systemic antimicrobial therapy for treating mildly infected diabetic foot ulcers: a randomized, controlled, double-blinded, multicenter trial of pexiganan cream. *Clinical Infectious Diseases*, vol. 47, no. 12, pp. 1537-1545.

LIU, J., JIANG, J., WU, Z. and XIE, F., 2012. Antimicrobial peptides from the skin of the Asian frog, Odorrana jingdongensis: de novo sequencing and analysis of tandem mass spectrometry data. *Journal of Proteomics*, vol. 75, no. 18, pp. 5807-5821.

LIU, T., WANG, Y., LUO, X., LI, J., REED, S.A., XIAO, H., YOUNG, T.S. and SCHULTZ, P.G., 2016. Enhancing protein stability with extended disulfide bonds. *Proceedings of the National Academy of Sciences*, vol. 113, no. 21, pp. 5910-5915.

LOHNER, K., 2001. The role of membrane lipid composition in cell targeting of antimicrobial peptides. *Development of Novel Antimicrobial Agents: Emerging Strategies*, pp. 149-165.

LÓPEZ, D., VLAMAKIS, H. and KOLTER, R., 2010. Biofilms. *Cold Spring Harbor Perspectives in Biology*, pp. a000398.

LÓPEZ-OTÍN, C. and BOND, J.S., 2008. Proteases: multifunctional enzymes in life and disease. *Journal of Biological Chemistry*.

LUDTKE, S.J., HE, K., HELLER, W.T., HARROUN, T.A., YANG, L. and HUANG, H.W., 1996. Membrane pores induced by magainin. *Biochemistry*, vol. 35, no. 43, pp. 13723-13728.

MADER, J.S., SALSMAN, J., CONRAD, D.M. and HOSKIN, D.W., 2005. Bovine lactoferricin selectively induces apoptosis in human leukemia and carcinoma cell lines. *Molecular Cancer Therapeutics*, vol. 4, no. 4, pp. 612-624.

MAHLAPUU, M., HÅKANSSON, J., RINGSTAD, L. and BJÖRN, C., 2016. Antimicrobial peptides: an emerging category of therapeutic agents. *Frontiers in Cellular and Infection Microbiology*, vol. 6, pp. 194.

MAISETTA, G., GRASSI, L., DI LUCA, M., BOMBARDELLI, S., MEDICI, C., BRANCATISANO, F.L., ESIN, S. and BATONI, G., 2016. Anti-biofilm properties of the antimicrobial peptide temporin 1Tb and its ability, in combination with EDTA, to eradicate Staphylococcus epidermidis biofilms on silicone catheters. *Biofouling*, vol. 32, no. 7, pp. 787-800.

MALANOVIC, N. and LOHNER, K., 2016a. Antimicrobial peptides targeting gram-positive bacteria. *Pharmaceuticals*, vol. 9, no. 3, pp. 59.

MALANOVIC, N. and LOHNER, K., 2016b. *Gram-positive bacterial cell envelopes: The impact on the activity of antimicrobial peptides.* Available from: http://www.sciencedirect.com/science/article/pii/S0005273615003697 ISBN 0005-2736. DOI //doi.org/10.1016/j.bbamem.2015.11.004.

MATTILA, J., SABATINI, K. and KINNUNEN, P.K., 2008. Oxidized phospholipids as potential molecular targets for antimicrobial peptides. *Biochimica Et Biophysica Acta (BBA)-Biomembranes*, vol. 1778, no. 10, pp. 2041-2050.

MCKERROW, J.H., ROSENTHAL, P.J., SWENERTON, R. and DOYLE, P., 2008. Development of protease inhibitors for protozoan infections. *Current Opinion in Infectious Diseases*, vol. 21, no. 6, pp. 668.

MECHLIA, M.B., BELAID, A., CASTEL, G., JALLET, C., MANSFIELD, K.L., FOOKS, A.R., HANI, K.and TORDO, N., 2018. *Dermaseptins as potential antirabies compounds.* Available from: http://www.sciencedirect.com/science/article/pii/S0264410X18301270 ISBN 0264-410X. DOI //doi.org/10.1016/j.vaccine.2018.01.066.

MICHAEL CONLON, J., GALADARI, S., RAZA, H. and CONDAMINE, E., 2008. Design of Potent, Non ‐ Toxic Antimicrobial Agents Based Upon the Naturally Occurring Frog Skin Peptides, Ascaphin ‐ 8 and Peptide XT ‐ 7. *Chemical Biology & Drug Design*, vol. 72, no. 1, pp. 58-64.

MILLER, R.E. and FOWLER, M.E., 2014. *Fowler's Zoo and Wild Animal Medicine, Volume 8-E-Book.* Elsevier Health Sciences.

MINCHINTON, A.I. and TANNOCK, I.F., 2006. Drug penetration in solid tumours. *Nature Reviews Cancer*, vol. 6, no. 8, pp. 583.

MOHNEKE, M., ONADEKO, A.B. and RÖDEL, M., 2011. Medicinal and dietary uses of amphibians in Burkina Faso. *African Journal of Herpetology*, vol. 60, no. 1, pp. 78-83.

MORIN, K.M., ARCIDIACONO, S., BECKWITT, R. and MELLO, C.M., 2006. Recombinant expression of indolicidin concatamers in Escherichia coli. *Applied Microbiology and Biotechnology*, vol. 70, no. 6, pp. 698-704.

MYHRMAN, E., HÅKANSSON, J., LINDGREN, K., BJÖRN, C., SJÖSTRAND, V. and MAHLAPUU, M., 2013. The novel antimicrobial peptide PXL150 in the local treatment of skin and soft tissue infections. *Applied Microbiology and Biotechnology*, vol. 97, no. 7, pp. 3085-3096.

NAGAOKA, I., KUWAHARA-ARAI, K., TAMURA, H., HIRAMATSU, K. and HIRATA, M., 2005. Augmentation of the bactericidal activities of human cathelicidin CAP18/LL-37-derived antimicrobial peptides by amino acid substitutions. *Inflammation Research*, vol. 54, no. 2, pp. 66-73.

NAGHMOUCHI, K., LE LAY, C., BAAH, J.and DRIDER, D., 2012. *Antibiotic and antimicrobial peptide combinations: synergistic inhibition of Pseudomonas fluorescens and antibiotic-resistant variants.* Available from: http://www.sciencedirect.com/science/article/pii/S0923250811002038 ISBN 0923-2508. DOI //doi.org/10.1016/j.resmic.2011.11.002.

NASTOUPIL, L.J., ROSE, A.C. and FLOWERS, C.R., 2012. Diffuse large B-cell lymphoma: current treatment approaches. *Oncology*, vol. 26, no. 5, pp. 488.

NGUYEN, L.T., HANEY, E.F.and VOGEL, H.J., 2011. *The expanding scope of antimicrobial peptide structures and their modes of action.* Available from:

http://www.sciencedirect.com/science/article/pii/S0167779911000886 ISBN 0167-7799. DOI //doi.org/10.1016/j.tibtech.2011.05.001.

NICOLAS, P. and EL AMRI, C., 2009. The dermaseptin superfamily: a gene-based combinatorial library of antimicrobial peptides. *Biochimica Et Biophysica Acta (BBA)-Biomembranes*, vol. 1788, no. 8, pp. 1537-1550.

NIIDOME, T., MATSUYAMA, N., KUNIHARA, M., HATAKEYAMA, T. and AOYAGI, H., 2005. Effect of chain length of cationic model peptides on antibacterial activity. *Bulletin of the Chemical Society of Japan*, vol. 78, no. 3, pp. 473-476.

NUTKINS, J.C. and WILLIAMS, D.H., 1989. Identification of highly acidic peptides from processing of the skin prepropeptides of Xenopus laevis. *European Journal of Biochemistry*, vol. 181, no. 1, pp. 97-102.

ODANI, S., KOIDE, T., ONO, T. and OHNISHI, K., 1983. Structural relationship between barley (Hordeum vulgare) trypsin inhibitor and castor-bean (Ricinus communis) storage protein. *Biochemical Journal*, vol. 213, no. 2, pp. 543-545.

OELKRUG, C., HARTKE, M. and SCHUBERT, A., 2015. Mode of action of anticancer peptides (ACPs) from amphibian origin. *Anticancer Research*, vol. 35, no. 2, pp. 635-643.

OHMER, M.E., 2016. Interactions between amphibian skin sloughing and a cutaneous fungal disease: infection progression, immune defence, and phylogenetic patterns.

OHSAKI, Y., GAZDAR, A.F., CHEN, H. and JOHNSON, B.E., 1992. Antitumor activity of magainin analogues against human lung cancer cell lines. *Cancer Research*, vol. 52, no. 13, pp. 3534-3538.

OURTH, D.D., 2011. Antitumor cell activity in vitro by myristoylated-peptide. *Biomedicine & Pharmacotherapy*, vol. 65, no. 4, pp. 271-274.

OVERHAGE, J., CAMPISANO, A., BAINS, M., TORFS, E.C., REHM, B.H. and HANCOCK, R.E., 2008. Human host defense peptide LL-37 prevents bacterial biofilm formation. *Infection and Immunity*, vol. 76, no. 9, pp. 4176-4182.

PAPAGIANNI, M., 2003. *Ribosomally synthesized peptides with antimicrobial properties: biosynthesis, structure, function, and applications.* Available from: http://www.sciencedirect.com/science/article/pii/S0734975003000776 ISBN 0734-9750. DOI //doi.org/10.1016/S0734-9750(03)00077-6.

PAZGIER, M. and LUBKOWSKI, J., 2006. Expression and purification of recombinant human α-defensins in Escherichia coli. *Protein Expression and Purification*, vol. 49, no. 1, pp. 1-8.

PEARCE, G., YAMAGUCHI, Y., MUNSKE, G. and RYAN, C.A., 2008. Structure–activity studies of AtPep1, a plant peptide signal involved in the innate immune response. *Peptides*, vol. 29, no. 12, pp. 2083-2089.

PIERRE, T.N., SEON, A.A., AMICHE, M. and NICOLAS, P., 2000. Phylloxin, a novel peptide antibiotic of the dermaseptin family of antimicrobial/opioid peptide precursors. *European Journal of Biochemistry*, vol. 267, no. 2, pp. 370-378.

POPOVIC, S., URBÁN, E., LUKIC, M. and CONLON, J.M., 2012. Peptides with antimicrobial and anti-inflammatory activities that have therapeutic potential for treatment of acne vulgaris. *Peptides*, vol. 34, no. 2, pp. 275-282.

PORTO, W.F., SILVA, O.N. and FRANCO, O.L., 2012. Prediction and rational design of antimicrobial peptides. In: *Protein Structure*InTech.

POUNY, Y., RAPAPORT, D., MOR, A., NICOLAS, P. and SHAI, Y., 1992. Interaction of antimicrobial dermaseptin and its fluorescently labeled analogs with phospholipid membranes. *Biochemistry*, vol. 31, no. 49, pp. 12416-12423.

PROAÑO-BOLAÑOS, C., LI, R., ZHOU, M., WANG, L., XI, X., TAPIA, E.E., COLOMA, L.A., CHEN, T. and SHAW, C., 2017. Novel Kazal-type proteinase inhibitors from the skin secretion of the Splendid leaf frog, Cruziohyla calcarifer. *EuPA Open Proteomics*, vol. 15, pp. 1-13.

QIN, T., ZHAO, X., YUN, J., ZHANG, L., RUAN, Z. and PAN, B., 2008. Efficacy and safety of gemcitabine-oxaliplatin combined with huachansu in patients with advanced gallbladder carcinoma. *World Journal of Gastroenterology: WJG*, vol. 14, no. 33, pp. 5210.

QUAN, Z., ZHOU, M., CHEN, W., CHEN, T., WALKER, B. and SHAW, C., 2008. Novel brevinins from Chinese piebald odorous frog (Huia schmackeri) skin deduced from cloned biosynthetic precursors. *Peptides*, vol. 29, no. 8, pp. 1456-1460.

RANASINGHE, S. and MCMANUS, D.P., 2013. Structure and function of invertebrate Kunitz serine protease inhibitors. *Developmental & Comparative Immunology*, vol. 39, no. 3, pp. 219-227.

RAWLINGS, N.D., TOLLE, D.P. and BARRETT, A.J., 2004. Evolutionary families of peptidase inhibitors. *Biochemical Journal*, vol. 378, no. 3, pp. 705-716.

RIEDL, S., ZWEYTICK, D. and LOHNER, K., 2011. Membrane-active host defense peptides–challenges and perspectives for the development of novel anticancer drugs. *Chemistry and Physics of Lipids*, vol. 164, no. 8, pp. 766-781.

RINK, R., ARKEMA-METER, A., BAUDOIN, I., POST, E., KUIPERS, A., NELEMANS, S.A., AKANBI, M.H.J. and MOLL, G.N., 2010. To protect peptide pharmaceuticals against peptidases. *Journal of Pharmacological and Toxicological Methods*, vol. 61, no. 2, pp. 210-218.

SANTRA, S., YANG, H., DUTTA, D., STANLEY, J.T., HOLLOWAY, P.H., TAN, W., MOUDGIL, B.M. and MERICLE, R.A., 2004. TAT conjugated, FITC doped silica nanoparticles for bioimaging applications. *Chemical Communications (Cambridge, England)*, Dec 21, no. 24, pp. 2810. Available from: http://www.ncbi.nlm.nih.gov/pubmed/15599418 MEDLINE. ISSN 1359-7345. DOI 10.1039/b411916a.

SASS, V., SCHNEIDER, T., WILMES, M., KÖRNER, C., TOSSI, A., NOVIKOVA, N., SHAMOVA, O. and SAHL, H., 2010. Human β-defensin 3 inhibits cell wall biosynthesis in Staphylococci. *Infection and Immunity*, vol. 78, no. 6, pp. 2793-2800.

SCHIBLI, D.J., HUNTER, H.N., ASEYEV, V., STARNER, T.D., WIENCEK, J.M., MCCRAY, P.B., TACK, B.F. and VOGEL, H.J., 2001. The solution structures of the human beta-defensins lead to a better understanding of the potent bactericidal activity of hBD-3 against Staphylococcus aureus. *Journal of Biological Chemistry*.

SCHMIDT, F.R., 2004. Recombinant expression systems in the pharmaceutical industry. *Applied Microbiology and Biotechnology*, vol. 65, no. 4, pp. 363-372.

SEIMON, T.A., AYEBARE, S., SEKISAMBU, R., MUHINDO, E., MITAMBA, G., GREENBAUM, E., MENEGON, M., PUPIN, F., MCALOOSE, D. and AMMAZZALORSO, A., 2015. Assessing the threat of amphibian chytrid fungus in the Albertine Rift: Past, present and future. *PloS One*, vol. 10, no. 12, pp. e0145841.

SEVIER, C.S. and KAISER, C.A., 2002. Formation and transfer of disulphide bonds in living cells. *Nature Reviews Molecular Cell Biology*, vol. 3, no. 11, pp. 836.

SHANG, D., YU, F., LI, J., ZHENG, J., ZHANG, L. and LI, Y., 2009. Molecular cloning of cDNAs encoding antimicrobial peptide precursors from the skin of the Chinese brown frog, Rana chensinensis. *Zoological Science*, vol. 26, no. 3, pp. 220-226.

SILVA, J.P., GONÇALVES, C., COSTA, C., SOUSA, J., SILVA-GOMES, R., CASTRO, A.G., PEDROSA, J., APPELBERG, R. and GAMA, F.M., 2016. Delivery of LLKKK18 loaded into self-assembling hyaluronic acid nanogel for tuberculosis treatment. *Journal of Controlled Release*, vol. 235, pp. 112-124.

SIMANSKI, M., GLÄSER, R., KÖTEN, B., MEYER‐HOFFERT, U., WANNER, S., WEIDENMAIER, C., PESCHEL, A. and HARDER, J., 2013. S taphylococcus aureus subverts cutaneous defense by d‐alanylation of teichoic acids. *Experimental Dermatology*, vol. 22, no. 4, pp. 294-296.

SIMMACO, M., MIGNOGNA, G. and BARRA, D., 1998. Antimicrobial peptides from amphibian skin: what do they tell us?. *Peptide Science*, vol. 47, no. 6, pp. 435-450.

SMITH, D., TIKHONOVA, I.G., JEWHURST, H.L., DRYSDALE, O.C., DVOŘÁK, J., ROBINSON, M.W., CWIKLINSKI, K. and DALTON, J.P., 2016. Unexpected activity of a novel Kunitz-type inhibitor: Inhibition of cysteine proteases but not serine proteases. *Journal of Biological Chemistry*, pp. jbc. M116. 724344.

SOEHNLEIN, O., 2009. Direct and alternative antimicrobial mechanisms of neutrophil-derived granule proteins. *Journal of Molecular Medicine*, vol. 87, no. 12, pp. 1157-1164.

SONOHARA, R., MURAMATSU, N., OHSHIMA, H. and KONDO, T., 1995. Difference in surface properties between Escherichia coli and Staphylococcus aureus as

revealed by electrophoretic mobility measurements. *Biophysical Chemistry*, vol. 55, no. 3, pp. 273-277.

SØRENSEN, O.E., BORREGAARD, N. and COLE, A.M., 2008. Antimicrobial peptides in innate immune responses. In: *Trends in innate immunity*Karger Publishers, pp. 61-77.

SRINIVAS, N., JETTER, P., UEBERBACHER, B.J., WERNEBURG, M., ZERBE, K., STEINMANN, J., VAN DER MEIJDEN, B., BERNARDINI, F., LEDERER, A. and DIAS, R.L., 2010. Peptidomimetic antibiotics target outer-membrane biogenesis in Pseudomonas aeruginosa. *Science*, vol. 327, no. 5968, pp. 1010-1013.

SU, L.Y., WILLNER, D.L. and SEGALL, A.M., 2010. An antimicrobial peptide that targets DNA repair intermediates in vitro inhibits Salmonella growth within murine macrophages. *Antimicrobial Agents and Chemotherapy*, vol. 54, no. 5, pp. 1888-1899.

TACHI, T., EPAND, R.F., EPAND, R.M. and MATSUZAKI, K., 2002. Position-dependent hydrophobicity of the antimicrobial magainin peptide affects the mode of peptide− lipid interactions and selective toxicity. *Biochemistry*, vol. 41, no. 34, pp. 10723-10731.

TAKAHASHI, D., SHUKLA, S.K., PRAKASH, O. and ZHANG, G., 2010. Structural determinants of host defense peptides for antimicrobial activity and target cell selectivity. *Biochimie*, vol. 92, no. 9, pp. 1236-1241.

TANG, M. and HONG, M., 2009. Structure and mechanism of β-hairpin antimicrobial peptides in lipid bilayers from solid-state NMR spectroscopy. *Molecular BioSystems*, vol. 5, no. 4, pp. 317-322.

TIANBAO, C., FARRAGHER, S., BJOURSON, A.J., PINGFAN, R. and CHRIS, S., 2003. Granular gland transcriptomes in stimulated amphibian skin secretions. *Biochemical Journal*, vol. 371, no. 1, pp. 125-130.

UBHI, R. and MATTHEWS, P.G., 2018. The transition from water to air in aeshnid dragonflies is associated with a change in ventilatory responses to hypoxia and hypercapnia. *Journal of Insect Physiology*, vol. 106, pp. 172-178.

ULMSCHNEIDER, J.P., 2017. Charged antimicrobial peptides can translocate across membranes without forming channel-like pores. *Biophysical Journal*, vol. 113, no. 1, pp. 73-81.

UMERSKA, A., CASSISA, V., MATOUGUI, N., JOLY-GUILLOU, M., EVEILLARD, M. and SAULNIER, P., 2016. Antibacterial action of lipid nanocapsules containing fatty acids or monoglycerides as co-surfactants. *European Journal of Pharmaceutics and Biopharmaceutics*, vol. 108, pp. 100-110.

van der Velden, Walter JFM, VAN IERSEL, T.M., BLIJLEVENS, N.M. and DONNELLY, J.P., 2009. Safety and tolerability of the antimicrobial peptide human lactoferrin 1-11 (hLF1-11). *BMC Medicine*, vol. 7, no. 1, pp. 44.

VAN ZOGGEL, H., CARPENTIER, G., DOS SANTOS, C., HAMMA-KOURBALI, Y., COURTY, J., AMICHE, M. and DELBÉ, J., 2012. Antitumor and angiostatic activities of the antimicrobial peptide dermaseptin B2. *PloS One*, vol. 7, no. 9, pp. e44351.

VELKOV, T., ROBERTS, K.D., NATION, R.L., THOMPSON, P.E. and LI, J., 2013. Pharmacology of polymyxins: new insights into an 'old'class of antibiotics. *Future Microbiology*, vol. 8, no. 6, pp. 711-724.

VIÉ, J., HILTON-TAYLOR, C. and STUART, S.N., 2009. *Wildlife in a changing world: an analysis of the 2008 IUCN Red List of threatened species.* IUCN.

VLIEGHE, P., LISOWSKI, V., MARTINEZ, J. and KHRESTCHATISKY, M., 2010. Synthetic therapeutic peptides: science and market. *Drug Discovery Today*, vol. 15, no. 1-2, pp. 40-56.

VOYLES, J., BERGER, L., YOUNG, S., SPEARE, R., WEBB, R., WARNER, J., RUDD, D., CAMPBELL, R. and SKERRATT, L.F., 2007. Electrolyte depletion and osmotic imbalance in amphibians with chytridiomycosis. *Diseases of Aquatic Organisms*, vol. 77, no. 2, pp. 113-118.

WANG, G., 2012. Post-translational modifications of natural antimicrobial peptides and strategies for peptide engineering. *Current Biotechnology*, vol. 1, no. 1, pp. 72-79.

WANG, K., JIA, F., DANG, W., ZHAO, Y., ZHU, R., SUN, M., QIU, S., AN, X., MA, Z. and ZHU, Y., 2016. Antifungal effect and action mechanism of antimicrobial peptide polybia‐CP. *Journal of Peptide Science*, vol. 22, no. 1, pp. 28-35.

WANG, M., WANG, L., CHEN, T., WALKER, B., ZHOU, M., SUI, D., CONLON, J.M. and SHAW, C., 2012. Identification and molecular cloning of a novel amphibian Bowman Birk-type trypsin inhibitor from the skin of the Hejiang Odorous Frog; Odorrana hejiangensis. *Peptides*, vol. 33, no. 2, pp. 245-250.

WELLS, K.D., 1977. The social behaviour of anuran amphibians. *Animal Behaviour*, vol. 25, pp. 666-693.

WELLS, K.D. and SCHWARTZ, J.J., 2007. The behavioral ecology of anuran communication. In: *Hearing and sound communication in amphibians*Springer, pp. 44-86.

WIEPRECHT, T., DATHE, M., KRAUSE, E., BEYERMANN, M., MALOY, W.L., MACDONALD, D.L. and BIENERT, M., 1997. Modulation of membrane activity of amphipathic, antibacterial peptides by slight modifications of the hydrophobic moment. *FEBS Letters*, vol. 417, no. 1, pp. 135-140.

WU, Y., LONG, Q., XU, Y., GUO, S., CHEN, T., WANG, L., ZHOU, M., ZHANG, Y., SHAW, C. and WALKER, B., 2017. A Structural and Functional Analogue of a Bowman Birk-type Protease Inhibitor from Odorrana Schmackeri. *Bioscience Reports*, pp. BSR20160593.

XU, N., WANG, Y., PAN, W., XIAO, B., WEN, Y., CHEN, X., CHEN, L., DENG, H., YOU, J. and KAN, B., 2008. Human α-defensin-1 inhibits growth of human lung adenocarcinoma xenograft in nude mice. *Molecular Cancer Therapeutics*, vol. 7, no. 6, pp. 1588-1597.

YANG, L., MEI, Y., FANG, Q., WANG, J., YAN, Z., SONG, Q., LIN, Z. and YE, G., 2017. Identification and characterization of serine protease inhibitors in a parasitic wasp, Pteromalus puparum. *Scientific Reports*, vol. 7, no. 1, pp. 15755.

YANG, X., LEE, W. and ZHANG, Y., 2011. Extremely abundant antimicrobial peptides existed in the skins of nine kinds of Chinese odorous frogs. *Journal of Proteome Research*, vol. 11, no. 1, pp. 306-319.

YE, C., FEI, L. and HU, S., 1993. *Rare and economic amphibians of China.* Sichuan Publishing House of Science & Technology.

YEUNG, A.T., GELLATLY, S.L. and HANCOCK, R.E., 2011. Multifunctional cationic host defence peptides and their clinical applications. *Cellular and Molecular Life Sciences*, vol. 68, no. 13, pp. 2161.

YIN, L.M., EDWARDS, M.A., LI, J., YIP, C.M. and DEBER, C.M., 2012. Roles of hydrophobicity and charge distribution of cationic antimicrobial peptides in peptide-membrane interactions. *Journal of Biological Chemistry*, pp. jbc. M111. 303602.

ZAIRI, A., TANGY, F., BOUASSIDA, K. and HANI, K., 2009. Dermaseptins and magainins: antimicrobial peptides from frogs' skin—new sources for a promising spermicides microbicides—a mini review. *BioMed Research International*, vol. 2009.

ZANETTI, M., 2004. Cathelicidins, multifunctional peptides of the innate immunity. *Journal of Leukocyte Biology*, vol. 75, no. 1, pp. 39-48.

ZHANG, L., PORNPATTANANANGKUL, D., HU, C. and HUANG, C., 2010. Development of nanoparticles for antimicrobial drug delivery. *Current Medicinal Chemistry*, vol. 17, no. 6, pp. 585-594.

ZHANG, S., SONG, J., GONG, F., LI, S., CHANG, H., XIE, H., GAO, H., TAN, Y. and JI, S., 2016. Design of an α-helical antimicrobial peptide with improved cell-selective and potent anti-biofilm activity. *Scientific Reports*, vol. 6, pp. 27394.

ZHAO, R., HAN, J., HAN, W., HE, H. and MA, J., 2011. Effects of two novel peptides from skin of Lithobates catesbeianus on tumor cell morphology and proliferation.